# COLOUR CENTRES DEVELOPMENT BY GAMMA-IRRADIATION OF NATURAL AND SYNTHETIC ROCK SALT SAMPLES

**C.de las Cuevas, L.Miralles**


## ABSTRACT

Laboratory gamma irradiations at a constant temperature (100ºC) were carried out in four sets of experiments. The starting materials for the experiments were both natural and synthetic rock salt. Dose rates were approximately constant for two of the experiments and variable for the other two. The total doses studied ranged from 20 kGy to 1154 MGy. Measurements of the concentration of colour centres (radiation induced defects) were performed using two methods: optical absorption and release of hydrogen after dissolution of irradiated salt. The results were compared with the dose absorbed, dose rate and chemical composition of the rock salt. The concentration of colour centres increases with increasing total dose, being lower dose rates slightly efficient in the generation of colour centres for samples irradiated at the same total dose. The mineralogical composition of the rock salt also affects the concentration of the defects, leading to a dispersion of one order of magnitude. In these experiments, mineralogical composition had more influence than dose rate in generating radiation-induced defects. The process of fluid-assisted recrystallization in the form of newly precipitated white halite was extensive in pure polycrystalline rock salt (natural and synthetic). These crystals, which precipitated after irradiation, included equivalent amounts of $H_2$ to the concentration of colloidal sodium developed in the damaged crystals. Comparison between experimental data and the Jain-Lidiard model predictions performed in the range of 20 kGy and 50 MGy, revealed that for doses higher than 5 MGy the model is a good aproximation.


## 1. INTRODUCTION

The disposal of high-level radioactive waste in rock salt can lead to a series of changes of state in the surrounding rock salt. The radiation emitted by radioactive waste canisters will be absorbed by the salt formation in the course of time. Most of the gamma radiation energy will be converted into heat, whilst a small part will induce radiation damage. This consists of the generation of defects in the crystal lattice of the halite (NaCl) which is the major mineral in rock salt (over 90 %). Although only the first meter in contact with the

wastes will be affected (Schulze, 1986), this phenomenon needs to be studied carefully in order to ensure that it will not threaten the long-term safety of the repository.

When sodium chloride is irradiated, the primary defects generated are pairs of F and H- centres. $Cl^-$ ions are ejected from their normal lattice sites to form interstitial chlorine atoms (H-centres). The former structural site of chloride traps an electron (F-centre), and the neutrality of the crystal is preserved. At temperatures above 30ºC, as is the case of heat-producing waste, the mobility of primary defects is increased (Hodgson *et al.*, 1979). Due to their high mobility the H-centres (activation energy about 0.1 eV) are easily trapped in the vicinity of dislocation lines, where molecular chlorine is formed, and the F-centres, which are less mobile (activation energy about 0.8 eV), tend to form clusters of two or more centres (e.g. M-, R-centres). Because of their optical properties, they all absorb light in the visible range of the electromagnetic spectrum (F, M, R and other centres), and are thus referred to as colour centres. If the clustering continues, larger aggregates of metallic sodium colloids are formed. The theory which describes the growth of the sodium colloids by irradiation of NaCl crystals was advanced by Jain and Lidiard (1977).

Radiation damage in halite has been extensively studied for low doses by several authors in the field of Solid State Physics (Przibram, 1956; Dale Compton, 1957). Over the last twenty years, its study has been extended to high doses (Jenks and Bopp, 1974; Levy, 1983) since a sudden recombination of the defects accumulated could constitute a possible hazard related to the radiation damage in salt repositories. As a consequence, the local temperature would rise around the emplacement of wastes (Mönig *et al.*, 1990)

In natural rock salt, there are large variations in the radiation damage as it depends on: temperature, the level of impurities, dose rate, total dose and strain on the rock sample (Levy, 1983). In addition, fluid-assisted recrystallization (García Celma *et al.* 1988) may take place, annealing the damage of the rock salt. For these reasons, a study of radiation damage in natural rock salt from several locations and in synthetic rock salt has been undertaken. Four sets of experiments were carried out at two Gamma-Irradiation Facilities (GIF A and GIF B) located at the cooling pool of the High Flux Reactor (Petten, The Netherlands), in which spent fuel elements are used as source of gamma radiation (article 5 in this volume).



## 2. EXPERIMENTAL PROCEDURE

Samples for the GIF A-1 experiment were irradiated at 100 ºC and atmospheric pressure. Dose rate was variable (between 200 and 20 kGy/h) and total doses ranged from 41 to 1223 MGy. Samples for the GIF A-2 experiment were irradiated at atmospheric pressure at a temperature that varied from 130 ºC at the beginning of the irradiation to 100 ºC after three days. Dose rate was variable (between 170 and 40 kGy/h) and total doses ranged from 19 to 48 MGy. The starting material used in the experiments was SP800 rock salt from the Asse Mine (Remlingen, Germany) for the GIF A-1 experiment, and rock salt from the Sallent Mine (Barcelona, Spain) for the GIF A-2 experiment.

The starting material for the GIF B-1 and GIF B-2 experiments were cores of both natural and synthetic rock salt. Samples of natural rock salt came from the Sallent Mine (Barcelona, Spain) at level 323 (coded PLL), from the Asse Mine (Remlingen, Germany) (coded SP800, Bha , Bhp or PS depending on stratigraphical position) and from Dutch salt formations (coded DS). Synthetic polycrystalline rock salt was obtained from an analytical NaCl reagent, and was divided into two types (coded PP, which is a fine grained rock salt, or SS, which is a coarse grained rock salt). Finally, pure monocrystals (manufactured by Harshaw Chemical Co., Ohio, USA; coded H) are also used. Samples were turned on a lathe until they reached a diameter of 24 mm and then cut to form cylinders (40 mm length) and tablets (10 mm length). Irradiations from the GIF B-1 experiment were performed at an approximately constant dose rate of 15 kGy/h (which ranged from 20 to 10 kGy/h) and the temperature during irradiation was kept constant at 100ºC. Total doses ranged from 20 kGy to 44 MGy. In each loading, 8 containers (6 of them pressurized at 20 MPa in order to simulate the confining pressure at depths of 800 m and the other two at atmospheric pressure) were irradiated simultaneously. Every container had inside a cylinder and a tablet shaped sample. The experimental conditions for the GIF B-2 experiment were identical to those of the GIF B-1 except that the dose rate was around 4 kGy/h.

The quantification of the fraction of the radiation-induced defects present in the NaCl lattice was performed by optical absorption measurement on translucent thin sections, 30 to 250 μm thick, depending on its opacity. Low-speed procedures were applied to obtain the thin sections in order to avoid damage induced by sample manipulation. Optical Absorption measurements (O.A) were performed using a double beam UV-Vis spectrophotometer. The spectral interval scanned was from 300 to 900 nm (Fig. 1), since F-centres show an absorption band at about 460 nm, M-centres at 700 nm, and the sodium colloids between 550 and 650 nm. In the case of halite containing impurities in its crystal lattice (Ikeda and Yoshida, 1967), F-centres are absent, being $F_A$ or $F_Z$ centres present (F-centres developed in

the vicinity of either a monovalent or a divalent cation impurity). These F-related centres show an absorption band between 380 and 420 nm. These bands commonly overlap and, in order to obtain better resolution, the spectra must be deconvolved (Fig. 2) using a Fast Fourier Transform filter. Afterwards, the concentration of colour centres was quantified from the absorbance of each band using Smakula's equations (1) (Markham, 1966) and (2) (Levy and Kiersted, 1984), which relate the absorption coefficient to the concentration of colour centres.

$$N = \alpha_{max} \frac{10^{16}}{2.06\, f} \qquad (1) \qquad \text{(for F-centres)}$$

$$FM = 4.42 \; 10^{-7} \; \alpha_{max} \qquad (2) \qquad \text{(for colloidal sodium)}$$

where $\alpha_{max}$ is the maximal absorption coefficient in $cm^{-1}$
f, the oscillator strength (between 0.8 and 0.9)
N is the number of F-centres per $cm^3$
FM is the molar fraction of colloidal Na.

The absorption coefficient is computed by the equation (3)

$$\alpha = \frac{\ln 10}{t} Abs \qquad (3)$$

where $\alpha$ is the absorption coefficient in $cm^{-1}$
t is the thickness of the sample in cm
Abs is the absorbance

Besides the concentration of colour centres, additional information can be obtained from the absorption spectra, such as the size of the colloids (Smithard and Tran, 1974) which can be related to the exact location of the optical absorption peak and/or to its width.

Moreover, quantification of sodium colloids by measuring the release of hydrogen during dissolution of irradiated salt samples (Jenks *et al.*, 1975) was also carried out, in order to contrast the aforementioned methodology. Grounded salt amounting 500 mg were dissolved in 1.5 ml of distilled water in a glass vial (V= 5 ml) which was closed with an



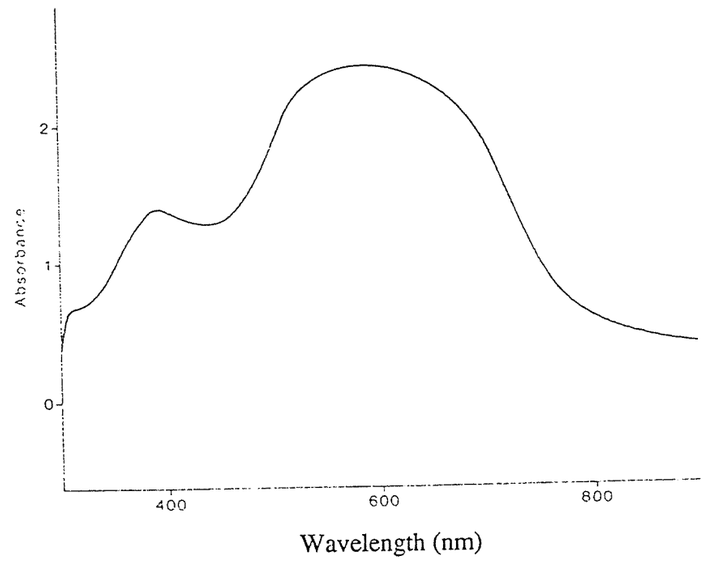


Figure 1: Absorbance spectrum of sample 1PLL.

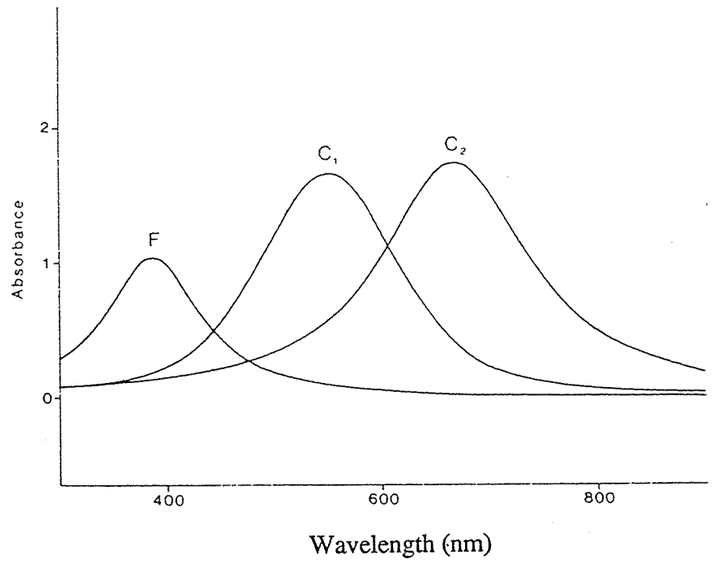


Figure 2: Deconvolved absorbance spectrum of sample 1PLL showing the presence of F-related centres and two populations of colloidal sodium particles.

open-hole screw-cap and a septum. The evolved hydrogen produced by the reaction of metallic sodium with water, was extracted via a gastight syringe and measured by gas chromatography. The working conditions were: Molecular Sieve column, Thermal Conductivity Detector, Argon as carrier gas and oven temperature hold to 60°C.

Geochemical characterization was performed only on the cylindrical samples from the GIF B-1 and GIF B-2 experiments. After crushing to a grain size of 2 to 3 mm, 250 mg was taken for water content analysis and quantified by thermogravimetry. In natural rock salt samples 5 to 10 g of the crushed material were further milled, and chemical and mineralogical analyses were performed. Chloride was determined volumetrically, sulphate by ICP-AES (Inductively Coupled Plasma Atomic Emission Spectroscopy), potassium by AES (Atomic Emission Spectroscopy) and calcium, magnesium and strontium by AAS (Atomic Absorption Spectroscopy). The insoluble fraction was calculated gravimetrically. The analytical procedures are described in detail elsewhere (Huertas *et al.*, 1992).

The mineralogical phases present in the irradiated rock salt from the GIF B-1 and GIF B-2 experiments were identified with a transmitted-light polarizing microscope in the aforementioned thin sections. The microscope study of thin sections also revealed microstructural changes in the starting material and permitted quantification of the damage-free halite precipitated in the experiments. The quantification was performed using an automated image analyzer.

## 3. RESULTS

### 3.1 Defect concentration in samples from the GIF A-1 experiment

F-related centres were quantified for all the samples of the GIF A-1 experiment from Optical Absorption spectra. Their concentrations ranged from $3.25 * 10^{-5}$ to $3.74 * 10^{-4}$ molar fraction. The colloidal sodium concentration of samples irradiated at doses of 41 and 86 MGy could be measured by O.A and release of hydrogen, both of which gave similar values. The amount of colloidal sodium ranged from $2.0* 10^{-4}$ to $6.0* 10^{-4}$ molar fraction. Moreover, two size of colloids (around 2 and 100 nm) could be determined. At higher doses (150 MGy and above), the O.A spectra of these samples are very complex to study, due to the high dose absorbed. For this reason the concentration of colloidal sodium was computed from the release of hydrogen from dissolved samples. The concentration of colloidal sodium ranged from $1.3* 10^{-3}$ to $4.9*10^{-3}$ molar fraction. The broad O.A band related to colloidal



sodium has been interpreted as the result of concentration of metallic sodium particles greater than $1* 10^{-3}$ molar fraction, with size ranging from 2 to 150 nm.

### 3.2 Defect concentration in samples from the GIF A-2 experiment

The irradiation experiment of GIF A-2 was performed with a similar dose rate to the GIF A-1 experiment but covering a lower dose region (between 19 and 50 MGy). In the samples studied, F-related centres, and one or two sizes of colloidal sodium particles (depending on the sample) were detected by O.A. The size of colloidal particles varied from 45 to 90 nm diameter. When the size of the colloids was around 90 nm, a second population of small size colloids was present (diameter between 1 and 50 nm). There is good correlation in the colloidal sodium measurements between Optical Absorption and evolved hydrogen methods, which give results of the same order of magnitude. The concentration of colloidal sodium was between $7.6 * 10^{-5}$ and $6.3 * 10^{-4}$ molar fraction and that of F-related centre was between $4.1 * 10^{-6}$ and $6.6 * 10^{-5}$ molar fraction.

The concentration of F-centres and colloids obtained in both variable dose experiments (GIF A-1 and GIF A-2) are plotted versus the total dose in Figures 3 and 4. A linearity of the amount of radiation induced defects in the range between 19 and 300 MGy is observed. Nevertheless, at higher doses there is a change in the slope suggesting decreasing efficiency in generating defects.

### 3.3 Defect concentration in samples from the GIF B-1 experiment

F- or F-related centres and sodium particles of colloidal size were found in all the samples. F-centres were present only in pure monocrystals, whereas F-related centres ($F_A$ or $F_Z$ centres) were found in polycrystalline rock salt. Moreover, M-centres were detected mainly in pure monocrystals, at concentration below $10^{-6}$ molar fraction. For doses below 430 kGy, the concentration of colloidal sodium is only measurable using the evolved hydrogen method since from the O.A spectra only F-centres could be quantified. At higher doses (430 kGy and above) colloidal sodium could also be measured from the O.A spectra. There is good correlation in the colloidal sodium measurements between both methods, Optical Absorption and evolved hydrogen, yielding results on the same order of magnitude. The amount of colloidal sodium, which increases with total dose, ranged between less than $10^{-7}$ to $5.25 * 10^{-4}$ molar fraction for doses of 48 MGy. The concentration of F-centre does not increase sensitively with total dose and ranged between $1.5* 10^{-6}$ to $1.0 * 10^{-4}$ molar

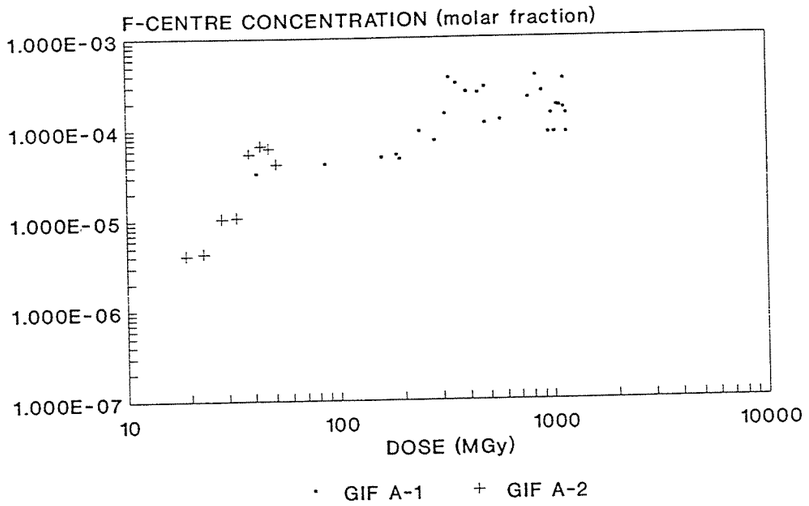


Figure 3: F-centre concentration versus total dose for samples from GIF A-1 and GIF A-2 experiments.

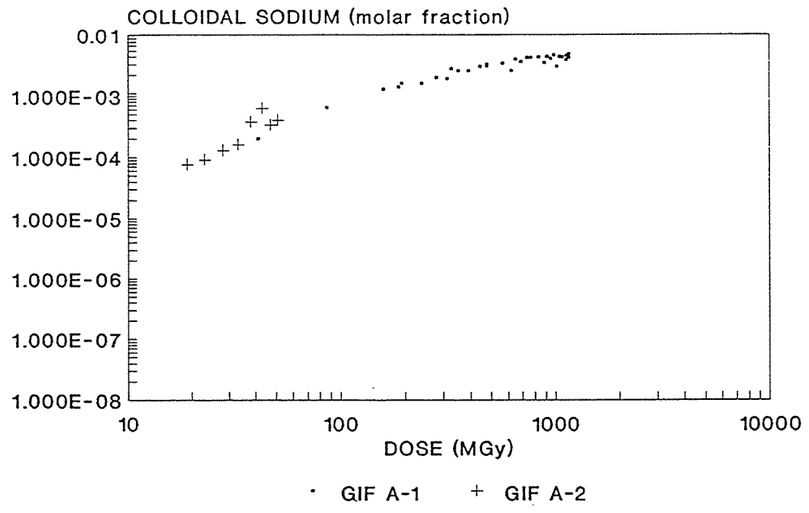


Figure 4: Colloidal sodium concentration versus total dose for samples from GIF A-1 and GIF A-2 experiments.



fraction. The concentration of the radiation induced defects are displayed in figures 5 and 6. Figure 5 shows the relationship between total dose and the amount of F- or F related centres. Figure 6 shows the relationship between total dose and the amount of colloidal sodium. For samples of the same type and irradiation conditions, the amount of defects varied widely, suggesting a substantial contribution of the geological parameters of the starting material. It has been observed that for the same total dose pure monocrystals developed less colloidal sodium (about one order of magnitude) than polycrystalline rock salt.

For polycrystalline rock salt the size of the colloidal particles usually grows with increasing total dose. Nevertheless, in several samples irradiated at doses higher than 16 MGy in addition to the colloidal sodium particles about 90 nm diameter, a second population of colloids of smaller size (about 5 nm diameter) was also present. In pure monocrystals, the size of the colloidal particles was always around 90 nm diameter, indepently on their concentration. In figure 7 the relationship between total dose and the size of the colloidal particles is plotted.

### 3.4 Defect concentration in samples from the GIF B-2 experiment

In all the samples F- or F-related centres and a population of colloidal sodium were present. In addition, in samples irradiated at doses higher than 10 MGy, a second population of colloidal sodium was detected in natural rock salt. In contrast for Pressed Powder samples and pure monocrystals, M-centres were normally found. The two population of colloids present in natural rock salt have been divided as small sized (between 1 and 60 nm diameter) and big sized (between 80 and 90 nm diameter). As in samples from the GIF A-2 and GIF B-1 experiments, there is also good correlation in the colloidal sodium measurements between Optical Absorption and evolved hydrogen methods.

The total amount of colloidal sodium particles ranged from $3 * 10^{-7}$ to $8.23 * 10^{-4}$ molar fraction, the amount of F-related centre ranges from $6 * 10^{-7}$ to $9.6 * 10^{-5}$ molar fraction and the amount of M-centre (when detected) ranged from $10^{-7}$ to $5.26 * 10^{-4}$ molar fraction. There is an increase of the amount of defects with increasing dose. Moreover, the size of the colloidal particles grows with increasing dose.

The behaviour of the radiation induced defects in these samples is similar to their equivalents of the GIF B-1 experiment. Figure 8 shows the relationship between total dose and the amount of F- or F related centres. Figure 9 shows the relationship between total dose and the amount of colloidal sodium particles, whereas in figure 10 the relationship between

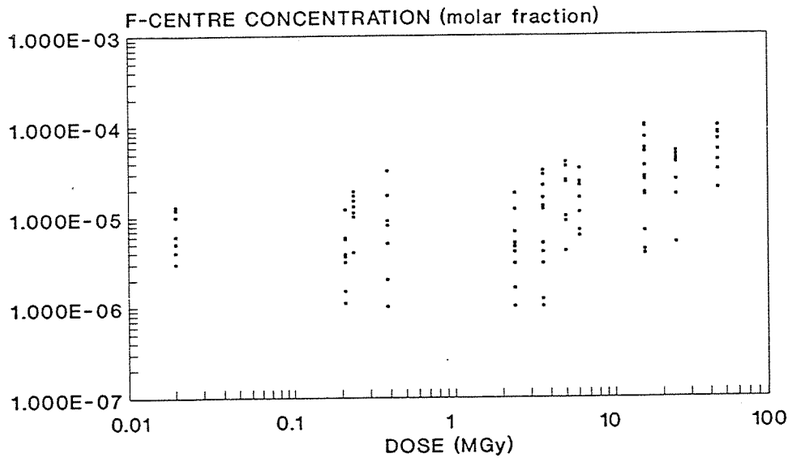


Figure 5: F-centre concentration versus total dose for samples from GIF B-1 experiment.

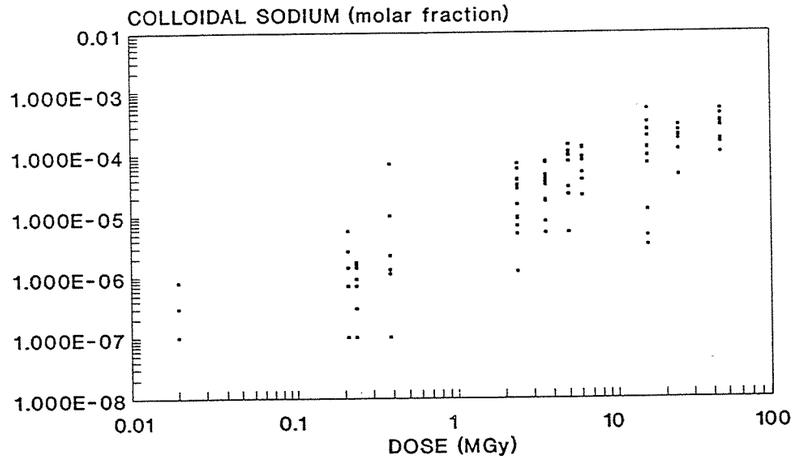


Figure 6: Colloidal sodium concentration versus total dose for samples from GIF B-1 experiment.



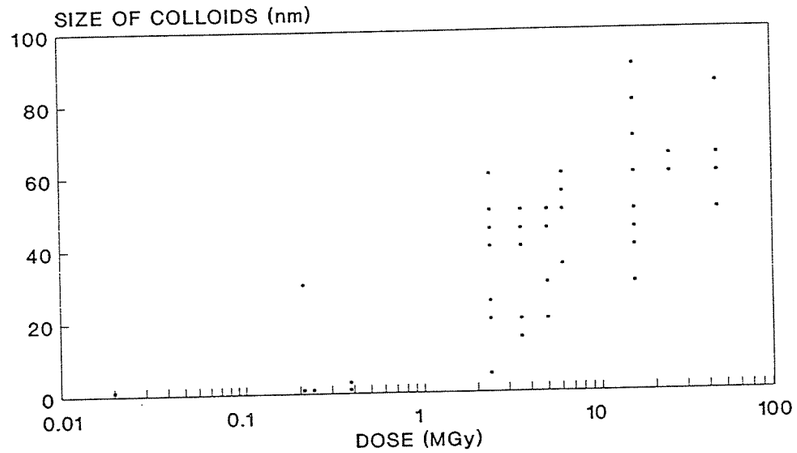


Figure 7: Size of colloidal sodium particles versus total dose for samples from GIF B-1 experiment.

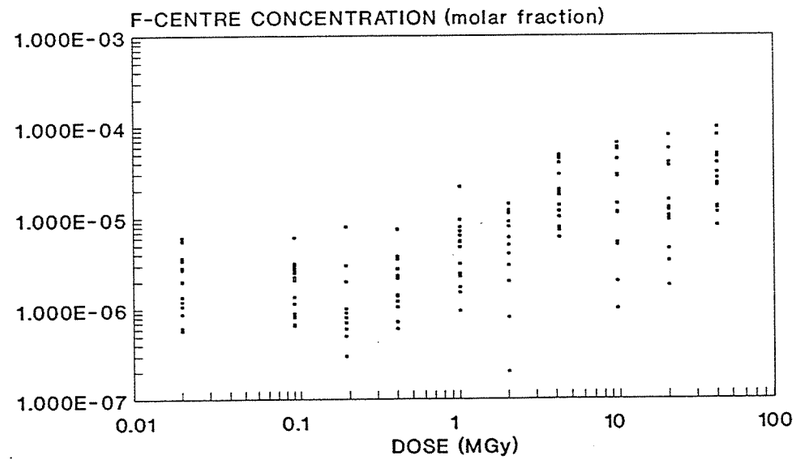


Figure 8: F-centre concentration versus total dose for samples from GIF B-2 experiment.

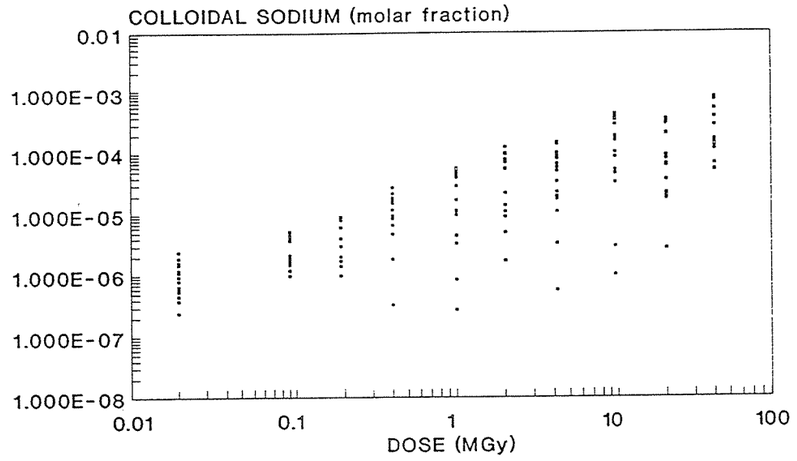


Figure 9: Colloidal sodium concentration versus total dose for samples from GIF B-2 experiment.

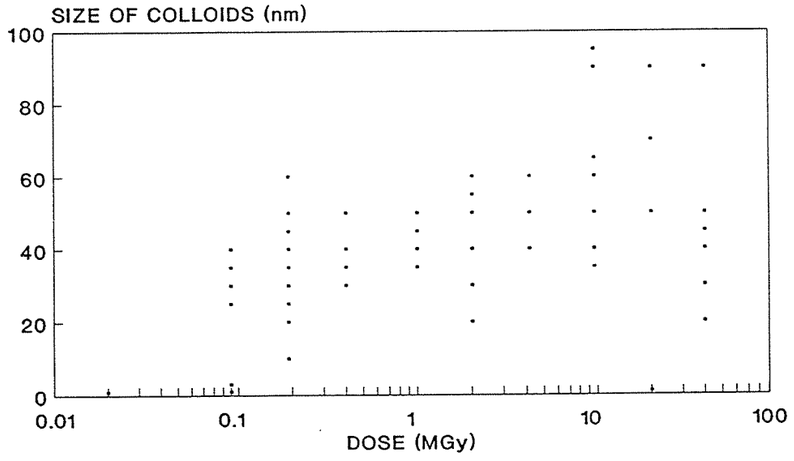


Figure 10: Size of colloidal sodium particles versus total dose for samples from GIF B-2 experiment.



total dose and the size of the colloidal particles is plotted.

It has been postulated by Van Opbroek and den Hartog (1985) that lower dose rates are more efficient in generating defects. Comparing absolute amounts of defects of the 15 kGy/h and 4 kGy/h experiments, the effect of dose rate in the efficiency in generating defects has been verified, although the concentrations are of the same order of magnitude. Although the amount of F-centre is one order of magnitude lower at 4 kGy/h for samples irradiated at doses below 2 MGy, at higher doses it is similar for both dose rates. In contrast, for colloidal sodium a slightly higher efficiency (2 or 3 times higher) at 4 kGy/h can be observed for the whole range of studied doses.

### 3.5 Microstructural observations

Microstructural observations were performed on samples from the GIF B-1 and GIF B-2 experiments with a transmitted light polarizing microscope. No microstructural changes were observed on samples of 20 kGy althought radiation induced defects (mainly F-centres) were generated. At doses between 110 and 430 kGy, samples show some light blue areas heterogenously distributed, which have colloidal sodium concentrations around $1.0 * 10^{-6}$ molar fraction. Nevertheless, it was observed that in rock salt having only hyaline halite grains (e.g. SP-800), the faintly blue areas are preferently related to the small grains, while the big grains remain uncoloured. At this dose range, which would represent the induction phase of radiation damage, not pressurized samples (brown-yellow colouration) exhibit higher amounts of F-centre and lower amounts of colloidal sodium than pressurized samples (pale blue colouration).

At doses ranging from 1.1 to 48 MGy, samples are dark blue decorated, having at least colloidal sodium concentrations of $10^{-5}$ molar fraction. Pressure enhances the generation of radiation induced defects at doses up to 5 MGy. Pressurized samples have between 1.5 and 2 times more sodium colloids than not pressurized, being F-centre concentration not affected by pressure. At doses between 5 and 48 MGy the effect of pressure in defect generation is unnoticeable.

Several microstructural features were visible because of difference in colouration, at doses higher than 1 MGy. These features mainly consist on: white colouration of subgrain boundary microstructures as well as white halos around fluid inclusions and polyhalite crystals, which are similar to those described by Urai et al. (1987), Holdoway (1974) and García Celma et al. (1988) respectively. The aforementioned features can represent an

important bleached zones, provided they are localized in certain grains.

The effect of fluid assisted recrystallization in the form of newly precipitated white halite crystals has also been observed in samples irradiated at doses higher than 1 MGy. These white crystals, free of damage, are the result of grain boundary migration asisted by fluids (García Celma et al. 1988). Solid impurities are rarely found around these white grains, which may act as physical barriers between the colloidal sodium and brine, thus hindering the dissolution-precipitation of halite. These new salt grains commonly contain biphasic fluid inclusions (gas and brine) as well as small rounded inclusions of hydrogen (2-3 μm in size). These grains tend also to grow by preserving at least two cubic faces of slow growth. In general, pressure enhances the neoprecipitation of halite.

In samples where high amounts of newly precipiteted halite were present (e.g. those irradiated under pressure at doses of 44 MGy and dose rate of 4 kGy/h; see figure 11), O.A spectra on white halite areas were performed. The spectra revealed that in those crystals no radiation-induced defects was present. This fact supports the hypothesis that precipitation of halite took place after irradiation stop and might be related either to the temperature decay (from 100°C to room temperature) and/or to the depressurization of the samples.

In the aforementioned samples, white halite grains were hand picked and high contents of $H_2$ (equivalent to $2 * 10^{-4}$ molar fraction of colloidal sodium) were measured. Blue halite grains of the same samples have colloidal sodium contents around $5 * 10^{-4}$ molar fraction. Since in the white halite crystals no radiation induced defects were detected, the measured $H_2$ has to be present as hydrogen inclusions. This $H_2$ comes from the reaction between colloidal sodium and water, indicating that the grain boundary of new salt grains migrated at the expense of former damaged rock salt, which had at least a molar fraction of colloidal sodium of $2 * 10^{-4}$. Since the measured amounts of $H_2$ in those samples is similar for the blue and white halite grains it can be concluded that most of the $H_2$ generated by the reaction of metallic sodium with brine is trapped in the neoprecipitated rock salt.

Quantification of the white halite fraction and the solid impurity content has also been performed. For samples having impuritiy contents higher than 2 %, the amount of white halite is below 1.5 % and usually related to subgrain boundary microstructures, and to the presence of white halos around fluid inclusions and polyhalite crystals. Nevertheless, for purer rock salt high amounts (up to 60 %) of white halite due to fluid assisted recrystallization has been measured (Figure 12). This means that this process may involve a substantial volume of the rock, wiping out the former accumulated defects.



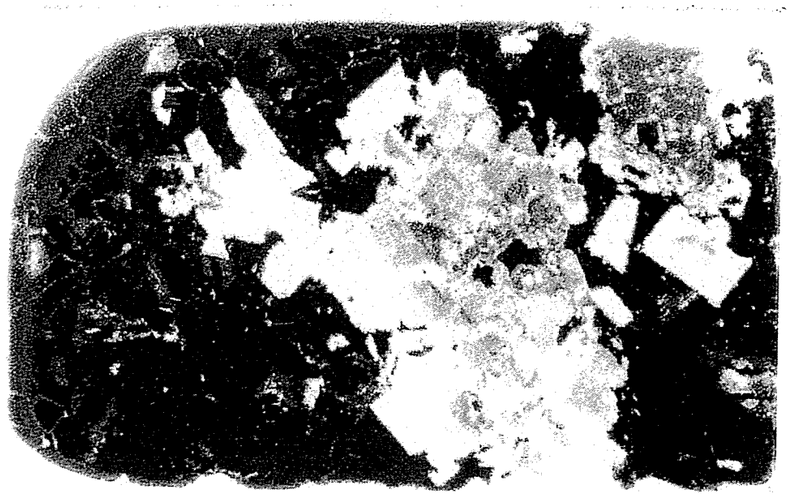

Figure 11: Transmitted light micrograph of the pressurized sample 40PLL irradiated to a dose of 44 MGy (dose rate 4 kGy/h). More than a half of the sample is represented by big crystals of new precipitated halite which tend to develope cubic faces. Long axis of the micrograph is 4 cm.

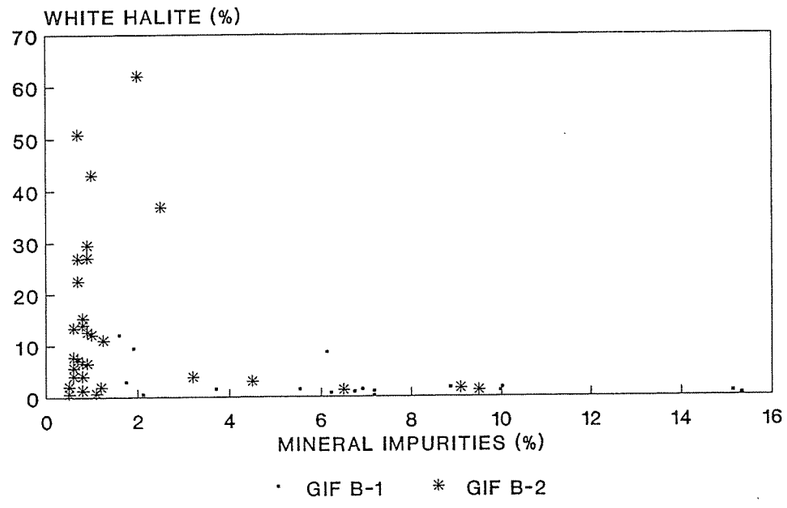


Figure 12: New precipitated white halite versus solid impurity content in irradiated rock salt.

## 3.6 Factors effecting the formation of radiation induced defects

In order to explain the relationships between the radiation-induced defects and the geological parameters, several Principal Component Analyses (PCA) using the correlation matrix were performed with the data from the GIF B-1 and GIF B-2 experiments. PCA is a statistical multivariate technique (Factor Analysis) which aims to explain the variability of a data set in terms of as few components (factors) as possible. The variables taken into account were: total dose, molar fraction of F-centre, molar fraction of colloidal sodium, size of colloids, confining pressure, as well as the amount of intergranular brine, and the contents of NaCl, $SO_4$, insoluble fraction, Ca, K, Mg and Sr.

The influence of total dose, confining pressure and brine content in the generation of colloidal sodium was checked in all the cylindrical samples (natural and synthetic). Six input variables were used in the analysis: total dose, molar fraction of F-centre, molar fraction of colloidal sodium, size of colloids, confining pressure and intergranular water content. The results of the Principal Component Analysis performed on samples from the GIF B-1 experiment are listed in Table 1. Similar results have been obtained for the samples of the GIF B-2 experiment.

The first component, which accounts for 50% of total variance, basically weights the contribution of total dose, and the amount of colloidal sodium and size of colloids, with intermediate loadings for the F-centres. Therefore the radiation-induced defects (molar fraction of F-centre, molar fraction of colloidal sodium and size of colloids) are the main parameter related to total dose. The contribution of intergranular water and confining pressure is negligible in this first component. The second and third components are not relevant in this context, reflecting respectively amount of water and pressurization.

The effect of pressure has been studied more in detail, by analyzing its effect in rock samples irradiated to the same total dose. Pressure has its influence in samples irradiated at doses up to 5 MGy, where pressurized samples exhibit more radiation induced defects than non pressurized samples. At higher doses the effect of pressure is negligible.

The influence of accesory minerals and trace elements in the radiation damage has also been analysed in a similar way. Thirteen input variables were used in the analysis: total dose, molar fraction of F-centre, molar fraction of colloidal sodium, size of colloids, confining pressure, and the contents in intergranular water, NaCl, $SO_4$, insoluble fraction, Ca, K, Mg and Sr. The results of the analysis performed on samples irradiated at the GIF B-1

Table 1: Composition of the first three Eigenvectors (Components) extracted from a data matrix of 6 variables and 84 irradiated rock salt samples in the GIF B-1 experiment.

| | COMPONENT 1 | COMPONENT 2 | COMPONENT 3 |
|---|---|---|---|
| DOSE | 0.94 | -0.09 | -0.01 |
| F CENTER | 0.69 | 0.21 | -0.14 |
| PRESSURE | 0.12 | 0.61 | 0.78 |
| SIZE COL. | 0.92 | -0.16 | 0.01 |
| COL. NA | 0.85 | -0.07 | 0.08 |
| IG. BRINE | 0.10 | 0.79 | -0.55 |
| TOTAL VARIANCE | 50.0 % | 18.0 % | 15.8 % |

Table 2: Composition of the first three Eigenvectors (Components) extracted from a data matrix of 13 variables and 61 irradiated natural rock salt samples in the GIF B-1 experiment.

| | COMPONENT 1 | COMPONENT 2 | COMPONENT 3 |
|---|---|---|---|
| DOSE | 0.67 | -0.67 | 0.13 |
| F CENTER | 0.65 | -0.31 | 0.38 |
| PRESSURE | 0.24 | -0.01 | 0.14 |
| SIZE COL. | 0.69 | -0.60 | 0.15 |
| COL. NA | 0.68 | -0.63 | 0.18 |
| IG. BRINE | 0.04 | 0.20 | 0.36 |
| NACL | -0.81 | -0.48 | 0.12 |
| S04 | 0.75 | 0.54 | 0.22 |
| INSOLUBLE | 0.72 | 0.35 | -0.34 |
| CA | 0.58 | 0.47 | 0.38 |
| K | 0.51 | -0.05 | -0.80 |
| MG | 0.45 | -0.07 | -0.74 |
| SR | 0.38 | 0.57 | 0.22 |
| TOTAL VARIANCE | 35.6 % | 20.0 % | 15.1 % |



experiment (dose rate of 15 kGy/h) are listed in Table 2. Similar results have been obtained for the samples of the GIF B-2 experiment (dose rate of 4 kGy/h).

For the first component, which accounts for 36% of total variance, radiation damage shares positive loadings with dose and impurity content. NaCl has negative loadings in this component. The second and third components are not relevant in the context of radiation damage, since they show the presence of celestite and the absence of polyhalite in the studied samples respectively. Since the chemical data reflect the mineralogical composition of the sample, the results of PCA show the influence of the amount of mineral impurities in the rock salt in the formation of radiation induced defects. Similar results have been obtained in a subset of natural non bearing polyhalite rock salt (PLL and BHA), since the presence of polyhalite as mineral impurity enhances the content of K and Mg interstitial ions.

## 4. DISCUSSION

### 4.1 Maximal expected damage at the repository

In order to use the experimental results for modelling or prediction at a real repository, one must be aware of the existence of uncertainties which arise from the limited understanding of the radiation damage process. The experimental data have shown the amount of radiation defects is strongly dose dependent. At doses below 10 MGy F-related centres, and one size of colloidal sodium particles are present. At doses between 10 and 50 MGy a second population of colloidal sodium may be present. At doses higher than 100 MGy colloidal sodium particles of sizes ranging between 2 and 150 nm are present.

In all the experiments there is a log-linearity of the amount of radiation induced defects vs. total dose. After reaching a dose of 300 MGy, a decreasing efficiency in generating defects is observed. In the range between 20 and 50 MGy, where the amount of defects has been measured for three diferent dose rates, a change in the efficiency in generating defects has been noted, although their concentration are of the same order of magnitude. Variable dose rate samples (GIF A-2) show 2 times less quantity of defects with regard to the ones of the 15 kGy/h irradiation (GIF B-1), which are also lower (2 or 3 times) with respect to the ones of the 4 kGy/h irradiation (GIF B-2).

An extrapolation of the experimental data with relative high dose rate and temperature of 100 °C to those to be present at a real repository after the first few hundred years (dose rates of 0.1 kGy/h, and probably higher temperatures) should be handled with caution. In addition, the amount of the defects is also governed by the composition of the rock salt, and can vary on one order of magnitude for the same absorbed dose. The effect of recrystallization, which in real repository would have more time to develop, and the fact that we could not observe the effect of back reactions at the early stage could give an erroneus idea of the understanding of the radiation damage process.

Despite these constraints, and since from the available laboratory measurements a probability density function could be defined, in the experiments GIF B-1 and GIF B-2 a probabilistic approach appeared to be the most suitable method for determining the damage which could be expected under these conditions in a repository. The Tchebychev theorem was used to compute the confidence interval for each dose, following the PAGIS methodology (Storck *et al.*, 1988), since the distribution of the amount of defects does not follow a gaussian curve.

The results of the analysis performed on both F-centres and colloidal sodium amount are summarised in Table 3 for the GIF B-1 experiment and in Table 4 for the GIF B-2 experiment. In each table the 50th percentile risk (mean value) and the 95th percentile risk for each total dose are listed. According to Bergsma *et al.*, (1985) and depending on several disposal strategies, the maximum dose for a 0.5 cm thick region in contact with the container over a 100,000 year period would range between 250 and 400 MGy. The different total doses would depend on specific waste parameters such as container diameter, container thickness and temperature. In both cases (GIF B-1 and GIF B-2 experiments), for F-centre the 95th percentile risk varies between $10^{-5}$ and $10^{-4}$. The extrapolation of these data to doses up to 400 MGy, leads us to expect the maximum value of F-centres around $10^{-4}$. For colloidal sodium, also in both experiments, the 95th percentile risk follows a quasilinear trend ranging between $10^{-6}$ and $10^{-3}$. The extrapolation to doses up to 400 MGy leads us to expect a maximum value of colloidal sodium below 1 %.

## 4.2 Comparison between experimental data with the Jain Lidiard model

The results obtained in terms of 50th and 95th percentile for both F-centre and colloidal sodium were compared with the values obtained with the extended version developed by Groote and Weerkamp (1990) of the Jain-Lidiard model. The results are plotted in figures 13 and 14 for the GIF B-1 experiment and in figures 15 and 16 for the GIF B-2



Table 3: Expected concentrations of F-centre and colloidal sodium for several doses (50th and 95th Percentile) for the GIF B-1 experiment.

| DOSE | F-CENTER | | COLLOIDAL SODIUM | |
|---|---|---|---|---|
| (MGy) | 50TH PC | 95TH PC | 50TH PC | 95TH PC |
| 0.02 | 1.1E-5 | 2.2E-5 | 3.1E-7 | 6.3E-7 |
| 0.23 | 4.5E-6 | 9.6E-6 | 1.6E-6 | 4.3E-6 |
| 0.26 | 1.4E-5 | 1.5E-5 | 1.0E-6 | 1.9E-6 |
| 0.42 | 1.1E-5 | 2.1E-5 | 4.1E-6 | 8.9E-6 |
| 2.61 | 5.7E-6 | 1.1E-5 | 2.6E-5 | 5.1E-5 |
| 3.91 | 1.3E-5 | 2.8E-5 | 3.5E-5 | 6.1E-5 |
| 5.47 | 2.3E-5 | 4.3E-5 | 7.2E-5 | 1.4E-4 |
| 6.95 | 2.1E-5 | 3.7E-5 | 9.3E-5 | 1.4E-4 |
| 16.00 | 4.8E-5 | 8.7E-5 | 2.0E-4 | 3.8E-4 |
| 24.00 | 3.4E-5 | 5.0E-5 | 1.8E-4 | 2.6E-4 |
| 44.65 | 5.3E-5 | 8.3E-5 | 3.2E-4 | 4.9E-4 |

Table 4: Expected concentration of F-centre and colloidal sodium for several doses (50th and 95th Percentile) for the GIF B-2 experiment.

| DOSE | F-CENTER | | COLLOIDAL SODIUM | |
|---|---|---|---|---|
| (MGy) | 50TH PC | 95TH PC | 50TH PC | 95TH PC |
| 0.02 | 2.5E-6 | 4.7E-6 | 9.6E-7 | 1.7E-6 |
| 0.10 | 1.7E-6 | 2.7E-6 | 2.6E-6 | 4.2E-6 |
| 0.21 | 1.5E-6 | 3.8E-6 | 4.1E-6 | 7.0E-6 |
| 0.44 | 2.3E-6 | 4.3E-6 | 1.2E-5 | 2.1E-5 |
| 1.10 | 6.0E-6 | 1.2E-5 | 3.0E-5 | 5.4E-5 |
| 2.22 | 7.6E-6 | 1.3E-5 | 5.6E-5 | 1.0E-4 |
| 4.60 | 2.3E-5 | 4.0E-5 | 6.7E-5 | 1.9E-4 |
| 10.66 | 3.0E-5 | 5.7E-5 | 2.0E-4 | 3.6E-4 |
| 22.70 | 1.9E-5 | 4.7E-5 | 1.1E-4 | 2.5E-4 |
| 44.01 | 3.4E-5 | 6.4E-5 | 2.7E-4 | 5.6E-4 |

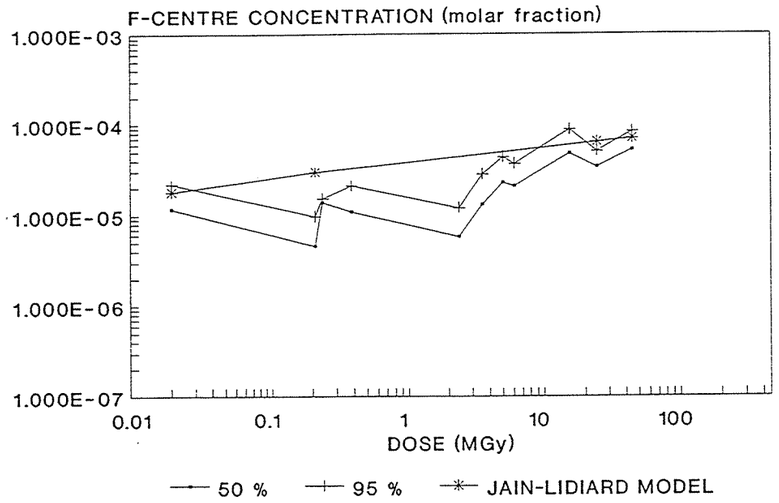


Figure 13: Comparison of the expected concentration of F-centre (50th and 95th Percentile) and the Jain-Lidiard simulation for several doses in the GIF B-1 experiment.

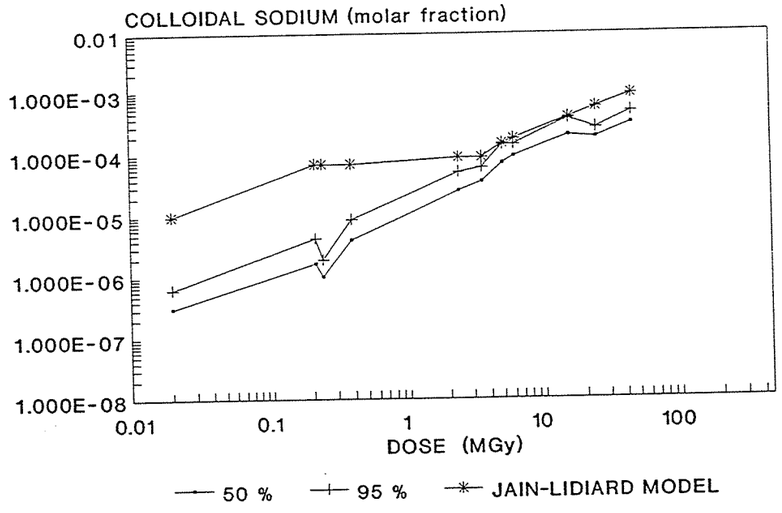


Figure 14: Comparison of the expected colloidal sodium concentration (50th and 95th Percentile) and the Jain-Lidiard simulation for several doses in the GIF B-1 experiment.



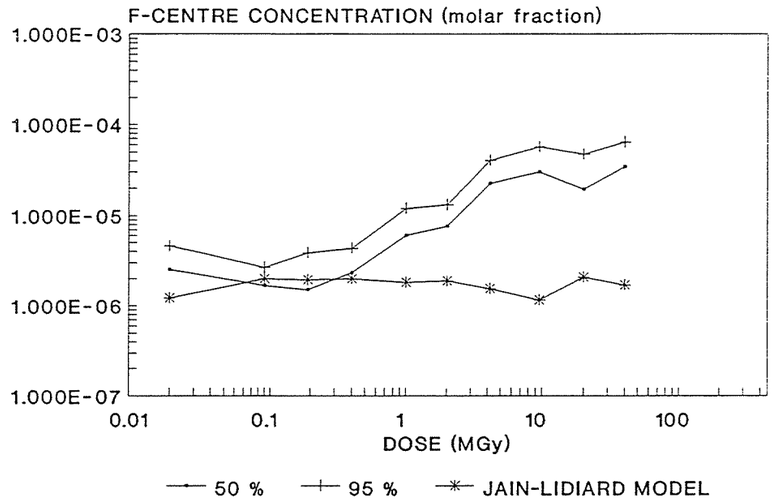


Figure 15: Comparison of the expected F-centre concentration (50th and 95th Percentile) and the Jain-Lidiard simulation for several doses in the GIF B-2 experiment.

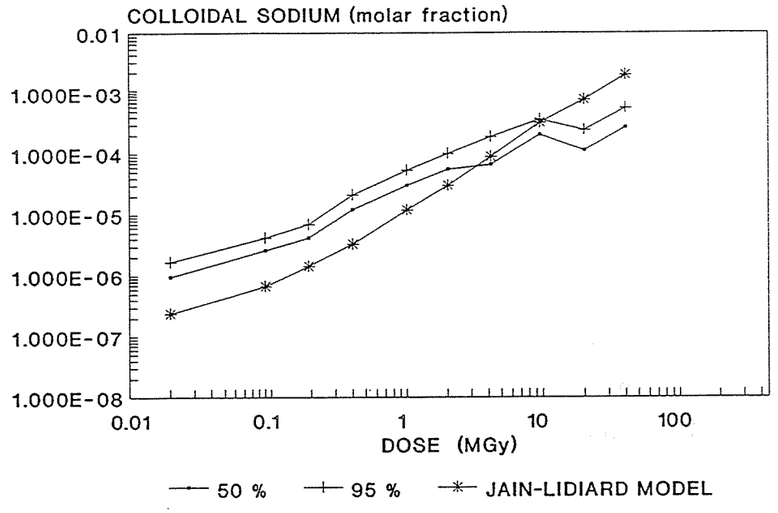


Figure 16: Comparison of the expected colloidal sodium concentration (50th and 95th Percentile) and the Jain-Lidiard simulation for several doses in the GIF B-2 experiment.

experiment respectively.

For the samples irradiated at a dose rate of 15 kGy/h, the 95th percentile of the measured F-centre is of the same order of magnitude than predicted by the Jain-Lidiard simulation. For colloidal sodium, at low doses (smaller than 3 MGy) the Jain Lidiard simulation gives values of one order of magnitude higher than the 95th percentile, while in contrast at higher doses both values tend to converge. However, it is worth noting that the simulation still gives higher values than the 95th percentile risk.

For the samples irradiated at a dose rate of 4 kGy/h, at doses up to 500 kGy, the 50th percentile of the measured F-centre is similar to the predictions of the Jain-Lidiard simulation. At higher doses, the 50th percentile of the measured F-centre is between one and two orders of magnitude higher than the Jain-Lidiard simulation. For colloidal sodium, at low doses (smaller than 2 MGy) the Jain Lidiard simulation gives values of an order of magnitude lower than the 95th percentile, while in contrast at higher doses both values tend to converge. At doses of 22 and 44 MGy, the simulation gives higher values than the 95th percentile which is explained by the extensive recristallization phenomena.

The obtained results focus that reliable predictions on the generation of colloidal sodium for doses higher than 5 MGy, can be obtained with this version of the Jain-Lidiard model. In contrast, F-centres are not accurately predicted. Nevertheless, and regarding safety relevant aspects of radiation damage, this model has proven its efficacy for the dose rates and temperatures used in the experiments. However, it should be further validated at other temperatures and realistic dose rates.

## 5. CONCLUSIONS

Laboratory irradiations at a temperature of 100ºC and several dose rates (variable dose rate between 200 and 20 kGy/h and constant dose rates of 15 and 4 kGy/h) have enabled the study of the radiation damage on several types of rock salt. The analyses take into account the concentration of radiation-induced defects in relation with dose, dose rate and the geological characteristics of the host rock.

In general, there is a good correlation between the two methods of determining radiation damage, yielding results of the same order of magnitude, except for samples irradiated at doses higher than 100 MGy. In those samples, and due to the complexity of the Optical absorption spectra, hydrogen measurements give a better resolution. Hydrogen



measurements are a very fast method of determining the colloidal sodium amount, but do not quantify other colour centres developed by irradiation. In contrast, Optical absorption is very time consuming.

The amount of F-centres as well as the amount of colloidal sodium increases log-linerily with increasing total dose. The concentration of colloidal sodium is very sensitive to the absorbed dose at doses up to 300 MGy. At higher doses (up to 1154 MGy) a decreasing efficiency in generating colloidal sodium particles is observed. The amount of F-centres increases not so sensitively reaching the steady state at a molar fraction of $4 * 10^{-4}$.

Another notable trend is that colloidal particle size grows with increasing dose. In samples irradiated at doses higher than 10 MGy, two populations of colloids may coexist: small colloids (about 5 nm diameter) and large colloids (between 80 and 90 nm diameter). At doses higher than 100 MGy, after reaching a colloidal sodium concentration of $10^{-3}$ the size of the particles ranges between 2 and 150 nm.

Comparing radiation damage between pure monocrystals and natural rock salt, the radiation damage in monocrystals is one order of magnitude less than in rock salt. This fact is explained by the low dislocation and impurity concentration of pure monocrystals and therefore they can not easily nucleate colloids. Despite its lower amount of colloidal sodium particles, their size is around 90 nm independently on the absorbed dose.

The effect of dose rate is also responsible of variations in the amount of defects for samples irradiated at the same total dose. Low dose rates shows a slightly higher efficiency in generating defects, althought their concentrations are of the same order of magnitude.

For samples of the same type and irradiation conditions the amount of measured defects is widely scattered (on one order of magnitude). Geochemical parameter intrinsic of the rock salt are more important in the generation of the radiation induced defects than the effect of the different studied dose rates. The mineralogical impurity of the rock salt enhances the development of radiation induced defects. Therefore, mineralogically pure rock salt formations may be more suitable to host radiactive waste than impure rock salt. This information can be very helpful in site characterization. In contrast, the influence of brine content in radiation damage is weak.

White halite (free of radiation induced defects) formed by grain boundary migration assisted by fluids has been extensively recognized in natural rock salt from GIF B-1 and GIF B-2 experiments. This process can be very important in pressurized and pure samples (halite content higher than 98 %). These white crystals commonly contain small hydrogen inclusions. Hidrogen is the product of the reaction between former halite grains, which had already developed colloids and intergranular brine. The major part of the $H_2$ generated in the reaction is trapped in the neoprecipitated halite, giving smaller releases of $H_2$ than expected in the repository. Since no radiation induced defects were detected in the white halite it has to be concluded that grain boundary migration took place after irradiation stop and therefore related to temperature and/or pressure decay.

It should be taken into account that for doses higher than 5 MGy, the amount of colloidal sodium obtained by the Jain-Lidiard simulation are slightly higher than the 95th percentile of risk based on the experimental results. However, extrapolations to repository conditions should be made after performing irradiation experiments at doses up to 5-10 MGy with realistic dose rate and temperature, in order to asssure that the emplacement of waste will not threaten the long-term safety of the repository.

ACKNOWLEDGEMENTS

The work reported here has been performed on behalf of ENRESA under contract No 70.2.3.13.03. We are indebted to Mr. J.M. Grosso and Ms. P. Teixidor from the LIFS for their assisstance at the laboratory. We make extensive our recognition to Dr. X. Dies of the Dept. d' Enginyería Nuclear de la Universitat Politècnica de Catalunya (UPC), who kindly performed the Jain-Lidiard simulations.



## 6. REFERENCES

BERGSMA, J., HELMHOLDT, R.B. and HEIJBOER, R.J, 1985: *"Radiation dose deposition and colloid formation in a rock salt waste repository"*, Nucl. Technology, **71**, 597-607

DALE COMPTON, W., 1957: *"Production of colloidal sodium in NaCl by ionizing radiation"*, Phys.Rev., **107**, 1271-1276

HOLDOWAY, K.A., 1974: *"Behaviour of fluid inclusions in salt during heating and irradiation"* in "Fourth Symp. on Salt. North. Ohio Geol. Soc.", 303-312

GARCIA CELMA, A., URAI, J.L. and SPIERS, C.J., 1988: *"A laboratory investigation into the interaction of recrystallization and radiation damage effects in polycrystalline salt rocks"*, Nuclear Science and Technology, EUR 11849 EN, 125p

GROOTE, J. and WEERKAMP, H.R., 1990: *"Radiation damage in NaCl; small particles"*, Ph.D. Thesis, Univ.Groningen, 270p

HODGSON, E.R., DELGADO, G. and ALVAREZ RIVAS, J.L., 1979: *"In-beam studies of M-centre production processes in NaCl"*, Jour.Phys. C: Sol.Sta.Phys., **12**, 1239-1244

HUERTAS, F., MAYOR, J.C. and DEL OLMO, C., 1992: *"Textural and Fluid Phase Analysis of Rock Salt subjected to the combined effects of Pressure, Heat and Gamma Radiation"*, Nuclear Science and Technology, EUR 14169 EN, 218p

IKEDA, T. and YOSHIDA, S., 1967: *"Effect of divalent cation impurities on the formation and bleaching of colloids in NaCl"*, Jour.Phys.Soc.Jap., **22**, 138-143

JAIN, U. and LIDIARD, A.B., 1977: *"The growth of colloidal centres in irradiated alkali halides"*, Phil.Mag., **35**, 245-259

JENKS, G.H. and BOPP, C.D., 1974: *"Storage and release of radiation energy in salt in radioactive waste repositories"*, ORNL-TM-4449, 77p

JENKS, G.H., SONDER, E., BOPP, C.D., WALTON, J.R. and, LINDEBAUM, S., 1975: *"Reaction products and stored energy released from irradiated sodium chloride by dissolution and by heating"*, Jour. Phys. Chem., **79**, 871-875

LEVY, P.W., 1983: *"Radiation damage on natural rock salt from various geological localities of interest to the radioactive waste disposal program"*, Nucl. Technology, **60**, 231-243

LEVY, P.W. and KIERSTEAD, J.A., 1984: *"Very rough preliminary estimate of the sodium metal colloid induced in natural rock salt by the radiations from radioactive waste canisters"*, Mat.Res.Soc.Symp.Proc., **26**, 727-734

MARKHAM, J.J., 1966: *"F-Centres in Alkali Halides"*. Academic Press Inc. 400p

MÖNIG J., GARCIA CELMA A., HELMHOLDT R.B., HINSCH H. HUERTAS F. and PALUT J.M., 1990: *"The HAW Project: Test disposal of high-level waste in the Asse salt mine. International test-plan for irradiation experiments"*, Nuclear Science and Technology EUR 12946 EN, 76p

PRZIBRAM, K., 1956: *"Irradiation colours and luminiscence; a contribution to mineral physics"*, Pergamon Press, 332p

SCHULZE, O., 1986: *"Der Einfluss radioaktiver Strahlung auf das mechanische Verhalten von Steinsalz"*, Z.dt.geol.Ges., **137**, 47-69

SMITHARD, M.A. and TRAN, M.Q., 1974: *"The optical absorption produced by small sodium metal particles in sodium chloride"*, Helv.Phys.Acta, **46**, 869-888

STORCK, R., ASCHENBACH, J., HIRSEKOM, R.P., NIES, A. and STELTE, N., 1988: *"Performance Assessment of Geological Isolation Systems for Radioactive Waste: Disposal in Salt formation"*, Nuclear Science and Technology, EUR 11778 EN, 788p

URAI, J.L.; SPIERS, C.J.; PEACH, C.J.; FRANSSEN, R.C.M.W. and LIEZENBERG, J.L., 1987: *"Deformation mechanisms operating in naturally deformed halite rocks as deduced from microstructural investigations"*, Geol.Mijn., **66**, 165-176

VAN OPBROEK, G. and DEN HARTOG, H.W., 1985: *"Radiation damage of NaCl: dose rate effects"*, Jour.Phys. C: Sol.Sta.Phys., **18**, 257-268



# COLLOID FORMATION AND STORED ENERGY DEPOSITION IN IRRADIATED NATURAL ROCK SALT SAMPLES

**J. Mönig, N. Jockwer, H. Gies**

## ABSTRACT

The temperature dependence of the radiation-induced formation of colloidal sodium, molecular chlorine gas and the associated deposition of energy in rock salt was determined between 100 °C and 250 °C. At each temperature the irradiation dose was varied between $10^6$ and $10^8$ Gy. After irradiation, the colloidal sodium content was measured via hydrogen evolution upon dissolving the salt in water. The amounts of chlorine gas were determined both in the gas phase above the salt and in the bulk of the sample. Stored energy was determined by DSC on selected halite specimens. The present study confirms the equivalence of the radiation-induced formation of the different products, i.e. colloidal sodium, molecular chlorine, and stored energy, over a substantial dose range and temperature range. The chosen range is of interest for radioactive waste repositories. From the data obtained it is concluded, that at temperatures above 150 °C, colloid formation starts to saturate with increasing dose. At 100 °C about 0.7 mol % sodium were detected for $10^8$ Gy but no saturation was indicated. Most of the molecular chlorine is found, after irradiation, inside the salt crystals of the bulk sample, but chlorine evaporation from the salt increases with increasing temperature. The stored energy follows the trends outlined for the molecular radiation products, i.e. it increases with dose. A conversion factor of about 70 J/g per mol % colloidal sodium in the rock salt is found by us. This value is lower than that proposed by Groote and Weerkamp of 125 J/g per mol % colloidal sodium [Groote and Weerkamp, 1990]. The reason for this difference is explained by Donker et al. [Donker et al., 1995 (article nr. 19, this volume)]. They obtained a value for the equivalence of stored energy and colloid content that is much nearer to one obtained by us than to that of Groote and Weerkamp. The influence of sulfate-containing minerals as anhydrite and polyhalite on the formation of radiation damage and stored energy was investigated but the present data do no allow to derive any final conclusion.

## 1. INTRODUCTION

Gamma irradiation of rock salt leads via a complex reaction scheme to radiation damage with accumulation of colloidal sodium and chlorine gas in the sodium chloride lattice (see for example [Hughes, 1983, Hobbs, 1973]). The formation of the irradiation products is associated with the storage of energy. In order to evaluate the long-term safety of a radioactive waste repository in rock salt, among other things quantitative information regarding the amount of radiation damage is required.

The formation of radiation defects depends on the following parameters: total dose, dose rate, temperature, microstructure of the salt, and the level of impurities. This has been the subject of numerous studies in the past (for an overview see [Gies et al., 1994]). In most of these studies, however, the radiation-induced formation of only one of the irradiation products was determined. Exceptions are the investigations of Jenks et al. [Jenks and Bopp, 1974, 1977, Jenks et al., 1975] and of Groote and Weerkamp [Groote and Weerkamp, 1990], but in these studies the temperatures were below 150 °C. Also, in many studies only fairly low radiation doses were employed at which the coagulation of radiation products has just begun. Extrapolation from these values to the conditions in a repository is, at its best, questionable.

There was a lack of data regarding chlorine development and its correlation with both sodium colloid development and stored energy deposition in NaCl, at least for the temperatures and total doses relevant for radioactive waste repositories. We have filled in this gap by irradiating samples in the temperature region above 150 °C, measuring the stored energy deposited and determining chemically the amounts of molecular chlorine and of sodium colloids in the same samples. Moreover, in order to allow comparison with previous research, the same experiments and measurements have also been performed at temperatures lower than 150 °C. The results of these investigations are presented here. The experimental methodologies are described in detail elsewhere [Mönig et al., 1995 (article nr. 8, this volume)].

## 2. RESULTS

The γ-radiation-induced generation of colloidal sodium depends strongly both on dose and temperature. This is shown in Fig. 1, which presents the data obtained for irradiations at temperatures of 100 °C, 150 °C, 200 °C, and 250 °C, respectively. The data points obtained from high dose irradiations have all been set to 100 MGy. This dose value was estimated from recorded decay curves for the gamma intensity of the spent fuel elements, since the solid state



dosimeters were not calibrated for such high dose ranges at the temperatures being used. Therefore, the deviations of the dose values from 100 MGy are not exactly known, but are expected to be within 30% of this value.

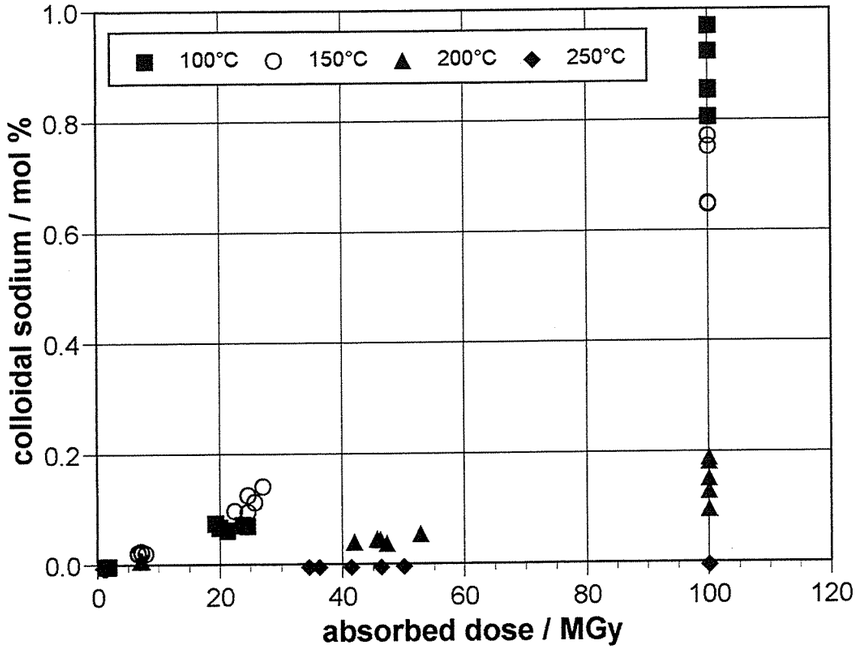


Figure 1: *Yield of colloidal sodium vs. irradiation dose in rock salt samples γ-irradiated at various temperatures*

Significant colloid formation is observed at temperatures of 100°C and 150°C, while only small amounts of colloids are produced at 200°C and hardly any colloid formation is found at 250°C (less than 0,003 mol % Na). At the latter temperature saturation in radiation damage is clearly observed. However, no saturation is indicated at 100°C and 150°C, while intermediate behavior is seen for 200°C.

The formation of molecular chlorine in these γ-irradiated rock salt samples depends also on dose and temperature (see Fig. 2). The total chlorine yields are given in Fig. 2. It was found that a small portion of the chlorine gas is released from the salt samples already during the irradiation and, thus, is found in the gas phase. The relative portion of chlorine gas released from the samples during irradiation increases with temperature. The corresponding data for

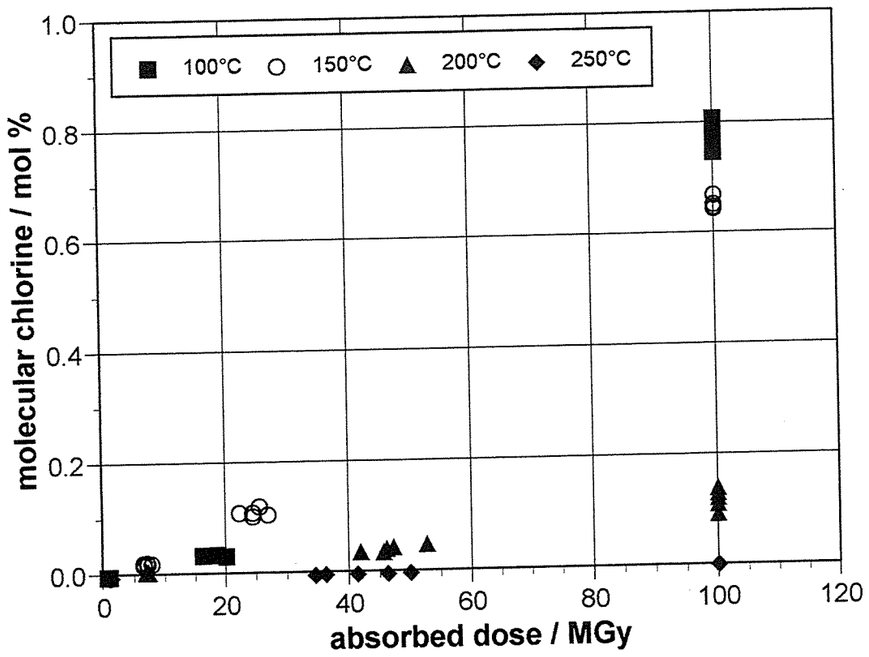


Figure 2: *Yield of molecular chlorine vs. irradiation dose in rock salt samples γ-irradiated at various temperatures*

high dose irradiations (duration 80 days, dose about 100 MGy) under helium are given in Table 1. At temperatures of 150 °C and lower, only insignificant amounts of chlorine were released during the experiment. However, it is conceivable, that the portion of chlorine gas being released from the salt increases with time. Since diffusion is slow and is often a temperature-activated process, at lower temperatures chlorine gas requires more time to diffuse through the crystal to the crystal's surface than at higher ones.

Table 1: *Relative portion and absolute chlorine yield released from rock salt during irradiation (duration 80 days, dose about 100 MGy, helium atmosphere)*

| irradiation temperature [°C] | relative portion in gas phase [%] | absolute amount in gas phase [mol/kg] |
|---|---|---|
| 100 °C | 0.003 | 0.0045 |
| 150 °C | 0.007 | 0.008 |
| 200 °C | 0.16 | 0.04 |
| 250 °C | 4.0 | 0.0045 |



As expected, the gas atmosphere during irradiation has neither an influence on the colloids yield nor on the chlorine yields. Identical results are obtained both for irradiations carried out in a nitrogen/oxygen (80/20 v/v) atmosphere and for irradiations carried out in a helium atmosphere (data not shown).

From the current understanding of the interaction of ionizing radiation with sodium chloride follows, that the γ-radiation-induced formation of metallic (colloidal) sodium is accompanied by the formation of equal amounts (on a molar basis) of molecular chlorine. Thus, plotting the chlorine yields versus the colloidal sodium yields should give a straight line with slope 1, irrespective of irradiation temperature, dose, and dose rate. This has indeed been observed in all our experiments (Fig. 3). Nonetheless, a small deviation from the expected straight line is apparent. In most cases, slightly lower chlorine yields than colloid yields are obtained. The deviation from the straight line increases at lower absolute yields. However, this finding does not invalidate the theoretical picture of radiation damage formation. It is rather attributed to small chlorine losses during the detection procedure, which inevitably occur even though extreme care has been taken in handling and preparing the equipment used. The scatter at very low yields (i.e. data for low dose irradiations and/or high temperatures) is most likely due to a decrease in the measuring accuracy as the lower detection limits of the hydrogen and hypochloride detection are approached.

The stored energy was measured in some of the samples. The available data are shown in Fig. 4 versus the amount of colloidal sodium detected in the same samples. Interestingly, no stored energy could be measured in samples irradiated at 200°C (triangles in Fig. 4), even though both colloidal sodium and molecular chlorine were clearly detected. This could be due to the low heating rate of 1 K/min that was employed in the DSC-measurements. The energy release peak is very broad under these conditions and may not be discernible from the baseline with its noise. In order to test this hypothesis, some of these measurements are being repeated at much higher heating rates, but the data are not yet available.

The two lines in Fig. 4 represent conversion factors between stored energy and the amount of colloidal sodium, that are published in the literature. The upper line corresponds to a conversion factor of 125 J/g stored energy per mol % colloidal sodium in rock salt. This number was taken from Groote and Weerkamp [Groote and Weerkamp, 1990]. The lower line corresponds to a value of 70 J/g stored energy per mol % colloidal sodium, that was derived by Jenks et al. [Jenks et al., 1975]. Clearly all our data fall close to the latter value.

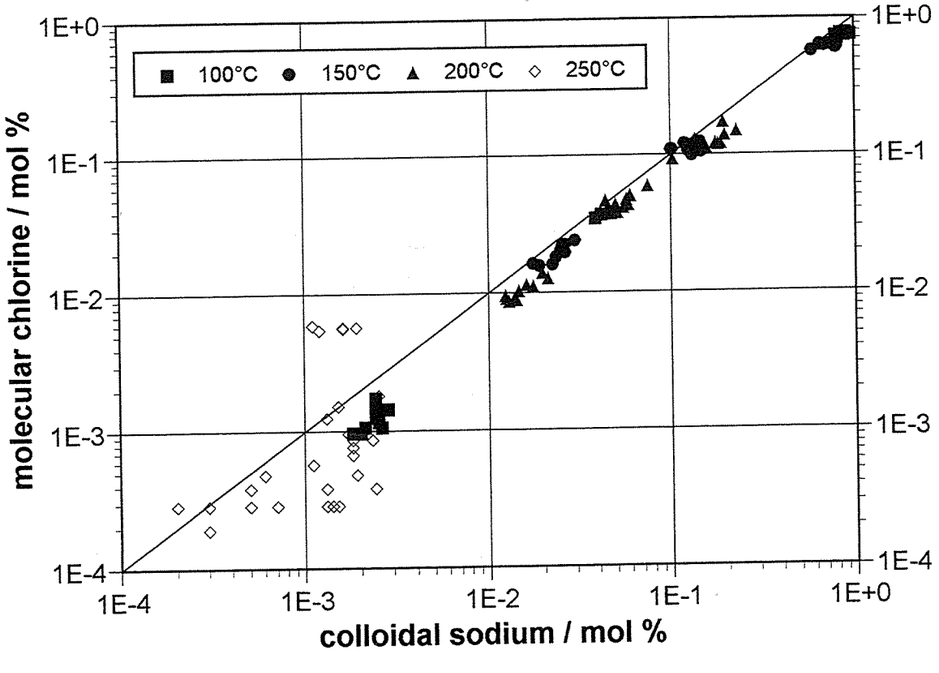


Figure 3: *Yields of colloidal sodium vs. yields of molecular chlorine. Each data point corresponds to different irradiation conditions. The range of irradiation conditions was: temperatures 100 - 250 °C, dose 1 - 100 MGy, dose rate varied between 240 and 40 kGy/h during the irradiation.*

Each data point in Fig. 4 represents the average of three independent DSC-measurements. In some cases it was observed that the individual results varied considerably (up to 40 %). Two reasons are conceivable for this finding:

Firstly, it could be due to the small rock salt specimens used in the DSC-measurements being different in their mineralogical composition from the bulk of the sample. As a rule, Asse rock salt consists of ~ 95 % halite and ~ 5 % of sulfates. Of the latter particularly the mineral anhydrite is known to be a very capable dosimeter material for ionizing radiation. It is expected, therefore, to contribute to the energy storage in rock salt, although it is not known to what extent. Generally, it is observed that the yield of the radiolysis mechanism in ionic crystals depends inversely on the charge of the ions. Thus, stored energy is expected to reach lower values in anhydrite and polyhalite than in halite. If the small specimens contain more sulfate minerals than the bulk, therefore, a lower value for the stored energy may be expected. Dehydration



of polyhalite is not the reason for these differences because the method used to determine the stored energy already takes it into account [Mönig et al., 1995 (article nr. 8, this volume]).

Secondly, the sample crystals being used in the measurements could have received significantly different radiation doses. The half-thickness of rock salt for γ-quanta from spent fuel elements (energy of several hundred keV) is about 30 - 40 mm. The diameter of the irradiation ampoule is 49.9±0.1 mm. Therefore, crystals lying at the perimeter of the ampoule have received a dose which is about 50 - 60 per cent higher compared to crystals which are located near the middle axis. These differences in dose are averaged out in the determination of colloidal sodium and molecular chlorine, as big sample volumes are used in these measurements. For DSC-measurements, on the contrary, only a few crystals are used, so that it is quite possible that no representative subsample was taken. Unfortunately this situation can not easily be avoided.

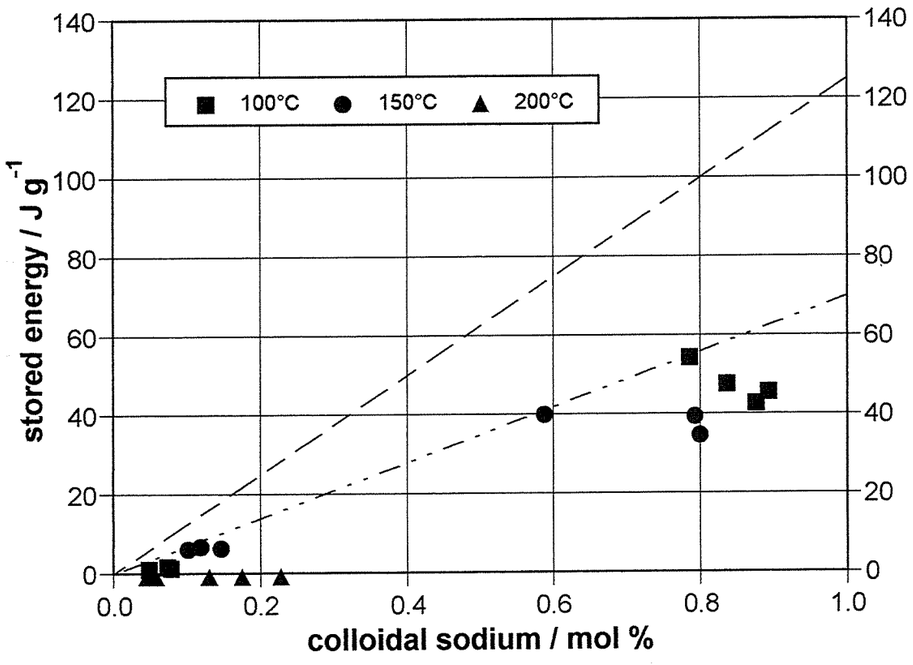


Figure 4: *Yield of colloidal sodium vs. stored energy for different irradiation temperatures (the broken line (upper line) reflects a conversion factor of 125 J/g stored energy per mol % colloidal sodium, while the dashed one corresponds to 70 J/g per mol % Na).*

The salt samples used in the DSC-measurements were chemically analyzed afterwards and their individual polyhalite and anhydrite content was calculated on the basis of elemental analyses. In order to find out whether the content of sulfate-containing minerals in the samples has an effect on the amount of stored energy, the individual results for two different sample series with identical irradiation history (100 MGy at 100°C and 100 MGy at 150°C) are listed in Table 2. Clearly, from these data no correlation between the amount of stored energy and the content of sulfate-containing minerals can be derived.

Table 2: *Results of the DSC measurements in individual subsamples and their respective anhydrite and polyhalite content.*

| irradiation conditions | subsamples for DSC | anhydrite [mg /kg] | polyhalite [mg / kg] | stored energy [J / g] |
|---|---|---|---|---|
| sample 101<br>100°C, 100 MGy | subsample 1<br>subsample 2<br>subsample 3 | 5583<br>3870<br>6046 | 1205<br>2131<br>1884 | 84,1<br>45,5<br>35,6 |
| sample 103<br>100°C, 100 MGy | subsample 1<br>subsample 2<br>subsample 3 | 3777<br>5067<br>5331 | 3441<br>2101<br>2731 | 45,2<br>40,1<br>45,3 |
| sample 104<br>100°C, 100 MGy | subsample 1<br>subsample 2<br>subsample 3 | 2245<br>2206<br>2742 | 3161<br>2664<br>3243 | 45,7<br>44,2<br>49,4 |
| sample 105<br>100°C, 100 MGy | subsample 1<br>subsample 2<br>subsample 3 | 1315<br>4378<br>2235 | 11692<br>9424<br>4930 | 37,0<br>50,8<br>57,5 |
| sample 131<br>150°C, 100 MGy | subsample 1<br>subsample 2<br>subsample 3 | 2168<br>1044<br>1403 | 6727<br>8130<br>3206 | 42,4<br>41,1<br>38,6 |
| sample 132<br>150°C, 100 MGy | subsample 1<br>subsample 2<br>subsample 3 | 1457<br>1957<br>1959 | 6746<br>3841<br>5490 | 37,2<br>33,6<br>49,9 |
| sample 133<br>150°C, 100 MGy | subsample 1<br>subsample 2<br>subsample 3 | 1818<br>1356<br>1605 | 5281<br>2854<br>4674 | 32,2<br>38,0<br>36,1 |

## 3. DISCUSSION

The present study confirms clearly that the irradiation of rock salt leads to the formation of equal amounts (on a molar basis) of the molecular products colloidal sodium and



chlorine gas over a broad temperature and dose range. This is one of the few investigations, in which the various products have been determined for the same sample. Other investigations are those of Jenks and Bopp [Jenks and Bopp, 1974, 1977] and of Groote and Weerkamp [Groote and Weerkamp, 1990]. However, in these studies the irradiation temperature was restricted to a range below 150°C. In order to quantify the formation of molecular chlorine, both the amount present in the crystals and the amount released into the gas phase above the salt must be determined. This is particularly true for temperatures above 150°C. A time dependence for the chlorine release is conceivable but was not investigated in the present study.

The formation of radiation defects and of molecular products in NaCl depends, in a complex manner, on the parameters dose, dose rate, and temperature. Also the microstructure of the salt and the level of impurity were suggested to have an influence. In principle, three phases can be distinguished in which the formation of defects is related to radiation dose. In an induction phase the density of F- and H-centers increases, while no significant growth of sodium colloids or other molecular irradiation products occurs. This is followed by a phase in which a more or less linear relationship exists between the formation of molecular defects and dose. At even higher radiation doses saturation occurs under specific conditions. While the beginning of the saturation depends on dose, the amount of irradiation products becomes independent of dose once saturation is reached. When considering waste disposal, one of the aspects of importance is the extent of radiation damage to the salt. Therefore, the linear phase and the possible saturation level are of most significance. In the present study saturation is clearly observed at a temperature of 250°C (at a very low level of less than 0,003 mol % damage). At 200°C saturation seems to begin at about 100 MGy. No saturation occurs at 100°C and 150°C in the investigated dose range. This is in accord with the extended Jain-Lidiard (JL) theory [Jain and Lidiard, 1977, Lidiard, 1979, van Opbroek and den Hartog, 1985], which predicts that at a dose rate of $10^4$ Gy/h damage saturation begins above 300 MGy. Unfortunately, under the boundary conditions of our experiments this dose range is only accessible using prohibitively long irradiation times. The absolute yield of radiation damage observed in our experiments is also in accordance with the JL-theory. At a dose of about 100 MGy, a damage level of about 0.8±0.1 mol % was determined. For comparison, using the JL-theory values of 1,4 mol % and 0,6 mol % are estimated for dose rates of $10^4$ Gy/h and $10^5$ Gy/h, respectively, for 100 MGy. Our stored energy data are slightly higher than those of Garcia Celma and Donker [Garcia Celma and Donker, 1994], who determined the stored energy in halite samples (Speisesalz) from the Asse salt mine, which were irradiated at 100°C in the same irradiation facility at Petten. They observed a stored energy of about 15 J/g at 100 MGy and of 40 J/g at about 160-180 MGy. Possibly these differences can be accounted

for by the different dosimetry systems utilized. Our high dose values have been roughly estimated, but in fact may be higher than 100 MGy.

The amount of energy that is deposited in the salt due to the formation of molecular radiation products is of particular importance when the thermo-mechanical consequences of a spontaneous release of the energy is considered. Our data seem to indicate that one mol % colloidal sodium corresponds to a stored energy of about 70 J/g. This value agrees well with the one given by Jenks et al. [Jenks et al., 1975]. From their data Groote and Weerkamp [Groote and Weerkamp, 1990] concluded a value of 125 J/g. Donker et al. [Donker et al., 1995 (article nr. 19, this volume] reviewed the available data and published calculations. They showed that the value of 125 J/g is based on erraneous assumptions. In their paper Donker et al. suggested to use a conversion factor between defect concentration and stored energy of 5 eV/defect, which corresponds to about 82 J/g. Our experimental value is very similar to this value and corroborates their conclusions.

## REFERENCES


A. GARCIA CELMA and H. DONKER, 1994: "*Stored Energy in Irradiated Salt Samples*", EUR-Report 14845 EN, 127 p.

H. GIES, W. HILD, T. KÜHLE, and J. MÖNIG, 1994: "*Radiation Effects in Rock Salt - A Status Report*", English translation of the GSF-Report 9/93, 149 p.

J. GROOTE and H.R. WEERKAMP, 1990: "*Radiation Damage in NaCl Small Particles*", Ph.D. Thesis at the Rijksuniversiteit Groningen, The Netherlands, 270 p.

L.W. HOBBS, 1973: "*Transmission Electron Microscopy of Defects in Alkali Halides*", J. Physique C9-227 - C9-241

A.E. HUGHES, 1983: "*Colloid Formation in Irradiated Insulators*", Radiat. Eff. **74**, 57 - 76

A.E. HUGHES and A.B. LIDIARD, 1989: "*The Growth of Colloids in Irradiated NaCl*", AERE-R-13319, United Kingdom Atomic Energy Authority HARWELL, 31 p.

U. JAIN and A.B. LIDIARD, 1977: "*The Growth of Colloid Centers in Irradiated Alkali Halides*", Phil. Mag. **35**, 245 - 259

G.H. JENKS and C.D. BOPP, 1974: "*Storage and Release of Radiation Energy in Salt in Radioactive Waste Repositories*", ORNL/TM-4449, Oak Ridge National Laboratory, Tennessee, USA





G.H. JENKS and C.D. BOPP, 1977: "*Storage and Release of Radiation Energy in Salt in Radioactive Waste Repositories*", ORNL-5058, Oak Ridge National Laboratory, Tennessee, USA, 97 p.

G.H. JENKS, E. SONDER, C.D. BOPP, J.R. WALTON, and S. LINDENBAUM, 1975: "*Reaction Products and Stored Energy Released from Irradiated Sodium Chloride by Dissolution and by Heating*", J. Phys. Chem. **79**, 871 - 875

A.B. LIDIARD, 1979: "*Energy Stored in Irradiated NaCl*", Phil. Mag. A **39**, 647 - 659

G. VAN OPBROEK and H.W. DEN HARTOG, 1985: "*Radiation Damage of NaCl: Dose Rate Effects*", J. Phys. C. **18**, 257 - 268

# STORED ENERGY IN IRRADIATED NATURAL ROCK SALT AS COMPARED TO SYNTHETIC HALITE OF DIFFERENT CHARACTERISTICS

**H. Donker and A. García Celma**

## ABSTRACT

In this paper the results of stored energy measurements performed on irradiated, natural and synthetic rock salt samples are presented and discussed. The samples were irradiated in the GIF B irradiation facility of the Dutch Energy Research Foundation (ECN) at approximately constant dose rates of 4 and 15 kGy/h, at a temperature of 100 °C and total doses varying between 0.022 and 44 MGy. It is shown that in general the measured stored energy values for samples irradiated to the same total dose and at the same dose rate are approximately equal.

## 1. INTRODUCTION

One of the safety aspects that has to be considered for a radioactive waste repository in rock salt is the formation of radiation damage in the halite crystals. Most of the energy irradiated by the radioactive waste is dissipated in the rock salt as heat, but a small part of it is used to create various lattice defects in the salt crystals. Agglomeration of these defects leads to partial decomposition of the halite crystals into sodium and chlorine. Recombination of the sodium and chlorine will set free the chemical energy stored in the defects. It has to be investigated whether this stored energy may form a thread to the safety of a repository.

Experiments for the length of time during which gamma radiation above the natural background will be present in a repository are however, impossible to carry out. One therefore has to rely on computer simulations based on theoretical models to predict the behaviour of a repository. Since the conditions in a repository are so far away from those which can be reached in a laboratory, heavy demands have to be applied to these models. It is necessarry that the models

describe all the processes influencing the damage formation (and anneal) that can occur under repository conditions. Theory development is usually based on experiments performed on pure, undeformed single crystals irradiated at atmospheric pressure. These crystals are however, very different from the impure, polycrystalline and deformed rock salt at the lithostatic pressure of a repository. Therefore, many irradiation experiments, under various conditions and with different types of salt were needed and have been performed in the GIF B irradiation facility in the spent fuel basin of the High Flux Reactor at Petten, The Netherlands [García Celma et al., 1995].

The irradiation experiments performed in the GIF B facility were initially performed to monitor the HAW–field experiments [Rothfuchs et al., 1988]. The main objective of these experiments was to establish the links between long term in situ and short term laboratory results of irradiation experiments. Due to repeated delays and finally cancelation of the emplacement of the radio–active sources in the HAW–field, the laboratory experiments were steadily extended. The main objective of both the GIF B experiments and the planned HAW field experiments was to find a link between the existing theories and the conditions to be expected in a repository. To achieve this a great number of samples were irradiated together, each sample differing from the others in one or more of the following factors: microstructure, composition, pressure or amount of added brine. The irradiation experiments were performed at dose rates which were as close as possible to those expected for a radio–active waste repository i.e. as low as possible.

The starting material consisted of pure NaCl single crystals, pressed pure NaCl powder samples, synthetic rock salt samples and different kinds of natural rock salt: Speisesalz of the 800 meter level, Borehole anhydritic salt, Borehole polyhalitic salt and Polyhalitic salt (all provinient from the Asse mine, Remlingen, Germany), Potasas del Llobregat salt (from the Potasas del Llobregat mine, Cardona, Spain) and Dutch rock salt (origin unknown, somewhere in the Netherlands).

In this paper the result of the stored energy measurements performed on these samples are presented and discussed.



## 2. MATERIAL CHARACTERIZATION

### 2.1. Harshaw crystals (H)

Harshaw single crystals are frequently used as standards for stored energy measurements in salt. They are poor in $OH^-$ content, have a very high purity and very low dislocation densities. They are produced by Harshaw Ltd. in the U.S.A., and are mainly used in optical instruments.

Stored energy determinations on several non–irradiated Harshaw crystals have been performed by Differential Thermal Analysis (DTA). The obtained results are not very reproducible, but some kind of general pattern could be observed. Below 500 K an endothermal effect is observed, while between 500 and 750 K an exothermal effect with a maximum around 600 K is observed. The magnitude of this exothermal effect varies between 0 and 15 J/g. Even samples taken from the same single crystal show large differences in thermal behaviour. No mass loss is observed during the DTA experiments. A full explanation for the observed features has not been found yet. Most probably they have to be ascribed to a rearrangement of dislocations in the crystals [García Celma, 1994; Schutjens, 1991].

At first these crystals were used as received in the irradiation experiments. Later when we knew that these non–irradiated crystals could contain considerable amounts of stored energy, they were annealed prior to irradiation in an open canister at 500°C for one hour in an Argon atmosphere. After anneal they were allowed to cool down slowly to room temperature. Stored energy measurements on these annealed crystals showed no significant endo– or exothermal ef–fects.

### 2.2. Pressed powder samples (PP)

Pressed powder samples are prepared by cold pressing NaCl powder (Merck, pro analysis) to which 0.2 weight% bi–distilled water has been added at 3 kbar. The NaCl powder was ana–lyzed by atomic emission spectroscopy (AES) using an inductively coupled plasma (ICP). Besides NaCl, only Fe (4.8 ppm) and Ca (13 ppm) were found in contents above the detection limit of the method. The average grain size of these samples is 66 $\mu$m. Most crystals present a cubic habitus.

The stored energy of these samples as measured with DTA is (4.2 ± 0.9) J/g. No endothermal decrepitation peaks are observed. It is therefore concluded that the pressed powder samples do not contain a significant amount of intragranular fluid inclusions.

## 2.3. Synthetic rock salt samples (SS)

The starting material used to produce these samples was the same as used for the pressed powder samples. Synthetic rock salt samples have been produced by:

a) forcing as much NaCl powder as possible into jackets;
b) vacuum emptying the jackets to extract the air from the pores;
c) pressing at 150°C and 1 kbar hydrostatic pressure for one day;
d) pressing at 150°C and 500 bar hydrostatic pressure for 30 days.

A detailed description of the method followed can be found in [García Celma et al., 1991].

Synthetic rock salt samples are real rock salt with respect to their microstructure, with real grain boundaries. In this they differ from pressed powder samples, which have more porosity and consist of loose grains.

The difference between synthetic rock salt and real (natural) rock salt is that the first is chemically pure and has a very perfect "foam microstructure", while the second is impure and has a granular microstructure. Foam microstructures are a special type of granular microstructure produced by grain boundary migration. Foam microstructures are special in that the grain boundaries present a sort of equilibrium: each grain boundary has the same tendency to intrude its neighbour as its neighbour has to intrude it. This produces grain shapes that resemble the shape of beer foam bubbles, with typical triple interferences of grain boundaries delineating three angles of 120 degrees.

Stored energy determinations of synthetic rock salt yielded (4.7 ± 0.5) J/g. During the DTA measurements a mass loss of 0.05 weight% was registered. This is assumed to correspond to the evaporation of water. Since no endothermal spikes are observed in the thermograms, this water is assumed to be intergranular water (grain boundary brine).



## 2.4. Asse Speisesalz of the 800–meter level (Sp–800)

The Sp–800 material consists of polycrystalline halite rock of a relatively high purity (> 99%), with a grain size of 3–10 mm. The main impurity phases are polyhalite ($K_2MgCa_2(SO_4)_4.2H_2O$) and minor anhydride. Besides the structurally bound water, the material contains about 0.05% intracrystalline $H_2O$, mainly in fluid inclusions at grain boundaries (i.e., halite–halite or halite–polyhalite) [Spiers et al., 1986].

As observed by Urai et al. [1986], original Asse Speisesalz samples have a granular microstructure produced by at least one episode of grain boundary migration in the mine. This was determined on the basis of grain overgrowths and substructure analyses. In a granular microstructure grain boundaries can have many different shapes.

The thermograms obtained by DTA characteristically consist of an exothermal peak between 485 and 705 K with a superimposed endothermal peak in the interval 565 to 635 K. During the DTA measurements a mass loss between 0.02 and 0.11 weight% was observed. The mass loss, which is assumed to be due to the loss of water, was observed to be proportional to the intensity of the endothermal peak. According to Jockwer [1981], polyhalite loses its crystal water between 235 and 350 °C. Therefore, the endothermal peak is ascribed to the dehydration of polyhalite. Mass losses less than 0.05 weight% are not reflected in endothermal peaks and are inferred to correspond to intergranular water.

In order to obtain the true stored energy in the halite of the Sp–800 samples, the observed exothermal effect is corrected for the endothermal dehydration peak of polyhalite. The shape of the true exothermal peak is estimated using the initial and final slope of this peak and the observed weight loss. Stored energy measurements of non–irradiated Sp–800 samples after performing the correction described above yielded 2.1 ± 0.7 J/g.

## 2.5. Borehole polyhalitic samples (Bhp)

Borehole polyhalitic samples are Asse samples from the same geological levels as the polyhalitic levels perforated by the HAW–test field boreholes. These samples present the same

type of microstructure as already discussed for the Asse Speisesalz, but contain more polyhalite.

The pre–irradiation stored energy of these samples is determined by correcting the exothermal signal for the endothermal dehydration of polyhalite in the same way as with the Asse Speisesalz samples. Due to the fact that more polyhalite is present in these samples, the corrected results are less accurate than those from the Sp–800 measurements. The corrected stored energy lies in the range between 4.4 and 1.9 J/g. The mass loss during the DTA experiments ranges between 0.01 and 0.32 weight% and is clearly related to the dehydration of polyhalite.

## 2.6. Borehole anhydritic samples (Bha)

Borehole anhydritic samples have also been taken from the boreholes of the HAW–test field. The difference with the borehole polyhalitic samples is that they contain anhydrite instead of polyhalite. From all the Asse samples, these are the most similar to the Potasas del Llobregat samples, although the borehole polyhalitic samples are more homogeneous at the mesoscale.

Pre–irradiation stored energy measurements yielded (2.6 ± 0.9) J/g. The mass loss during these measurements varied between 0.01 and 0.11 weight%. This mass loss is not accompanied by any endothermal peaks in the temperature interval where the stored energy is set free, as was the case with samples containing polyhalite.

## 2.7. Polyhalitic salt samples (PS)

Polyhalitic salt samples have also been taken from the boreholes of the HAW–test field. They contain extremely high amounts of polyhalite.

## 2.8. Potasas del Llobregat samples (PLL)

The solid phase of Potasas del Llobregat samples mainly consists of halite (85 to 99%) and anhydrite (1 to 15%). Clay, coelestine, an undetermined magnesium mineral and quartz are



present in minor proportions as determined by microprobe analyses [García Celma et al., 1991].

The amount of inherent brine was measured by us with TG–DTA and ranges between 0.1 and 0.9 weight%. For 175 thermogravimetric analyses (performed at the Barcelona University) where mass loss was measured up to 725 K, the mean content of brine was calculated to be 0.3 weight% with values ranging between 0.04 and 1.0 weight% [Pueyo et al., 1992]. This corresponds well with our measurements.

Observations of decorated microstructures in the irradiated Potasas del Llobregat samples revealed the presence of different subgrain microstructures, which points to at least two recrystallization periods in the starting material. After these recrystallization episodes, veins developed [García Celma et al., 1991]. Many intragranular fluid inclusions are found within hopper crystals. Intergranular fluid inclusions show the normal vermicular grain boundary structures [Urai et al., 1986].

In the temperature interval of 305 to 495 K several endothermal peaks are observed, which are ascribed to the evaporation of grain boundary water and production of $CH_4$. Due to these endothermal peaks the onset of the exothermal signal is difficult to determine and can vary from 395 to 505 K. The end of the exothermal signal is difficult to determine as well due to fluid inclusion decrepitation and can vary from 645 to 695 K. The endothermal effect of decrepitation does not usually represent more than 0.5 J/g. To avoid arbitrary interpretations the choice was made to integrate the thermal effect, assuming a base line as near as possible to the line where $\Delta H = 0$. The mean stored energy of non–irradiated Potasas del Llobregat samples determined in this way is (0.6 ± 2.2) J/g. This average has been established for samples containing low amounts of impurities. Low amounts of impurities are also reflected by the colour of the samples and the mass loss

## 2.9. Dutch salt samples (DS)

Dutch salt samples are samples of unknown composition and origin except that they were taken from somewhere in the Netherlands.

## 3. EXPERIMENTAL

### 3.1. Irradiation experiments

The samples mentioned above have been irradiated in the GIF B facility of the ECN at a temperature of 100 °C [García Celma et al., 1995]. They were irradiated at a low dose rate which was kept as constant as possible. To achieve this, old spent fuel elements which have a slow decay were used. Two different mean dose rates were applied in these experiments i.e. 15 and 4 kGy/h. In each experiment 16 samples were irradiated simultaneously. Twelve of these samples were irradiated under enhanced pressure, the other four at atmospheric pressure. To some of the samples an extra amount of brine was added previous to the irradiation experiment.

The first series of experiments (GIF B1) was performed at dose rates varying between 20 and 10 kGy/h . The average dose rate was 15 kGy/h. In these experiments the samples were wrapped in silver foil and then placed in an aluminum sample holder (in stead of the later used golden sample holders). The Harshaw crystals used in this series were not annealed prior to irradiation.

A second series of experiments (GIF B2) was performed at dose rates varying between 8 an 1 kGy/h. The average dose rate was 4 kGy/h. In these experiments the golden sample holders were used and the Harshaw crystals were annealed prior to irradiation.

Finally a third series of experiments (GIF B3) with a limited number of sample types was performed at dose rates varying between 21 and 12 kGy/h. The average dose rate was 15 kGy/h. This to check some controversial results obtained in the GIF B1 experiments and also to check the effect of annealing prior to irradiation on the radiation damage development. To achieve this annealed and non–annealed Harshaw crystals were irradiated simultaneously in each experiment of this series. For these experiments also golden sample holders were used.



### 3.3. Stored Energy Measurements

The stored energy measurements were carried out by means of differential thermal analysis on a SETARAM DSC–111. Calibrations were performed by melting Indium metal. Anneals took place in "closed" Pt capsules with a small capillary hole to allow gases to escape in order to avoid explosion of the capsule when pressure builds up. The heating rate used for these measurements was either 5 (GIF B1) or 10 (GIF B2 and B3) K/min. In a first run the sample is measured against an empty reference sample holder up to a temperature of 750 K. Then the sample and reference are allowed to cool down and a background signal is measured in a second run. The result of the second run is subtracted from that of the first. The area closed by the resulting curve and the base line is then integrated to obtain the released stored energy. Due to the difference in heating rate the stored energy peaks for the samples measured with a rate of 10 K/min will be observed at slightly higher temperatures than the peaks observed for the samples measured with a rate of 5 K/min.

For the stored energy measurements, parts of the irradiated samples were cut in small pieces. From those pieces, the darkest i.e. free from secondary minerals and recrystallized material were selected with the naked eye. Small portions of secondary minerals and recrystallized material may however, still have been present in the analyzed material. This procedure worked quite well for most of the samples, except for the pressed powder and synthetic salt samples. For these materials the grains were so small that it was impossible to separate dark and light material. Therefore the stored energy values given for these samples represent the bulk stored energy

According to the measurements of Jockwer [1981], polyhalite loses its crystal water between 235 and 350 °C. As already discussed in section 2 our analysis showed that the dehydration of polyhalite takes place in the same temperature interval as the release of stored energy. This results in the presence of an endothermal peak superposed on the exothermal release of stored energy. When necesarry our results have therefore, been corrected for the dehydration of polyhalite.

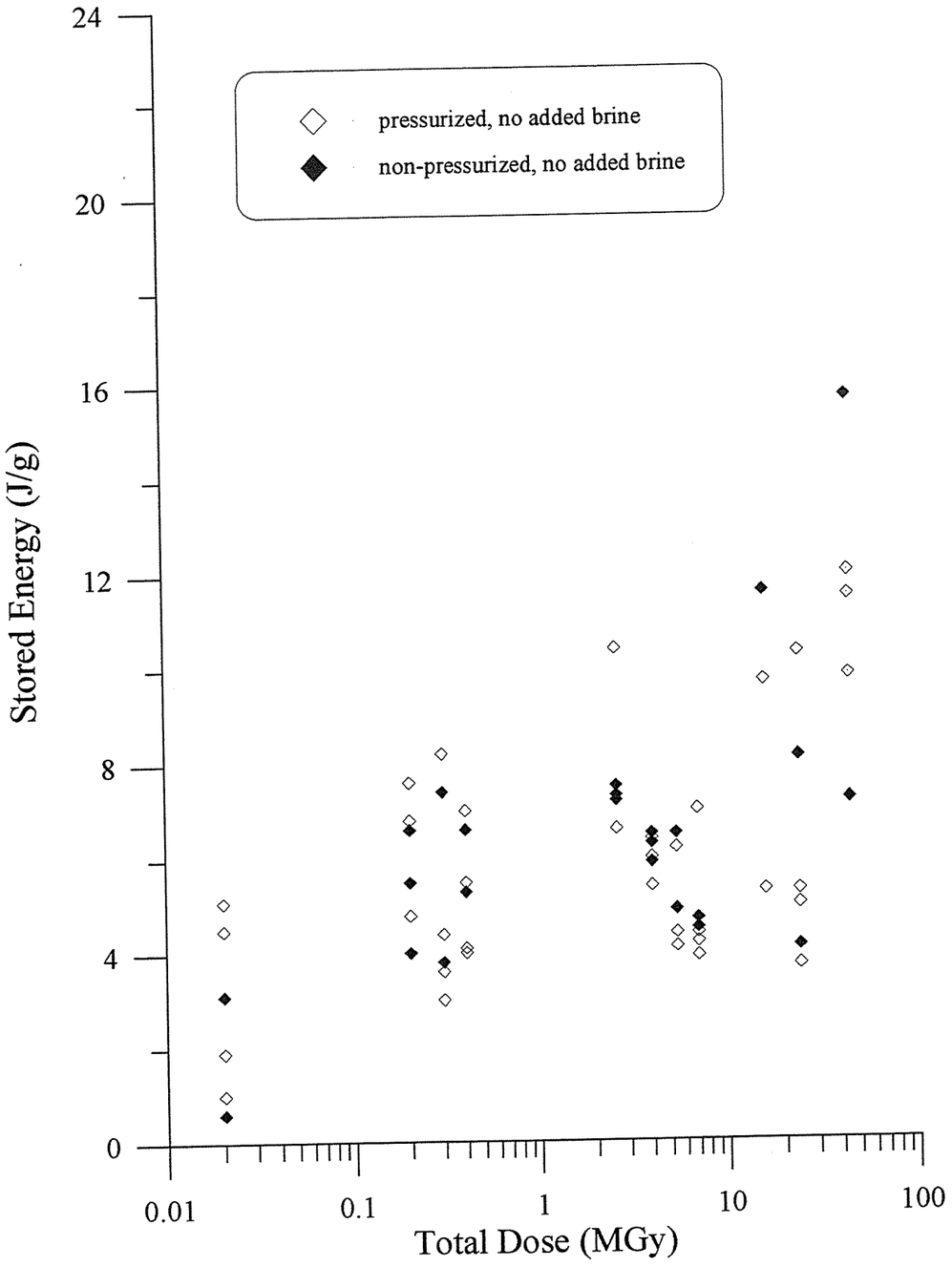


Figure 1a: *Stored energy of salt samples of various composition irradiated in GIF B1 (15 kGy/h, 100 °C)*



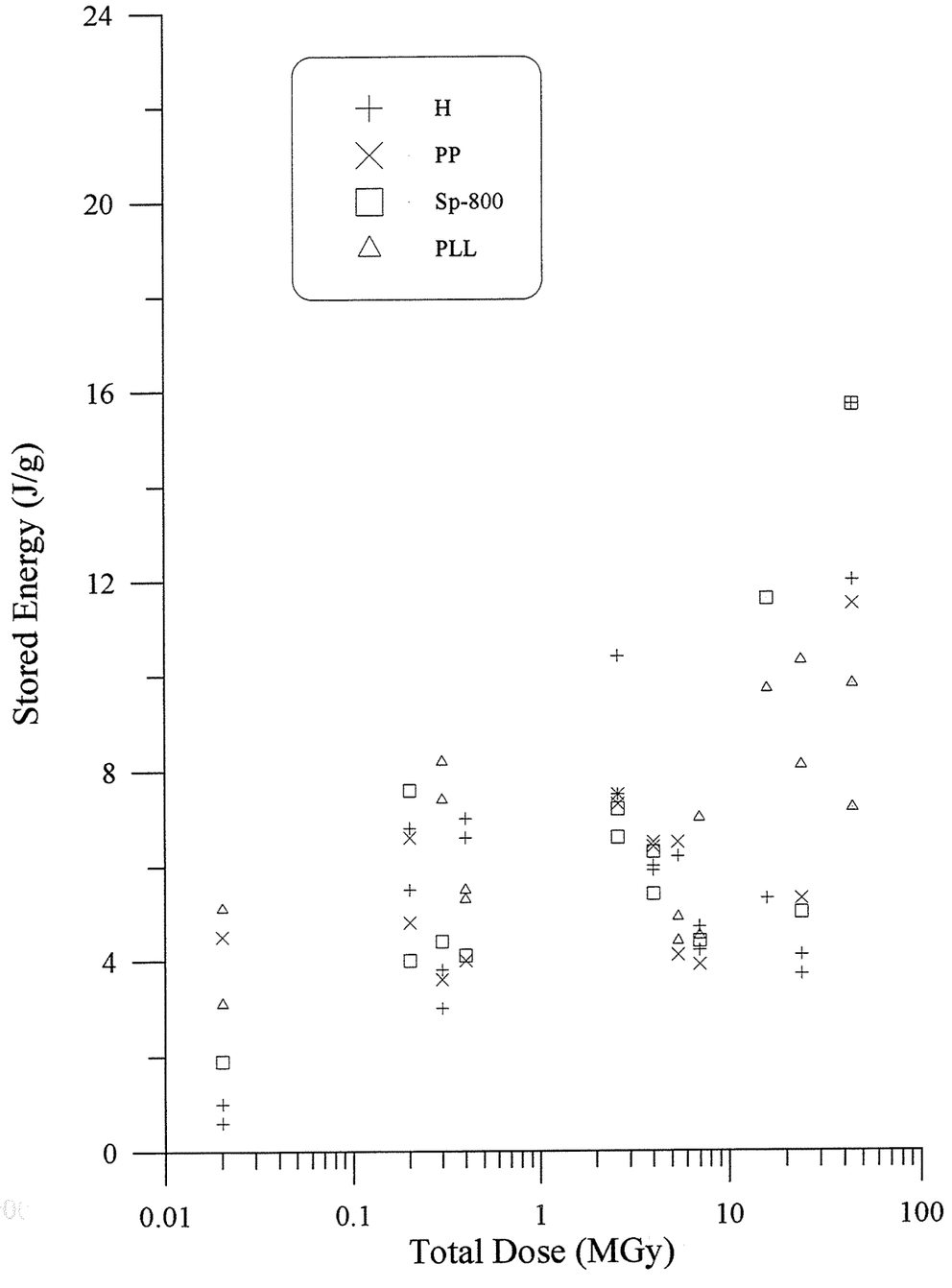


Figure 1b: *Stored energy of salt samples, pressurized and non-pressurized, with and without added brine, irradiated in GIF B1 (15 kGy/h, 100 °C)*

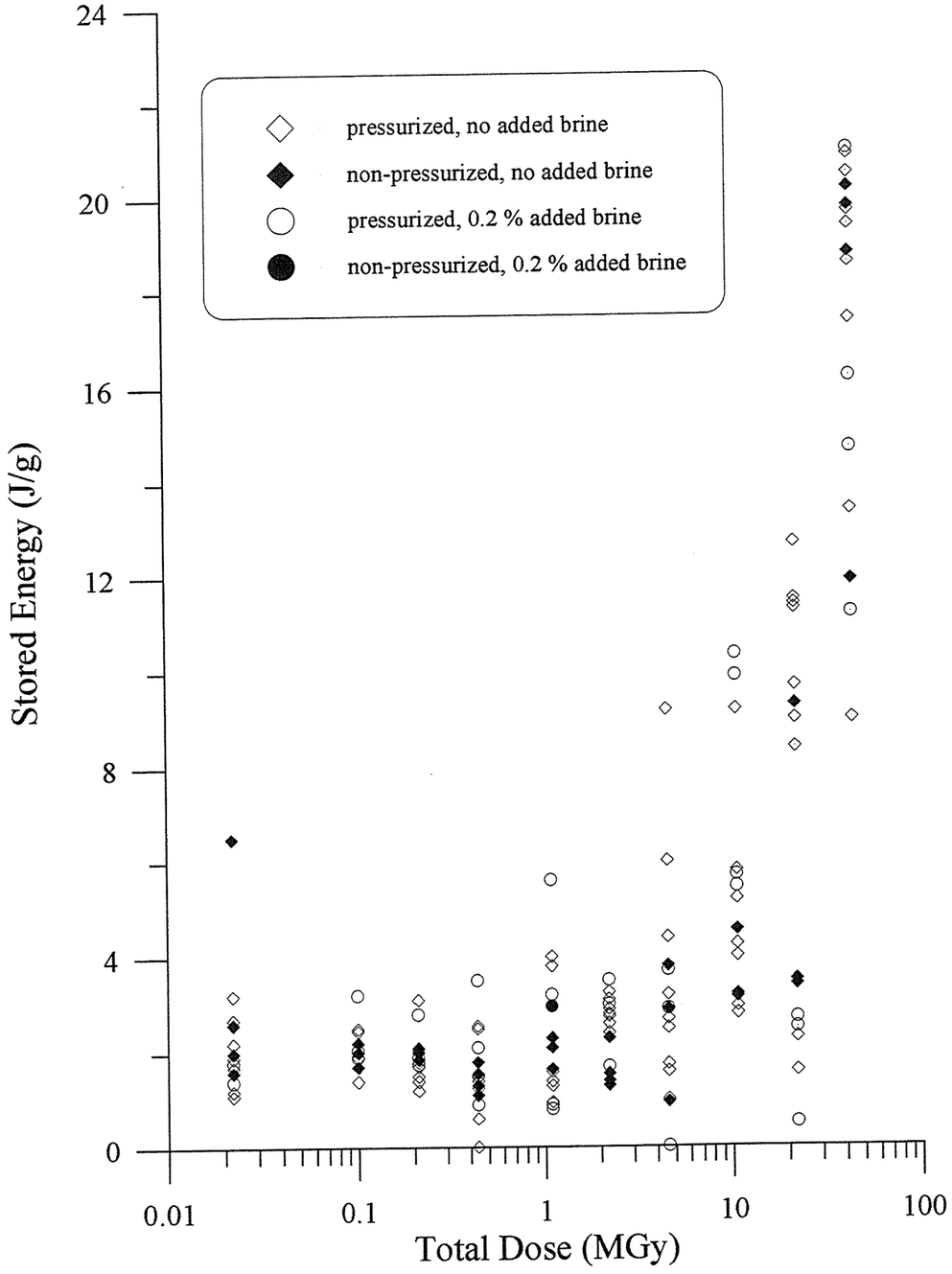


Figure 2a: *Stored energy of salt samples of various composition irradiated in GIF B2 (4 kGy/h, 100 °C)*



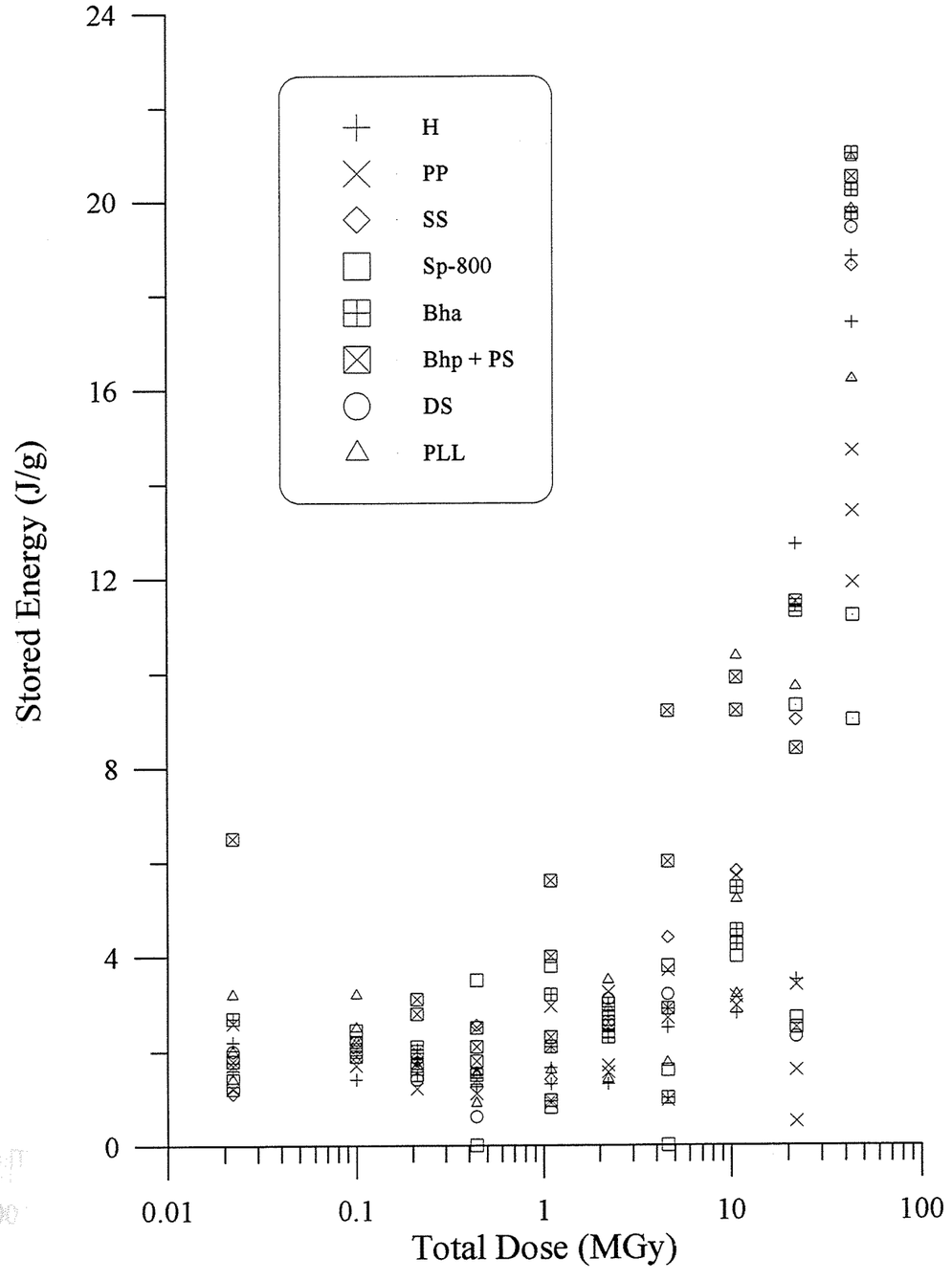


Figure 2b: *Stored energy of salt samples, pressurized and non-pressurized, with and without added brine, irradiated in GIF B2 (4 kGy/h, 100 °C)*

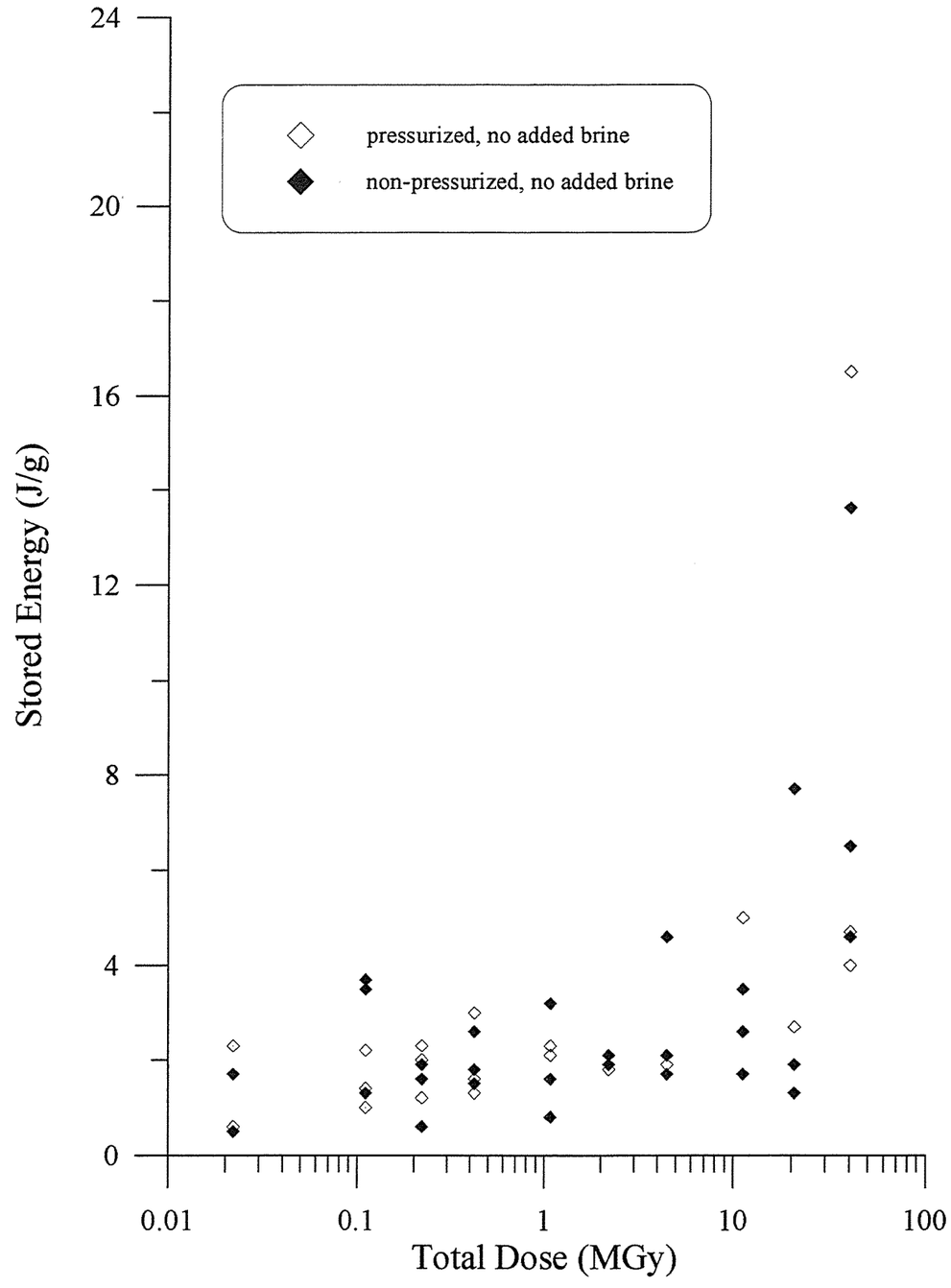


Figure 3a: *Stored energy of salt samples of various composition irradiated in GIF B3 (15 kGy/h, 100 °C)*



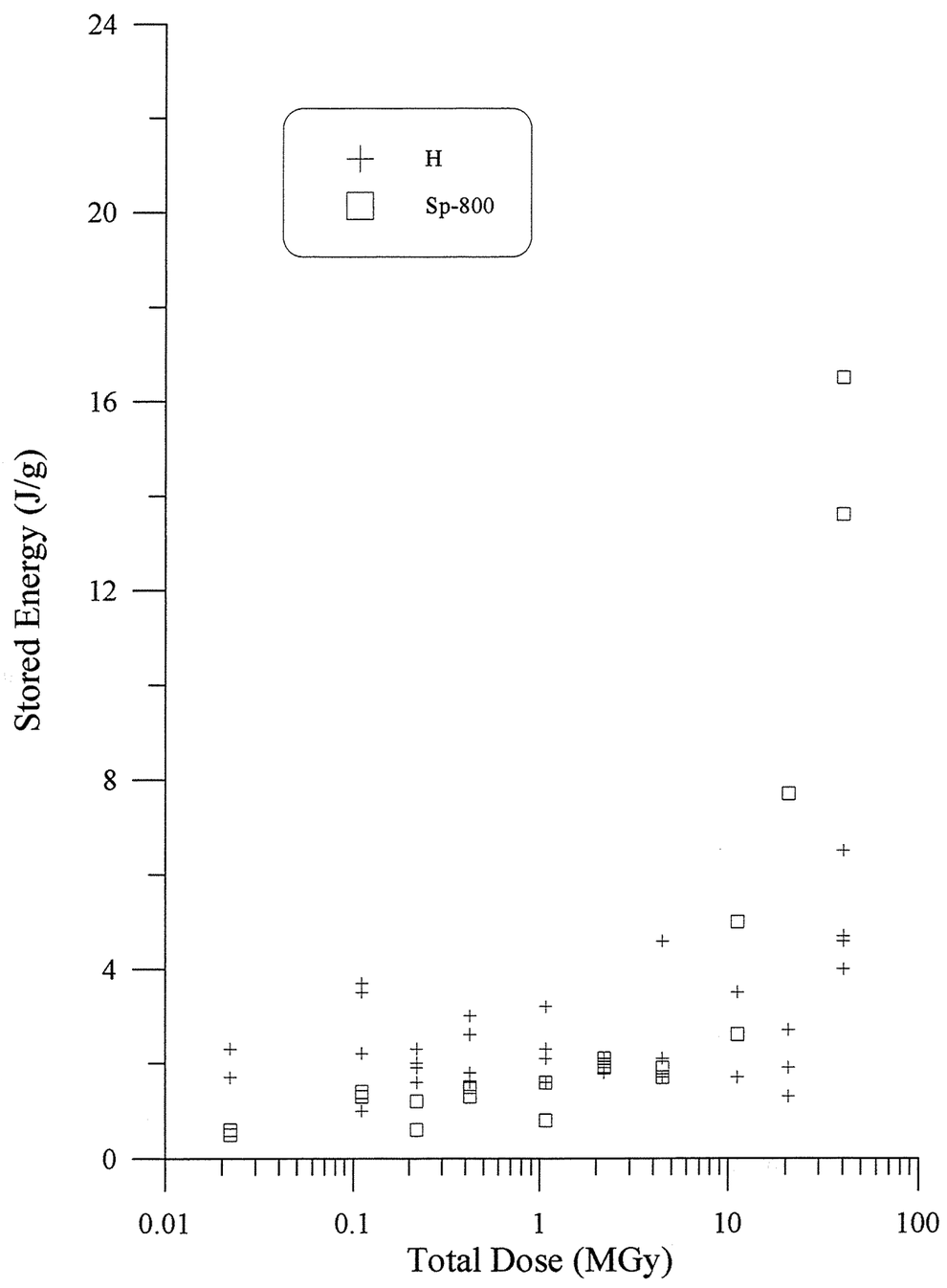


Figure 3b: *Stored energy of salt samples, pressurized and non-pressurized, without added brine, irradiated in GIF B3 (15 kGy/h, 100 °C)*

## 4. RESULTS AND DISCUSSION

### 4.1. General

The measured stored energy values for all samples irradiated in the three series of experiments in GIF B are shown in Fig. 1 to 3. In these figures no clear tendencies resulting from pressurizing the samples or adding extra brine to the samples can be observed. Also no clear distinction of some kind of sample developing systematically more or less damage than the others can be made, except maybe for the pressed powder samples irradiated in the GIF B2 experiments. At high total doses, low stored energy values have been systematically observed for these samples. Note, however, that for these samples bulk stored energy values have been measured whereas for the natural samples the darkest i.e. most damaged parts of the irradiated samples have been selected for stored energy measurements. The large variation in stored energy values observed for the different samples irradiated to the same total doses is probably caused by differences in the samples at the microstructural (or even submicrostructural) level.

The results of the GIF B1 experiments show that in most types of samples an initial increase of the stored energy with increasing total dose up to a maximum value at a total dose of about 2.6 MGy, is followed by a decrease of stored energy with increasing total dose. At a total dose between 5 and 15 MGy a minimum is reached after which the stored energy increases again with increasing total dose (see Fig. 1). Below integrated doses of 15 MGy a comparison of our stored energy results with the results of the Light Absorption measurements shows that the irradiated samples yield higher stored energy levels than could be attributed to colour centres [García Celma et al., 1992; García Celma and Donker, 1994a, García Celma, 1993; García Celma et al.,1993]. The initial increase and the ensuing decrease of stored energy was therefore ascribed to the development of dislocations and their anneal, also because the stored energy peaks were observed at a higher temperature than the colloid anneal peak in the thermograms of the Harshaw crystals irradiated to higher doses [García Celma and Donker, 1994a]. Moreover, the development of low energy dislocation arrangements has been shown by means of microstructural analysis [García Celma and Donker, 1994b]. However, the results of the GIF B3 experiments shed some doubts on this interpretation.



A comparison of Fig. 1 and 3 shows that for the samples of the GIF B3 experiments the measured stored energy values are systematically lower than for the samples of the GIF B1 experiments, while the experimental conditions (dose rate, total doses, temperature, etc) under which these two series were performed were similar. Also the initial rise and ensuing decrease of stored energy as found in the GIF B1 experiments, is not observed for the samples of the GIF B3 (or GIF B2, see Fig. 2) experiments. In the GIF B3 experiments the stored energy observed for samples irradiated up to total doses of 11 MGy has an approximately constant value of about 2 J/g. The reason for these differences is not yet very clear but we think that they might be caused by surface effects. Jiménez de Castro and Álvarez Rivas [1990] have reported that samples cut from the surface of their irradiated samples show an enhanced stored energy. This additional stored energy, as compared to samples cut from the interior of the same irradiated crystal, is released in the temperature region above 300 °C. In the GIF B2 and GIF B3 experiments the samples for stored energy measurements were all selected from the interior of the irradiated samples while this was most probably not the case in the GIF B1 experiments. For all our samples irradiated up to total doses of 22 MGy the maximum of the stored energy peak in the DTA scans is found at about 600 K, i.e. in the same temperature region as the enhanced stored energy of Jiménez de Castro and Álvarez Rivas.

Since we do not know to what extent surface effects have played a role in each individual stored energy measurement for samples irradiated in GIF B1 we will only briefly discuss the results of these measurements in what follows and not really use them for the conclusions.

For the samples irradiated in the GIF B2 experiments, the results of the stored energy measurements at low total dose are similar to those obtained for the samples irradiated in the GIF B3 experiments. At low total doses there is an approximately constant stored energy at a value of about 2 J/g. Above a total dose of 10 MGy this stored energy starts to increase. The maximal stored energy value observed at 44 MGy total dose is approximately 22 J/g

.

Note that for the natural samples we measured the stored energy in the most damaged parts of these samples. Bulk stored energy values for these samples will be lower than the values discussed in this paper since the microstructural analysis of these samples showed that they contain considerable recrystallized areas with less or no damage.

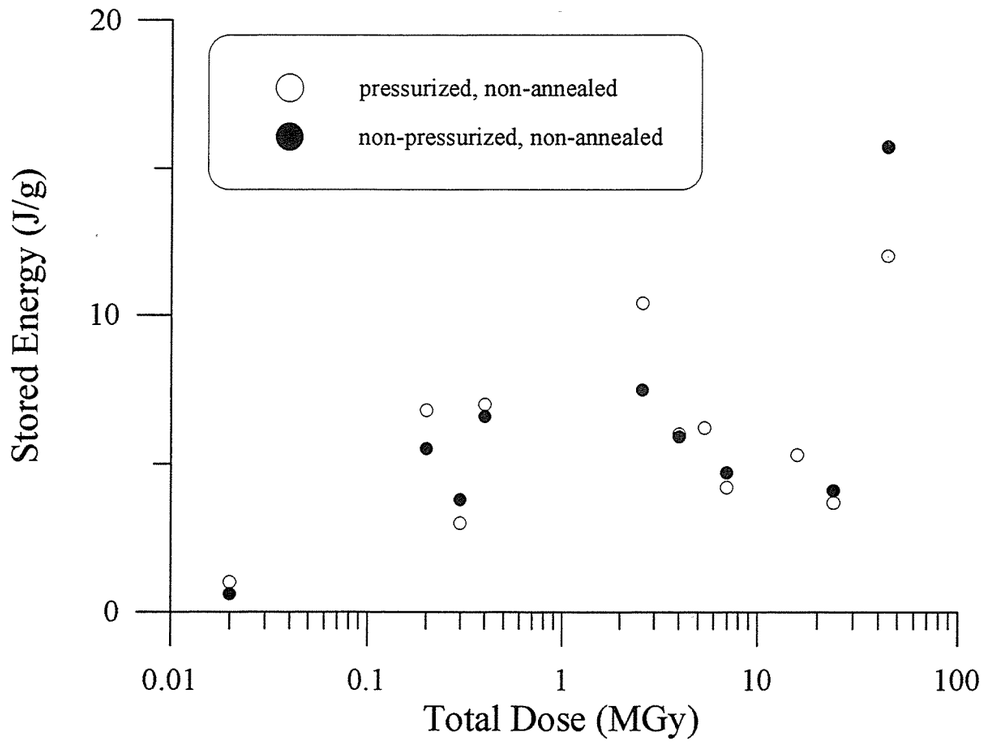


Figure 4: *Stored energy of Harshaw single NaCl crystals irradiated in GIF B1 (15 kGy/h, 100 °C)*

### 4.2. Harshaw crystals

In Fig. 4 the stored energy of the Harshaw crystals irradiated in GIF B1 is shown as a function of total dose. Below 2.6 MGy the stored energy increases rapidly with increasing total dose. Between 2.6 and 24 MGy a decrease in stored energy with increasing total dose is observed, while above 24 MGy it increases again although not as fast as in the interval between 0 and 2.6 MGy.

Of the Harshaw crystals irradiated in the GIF B1 experiments, those irradiated to integrated doses up to 24 MGy only show one exothermal peak with a maximum at about 600 K (see Fig. 5). At an integrated dose of 44.6 MGy two exothermal peaks are observed: the aforementioned peak at 600 K and another one at about 540 K (see Fig. 6). In previous reports we



have ascribed the 600 K stored energy peak to the anneal of dislocations, while the 540 K peak was ascribed to the anneal of colloids. In other (not Harshaw) samples we have observed only one stored energy peak with a maximum at a temperature of about 600 K. Also when these samples definitely contained a considerable amount of colloids. This means that in these samples the anneal of colloids takes place at a higher temperature than in the Harshaw crystals. The origin of this temperature shift is not yet clear. It does however indicate that there are possibly different kinds of colloids

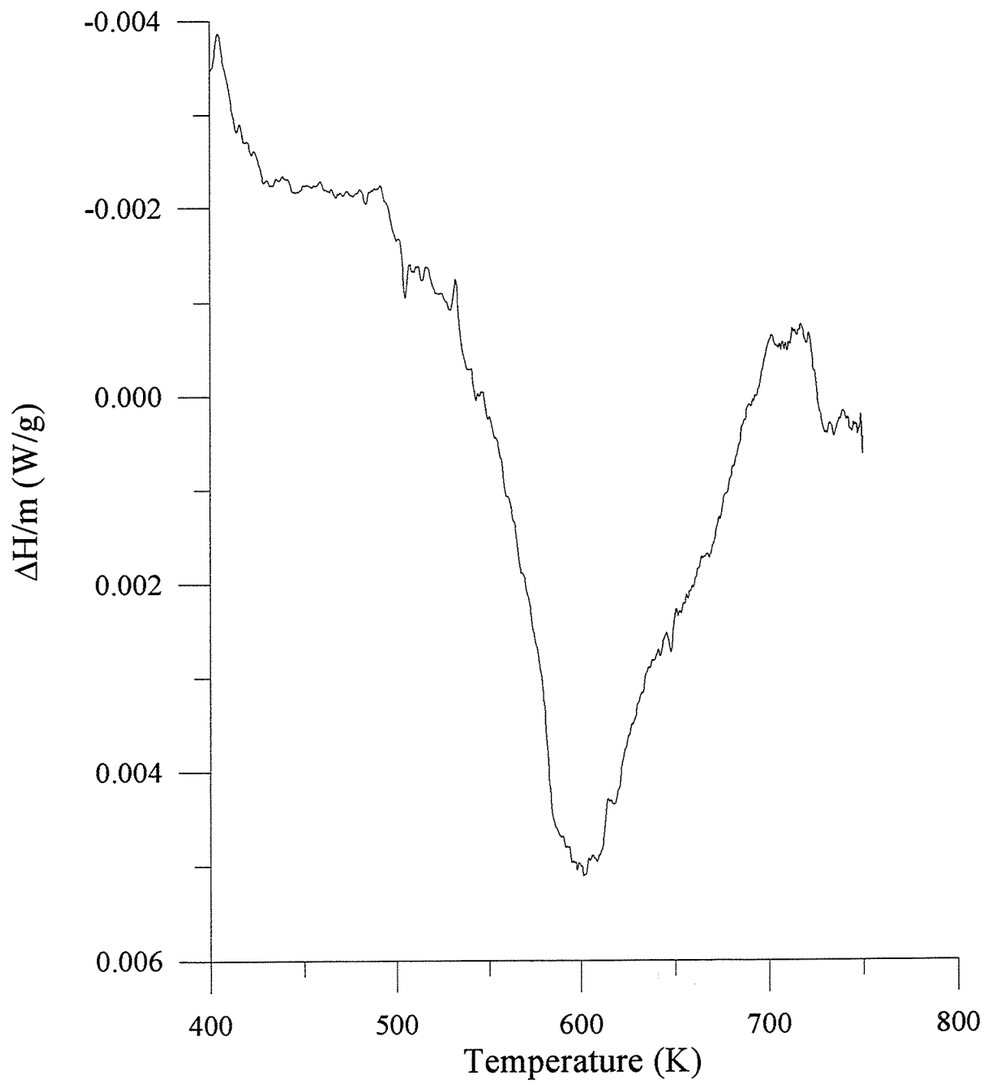


Figure 5: *DTA curve of sample 25 H (0.4 MGy, 15 kGy/h, 100 °C, 200 bar)*

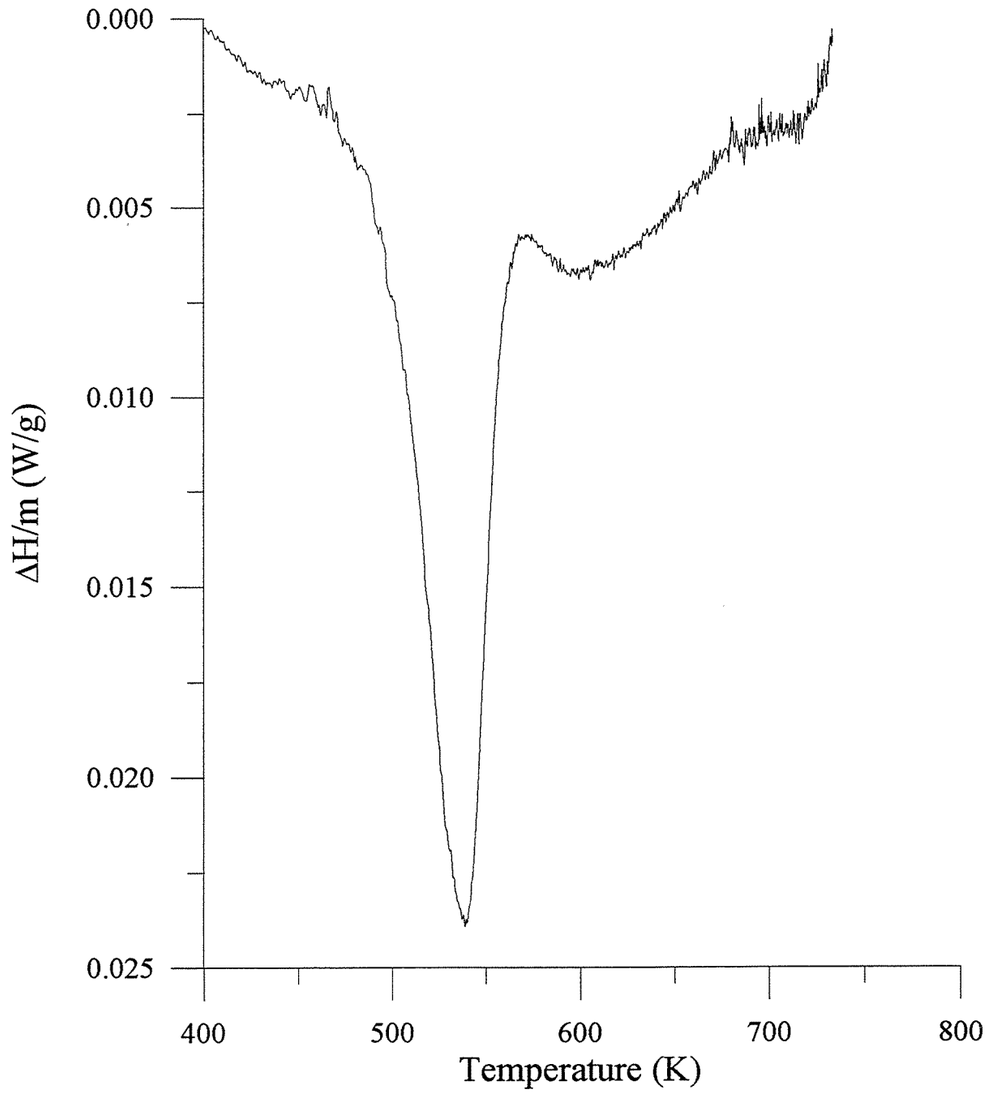


Figure 6 *DTA curve of sample 33 H (44.6 MGy, 15 kGy/h, 100 °C, 200 bar)*

In the GIF B2 experiments, performed at an average dose rate of 4 kGy/h, the samples irradiated up to a total dose of 4.4 MGy only show a weak exothermal peak at about 600 K similar to the one observed in the previous experiments. At 11 MGy the pressurized sample still only shows this peak, however, for the non–pressurized sample another much stronger exothermal peak at about 650 K is also observed. Also a small mass loss during the DTA measurement is observed for the non–pressurized sample. At 22 MGy the non–pressurized sample only shows



a weak exothermal peak at about 600 K again, while the pressurized sample shows a strong exothermal peak at about 560 K. According to our interpretation of the stored energy peaks, in the pressurized sample colloids have already nucleated while, in the non–pressurized sample they have not, at least not in significant amounts. This single observation, however is to little evidence to state that pressure enhances colloid nucleation. At 44 MGy both (pressurized and non–pressurized) irradiated Harshaw crystals only show an exothermal peak at about 570 K and their stored energy is approximately equal. Except for the mentioned sample none of the other samples show a significant mass change during the DTA measurement.

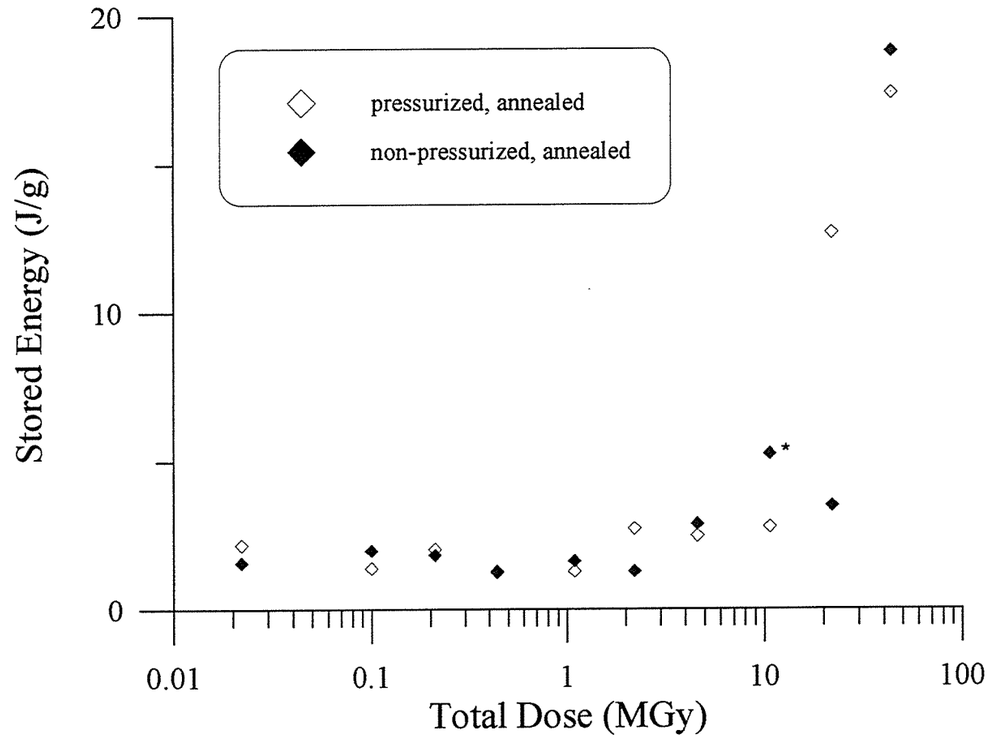


Figure 7: *Stored energy of Harshaw single NaCl crystals irradiated in GIF B2 (4 kGy/h, 100 °C)*

In Fig. 7 the stored energy of the Harshaw crystals irradiated in GIF B2 is shown as a function of total dose. The measured stored energy remains approximately constant for both pressurized and non–pressurized samples at about 2 J/g up to total doses of 1.1 MGy. Above 1.1 MGy the stored energy starts to increase with increasing total dose. Although, large differences

between the behaviour of pressurized and non–pressurized samples are observed, at 44 MGy the stored energy in both samples is again approximately equal and has reached a value of about 18 J/g.

Figure 8 shows the stored energy values obtained for the Harshaw crystals irradiated in the GIF B3 experiments. The generally observed tendency is the same as that observed in the 4 kGy/h experiments. At low total doses only a peak at about 600 K is observed in the DTA curves, while at high total doses a peak in the region between 525 and 570 K is observed. However, for some samples (marked with an asterisk in the figures) also an exothermal peak at about 650 K is observed.

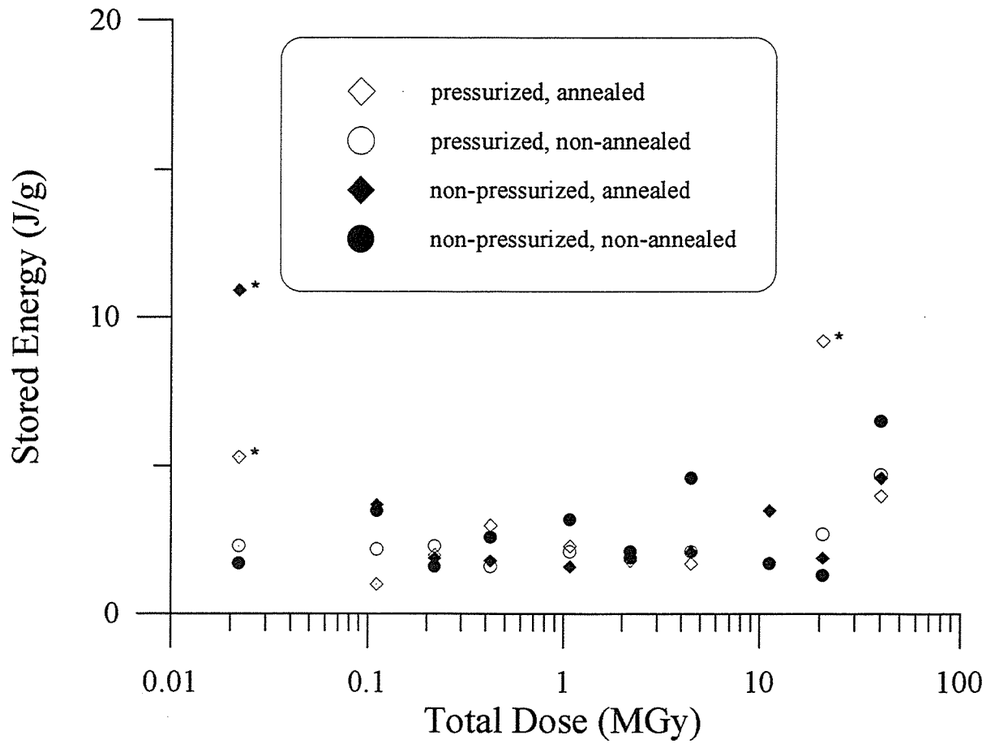


Figure 8: *Stored energy of Harshaw single NaCl crystals irradiated in GIF B3 (15 kGy/h, 100 °C)*



The occurrence of the peak at 650 K always goes accompanied by a considerable mass loss during the DTA measurement. Notice also that this 650 K peak is only observed for samples which have been annealed prior to irradiation. The Harshaw crystals were annealed in batches of four. Notice that altogether we have found exactly four Harshaw crystals in which the 650 K peak occurs. Although we have not kept record whether these Harshaw crystals were annealed simultaneously we do have this suspicion. Also we assume that during the anneal of these crystals something went wrong and that the 650 K peak has nothing to do with the irradiation experiments but is possibly due to a contamination of our samples.

As can be seen in Fig. 8, there are no systematic differences in stored energy values for either annealed or non–annealed and pressurized or non–pressurized Harshaw crystals. Although at 44 MGy total dose non–pressurized Harshaw crystals seem to contain more stored energy than the pressurized crystals. The differences are, however, within the experimental error.

As already discussed in section 4.1 comparison of Fig. 4 and 8 shows that for the Harshaw crystals irradiated in the GIF B3 experiments the obtained stored energy values are lower than those obtained in GIF B1. Also the trend of first an increasing and then a decreasing stored energy with increasing total dose in the total dose region up to 24 MGy as observed in GIF B1 is not found in GIF B3. As already explained in section 4.1 these differences are possibly due to surface effects.

Another remarkeble observation is that none of the irradiated non–annealed Harshaw crystals show any sign of the endo–and/or exothermal effects observed for the non–irradiated, non–annealed Harshaw crystals. Not even at total doses as low as 22 kGy. This means that the gamma radiation, at least at a temperature of 100 °C, is very effective in removing these effects.

Comparison of Fig. 7 and 8 shows that at total doses below 11 MGy the amounts of stored energy developed at 4 or 15 kGy/h are not very different. At higher total doses the amounts of stored energy developed at 4 kGy/h are much higher than at 15 kGy/h for the same total dose. At 44 MGy total dose the difference in stored energy is about a factor 3.

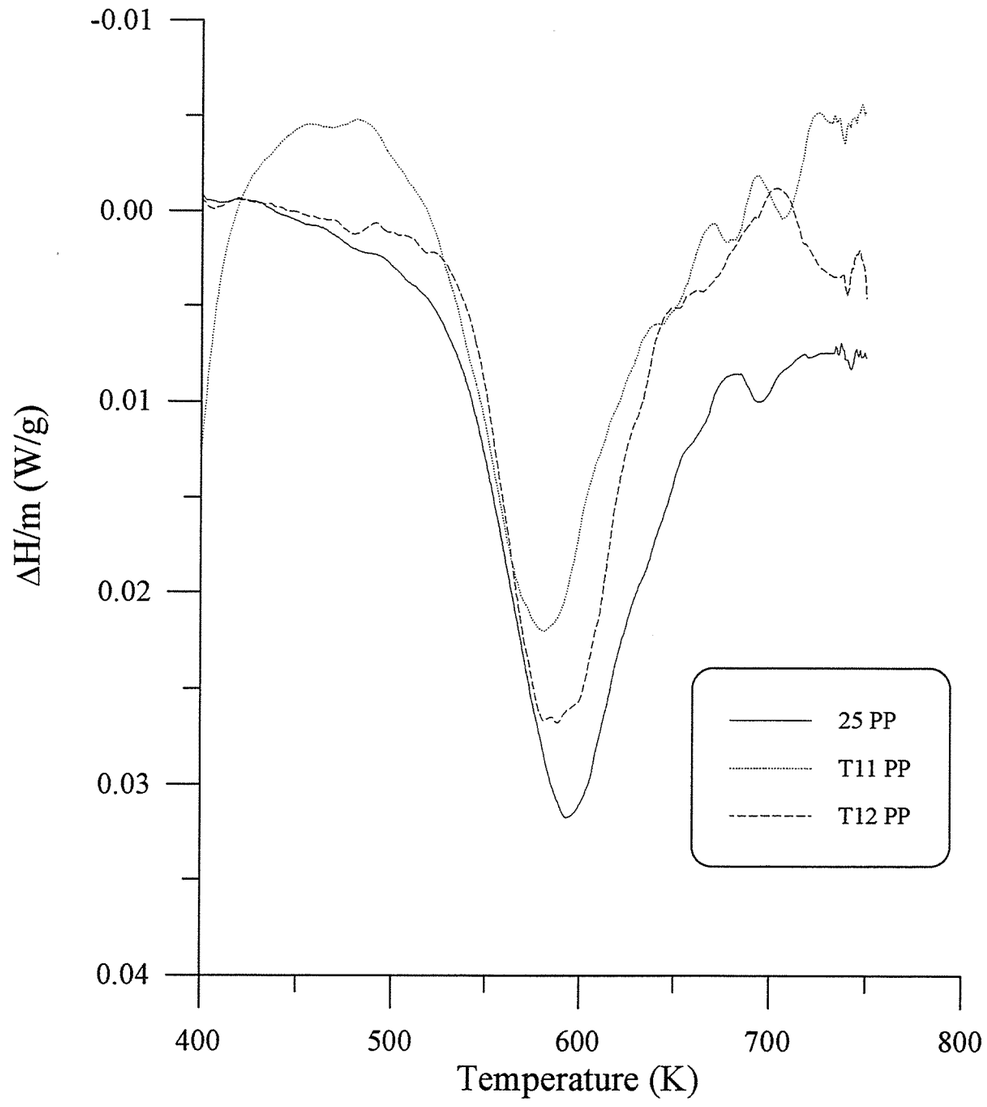


Figure 9: *DTA curves of Pressed Powder samples irradiated in GIF B2 (44 MGy, 4 kGy/h, 100 °C)*

## 4.2. Pressed Powder Samples

The DTA curves obtained for irradiated pressed powder samples show only a single exothermal peak with a maximum at about 600 K. Some of the obtained DTA curves are shown



in Fig. 9. In Fig. 10 the stored energy values obtained for the samples irradiated in GIF B2 at a dose rate of 4 kGy/h are shown as a function of total dose. The dashed line indicates the average stored energy of non–irradiated pressed powder samples. At low total doses the stored energy of the irradiated samples is lower than that of non–irradiated samples At each total dose the stored energy values observed for the various samples are within experimental error equal to each other. Up to total doses of 22 MGy the measured stored energy is approximately constant at a level of about 2 J/g. Only at a total dose of 44 MGy a higher stored energy is observed i.e. about 14 J/g.

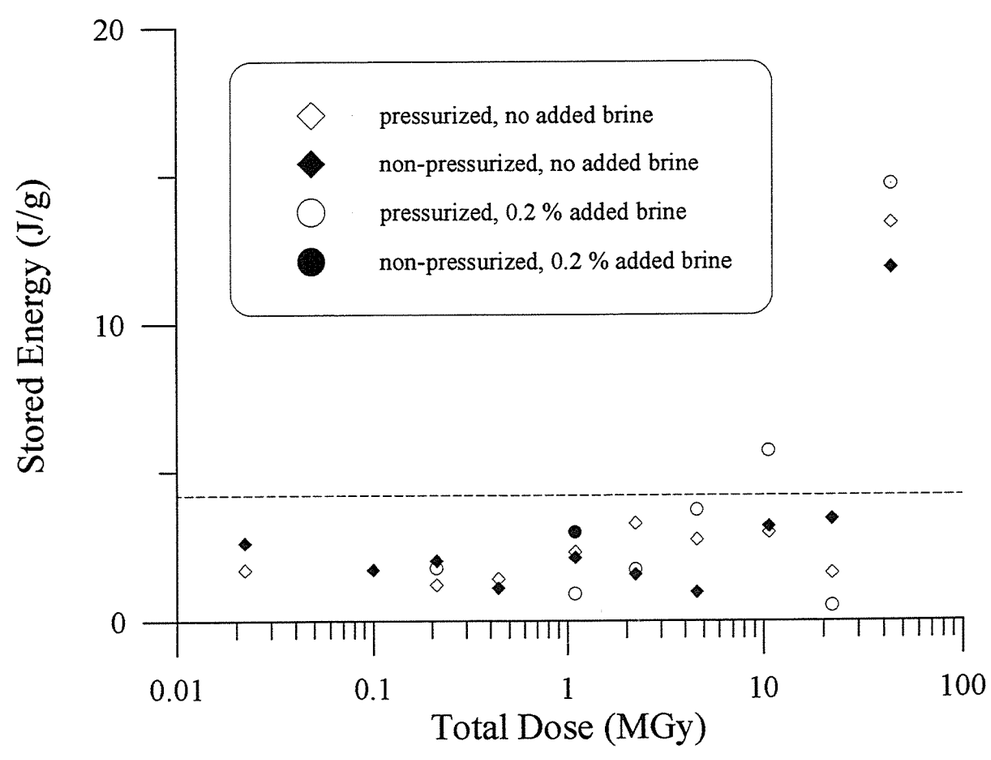


Figure 10: *Stored energy of Pressed Powder samples irradiated in GIF B2 (4 kGy/h, 100 °C)*

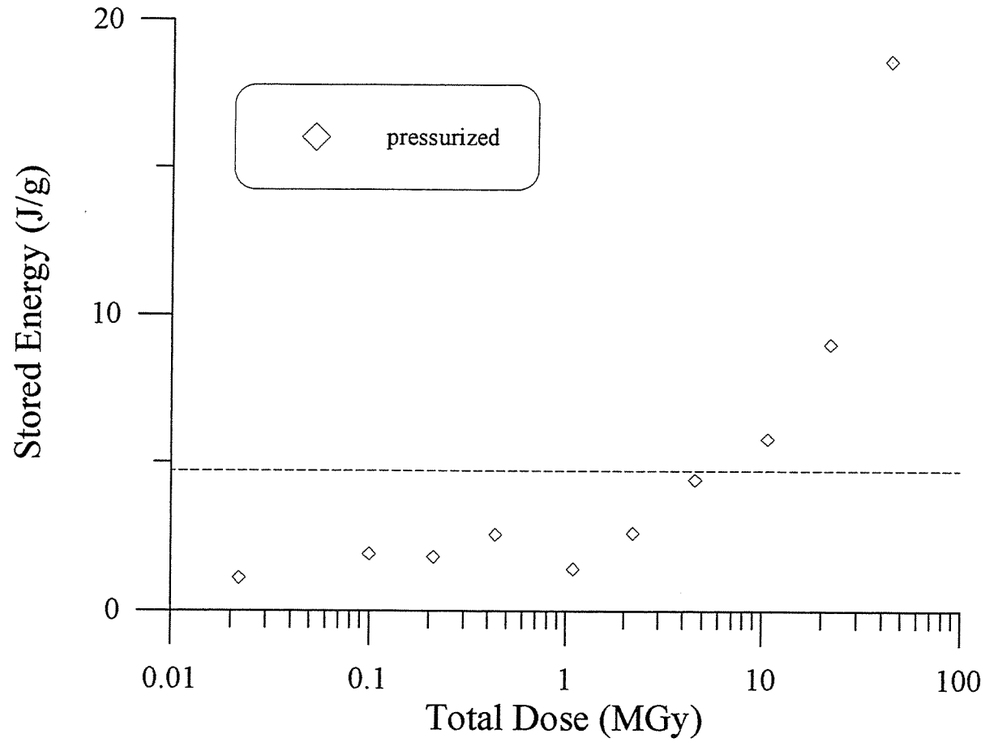


Figure 11: *Stored energy of Synthetic Salt samples irradiated in GIF B2 (4 kGy/h, 100 °C)*

### 4.3. Synthetic Rock Salt samples

For the synthetic rock salt samples we only have data from the GIF B2 experiments, i.e. only for samples irradiated at a dose rate of 4 kGy/h. Also only for pressurized samples. The DTA curves for these samples are similar to those observed for the pressed powder samples, i.e. only a broad exothermal peak at about 600 K. In Fig. 11 the stored energy observed for these samples is shown as a function of total dose. The observed dose dependence is similar to that observed for the Harshaw crystals i.e. a stored energy approximately constant at a level of about 2 J/g for total doses below 1.1 MGy and an increasing stored energy with increasing total dose above 1.1 MGy. For all studied total doses the measured stored energy values are approximately equal to those of the simultaneously irradiated Harshaw crystals.



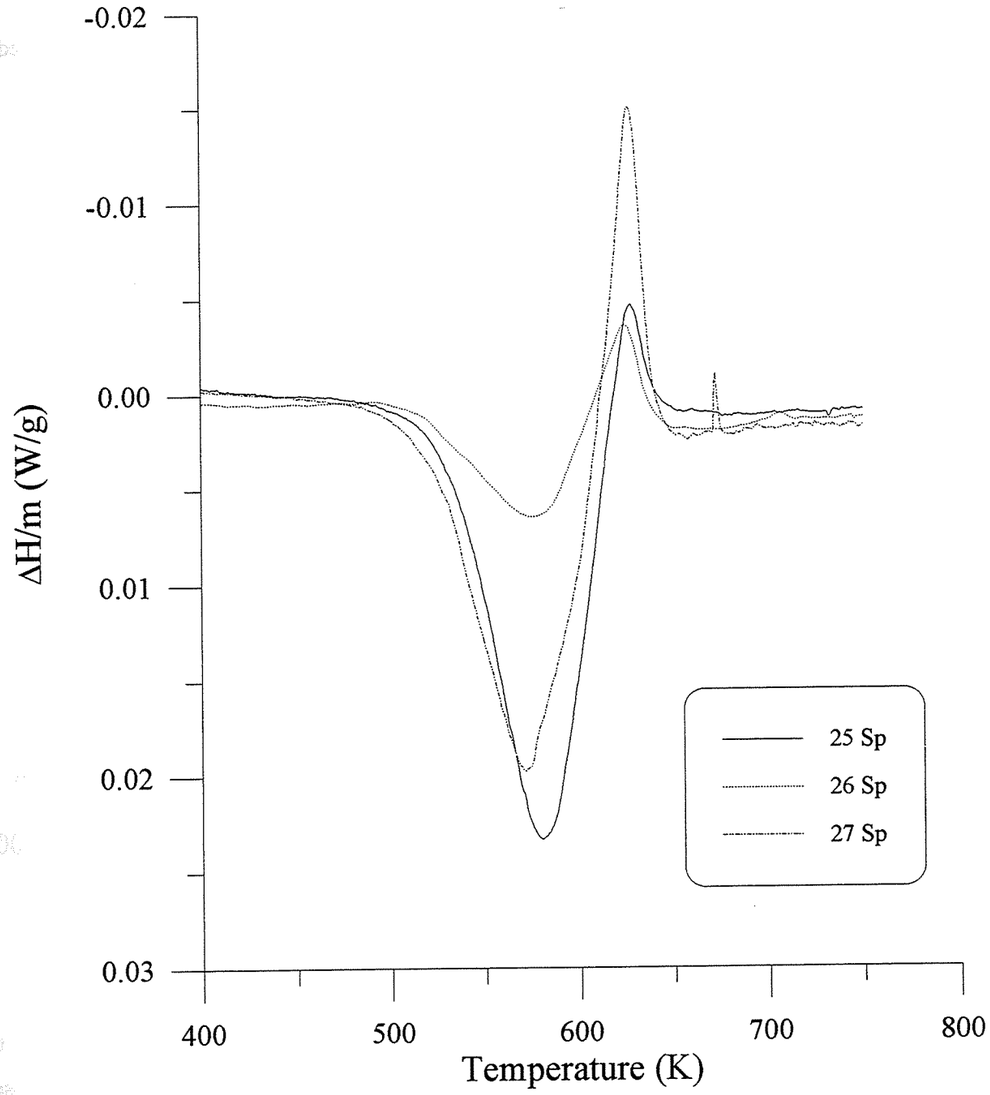


Figure 12: *DTA curves of Sp–800 samples irradiated in GIF B2 (22 MGy, 4 kGy/h, 100 °C)*

### 4.4. Asse Speisesalz of the 800 meter level (Sp–800) samples

The DTA curves obtained for irradiated Asse Speisesalz (Sp–800) samples show a similar pattern to those obtained for the non–irradiated Sp–800 samples: an exothermal peak between 485 and 705 K with a superimposed endothermal peak between 565 and 635 K due to the

dehydration of polyhalite. (see Fig. 12) Just as for the non–irradiated Sp–800 samples the stored energy values have been corrected for this endothermal effect.

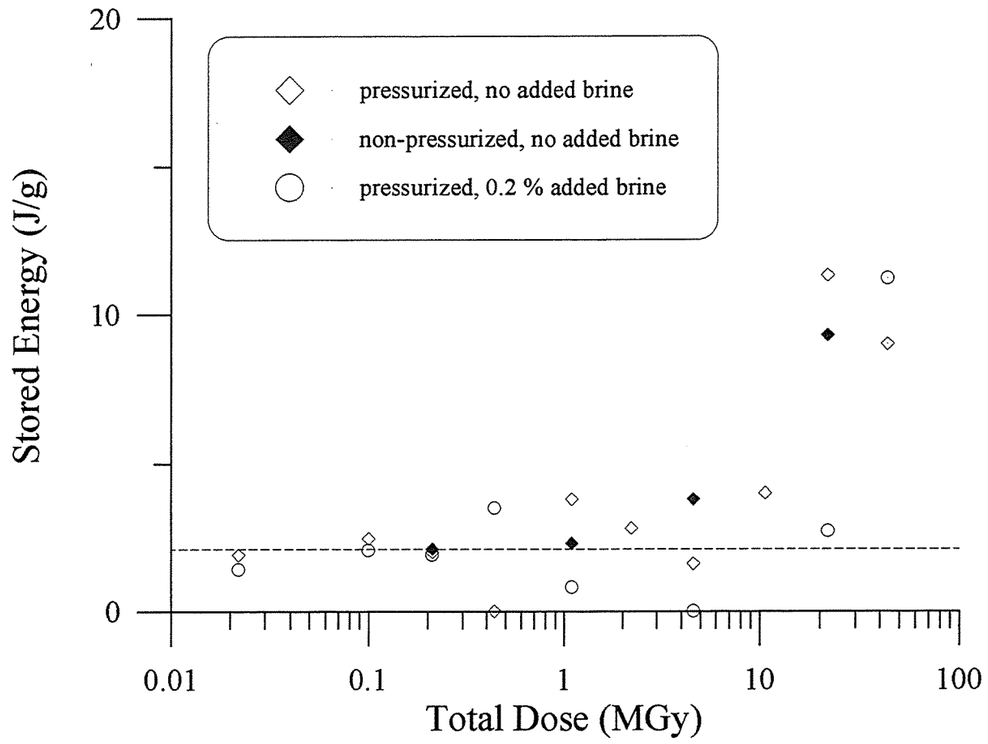


Figure 13: *Stored energy of Sp–800 samples irradiated in GIF B2 (4 kGy/h, 100 °C)*

Figure 13 shows the stored energy values obtained for the Sp–800 samples irradiated in GIF B2 at 4 kGy/h. At low total doses the stored energy values are approximately equal to those observed for the simultaneously irradiated Harshaw crystals. However the stored energy observed for the samples irradiated up to 44 MGy is much lower than that observed for the Harshaw crystals, i.e. 10 versus 18 J/g. A possible explanation for this observation is that for the stored energy measurements of the Sp–800 samples irradiated up to a total dose of 44 MGy, recrystallized and then redamaged material was selected.



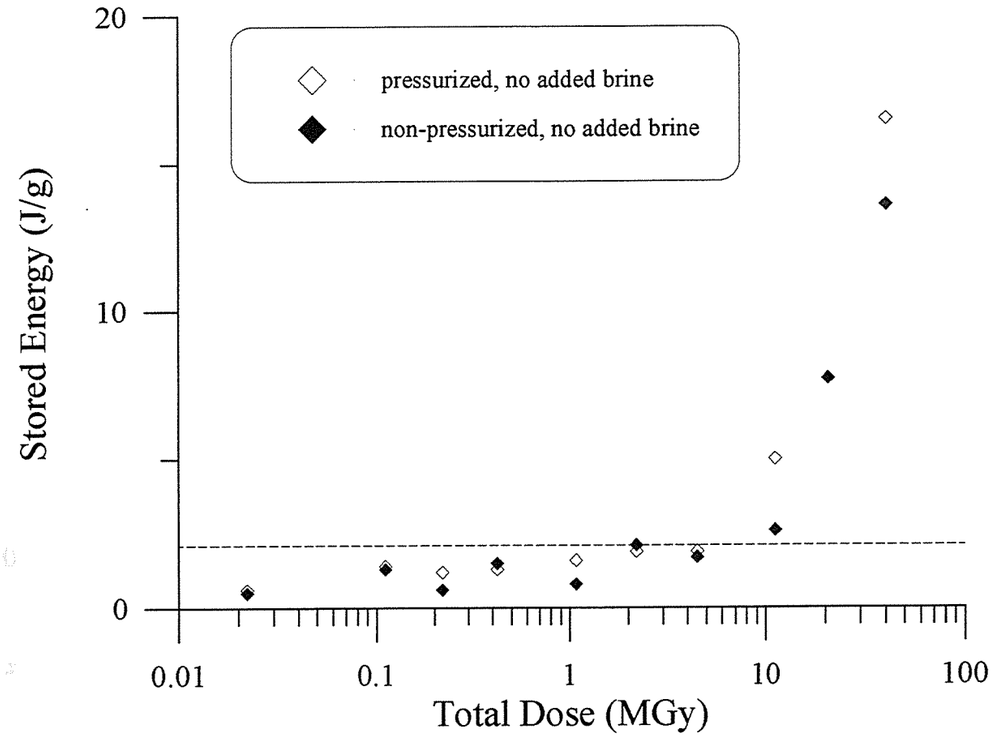


Figure 14: *Stored energy of Sp–800 samples irradiated in GIF B3 (15 kGy/h, 100 °C)*

The stored energy values obtained for the Sp–800 samples irradiated in the GIF B3 experiments are shown as a function of total dose in Fig. 14. The results obtained for the Sp–800 samples in the GIF B3 experiments are also similar to those obtained for the Harshaw single crystals, at least up to total doses of 11 MGy. At 22 and 40 MGy total dose, however, the stored energy values obtained for the Sp–800 samples are higher than those for the Harshaw crystals.

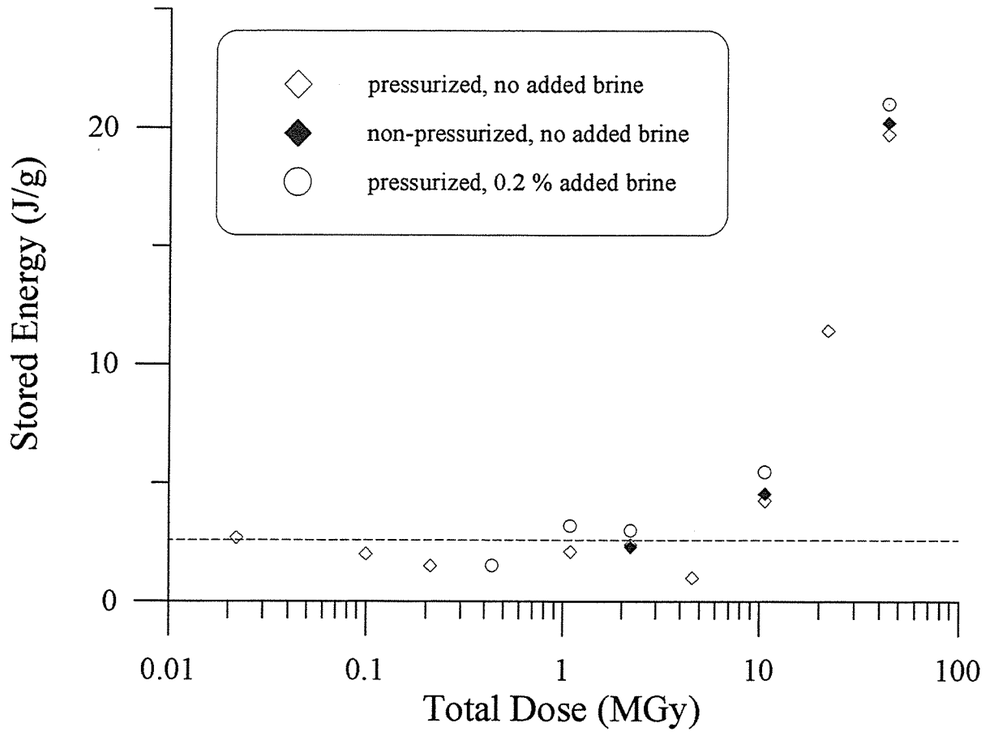


Figure 15: *Stored energy of Borehole Anhydritic samples irradiated in GIF B2 (4 kGy/h, 100 °C)*

### 4.5. Borehole Anhydritic Samples

For the borehole anhydritic samples we only have stored energy data from GIF B2, i.e. samples irradiated with a dose rate of 4 kGy/h. The DTA curves obtained for these samples only show an exothermal peak with a maximum at about 600 K. In Fig. 15 the dependence of the stored energy of these samples on total dose is shown. The observed dependence is similar to that for the Harshaw crystals irradiated in this experiment. The stored energy for the samples irradiated to 44 MGy total dose is a little higher than that of the simultaneously irradiated Harshaw crystals, 20 and 18 J/g respectively.



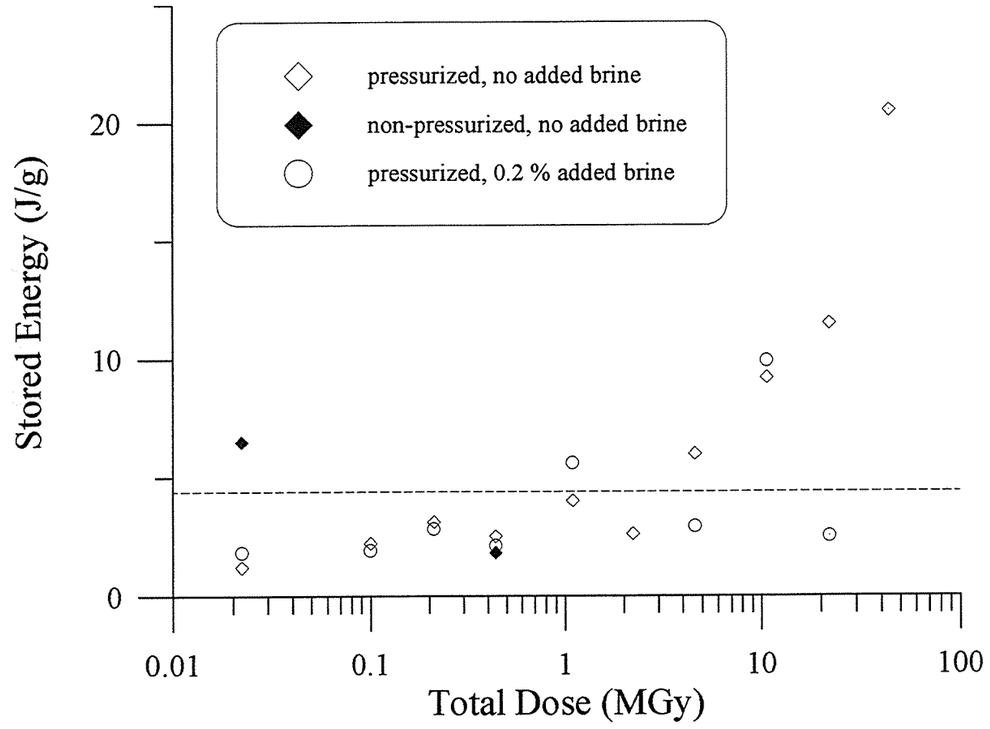


Figure 16: *Stored energy of Borehole Polyhalitic samples irradiated in GIF B2 (4 kGy/h, 100 °C)*

### 4.6. Borehole Polyhalitic Samples

The DTA curves obtained for these samples are similar to those observed for the Sp–800 samples, only the endothermal signal due to the dehydration of polyhalite is often a lot stronger. This makes it more difficult to estimate the stored energy. It is therefore not surprising that in Fig. 16, where the obtained stored energy values are shown as a function of total dose, the spread in the data points is much larger than that of the other samples. The dependence of the stored energy on total dose is however similar to that of the other samples.

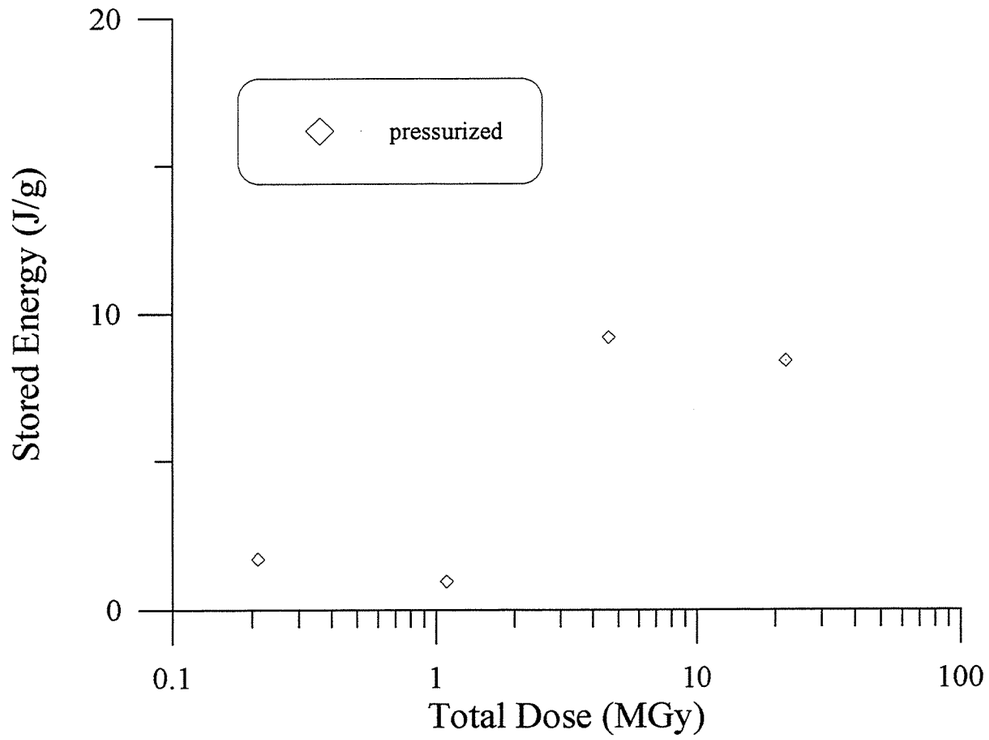


Figure 17: *Stored energy of Polyhalitic Salt samples irradiated in GIF B2 (4 kGy/h, 100 °C)*

### 4.7. Polyhalitic Salt samples

Only a few data points for these samples have been obtained and are shown in Fig. 17. The DTA curves for these samples are similar to those of the borehole polyhalitic samples.



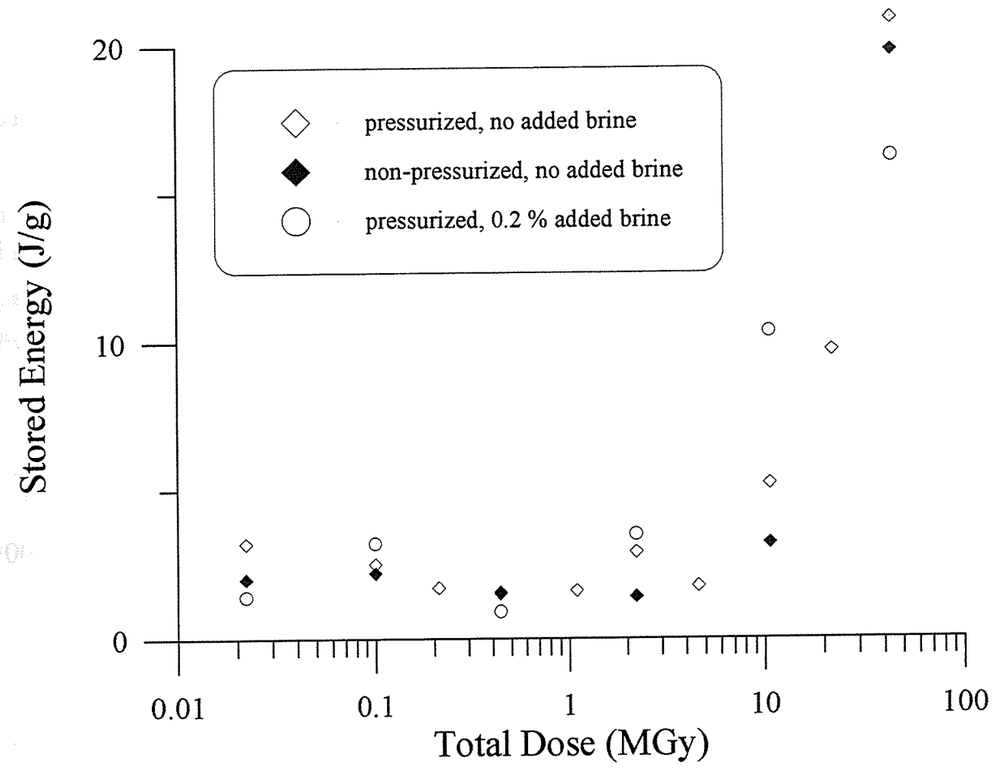


Figure 18: *Stored energy of Potassas de Llobregat samples irradiated in GIF B2 (4 kGy/h, 100 °C)*

### 4.8. Potasas de Llobregat samples

The measured stored energy values obtained for the irradiated Potasas del Llobregat samples irradiated in GIF B2 are shown in Fig. 18. The results obtained for these samples are similar to those of the other samples.

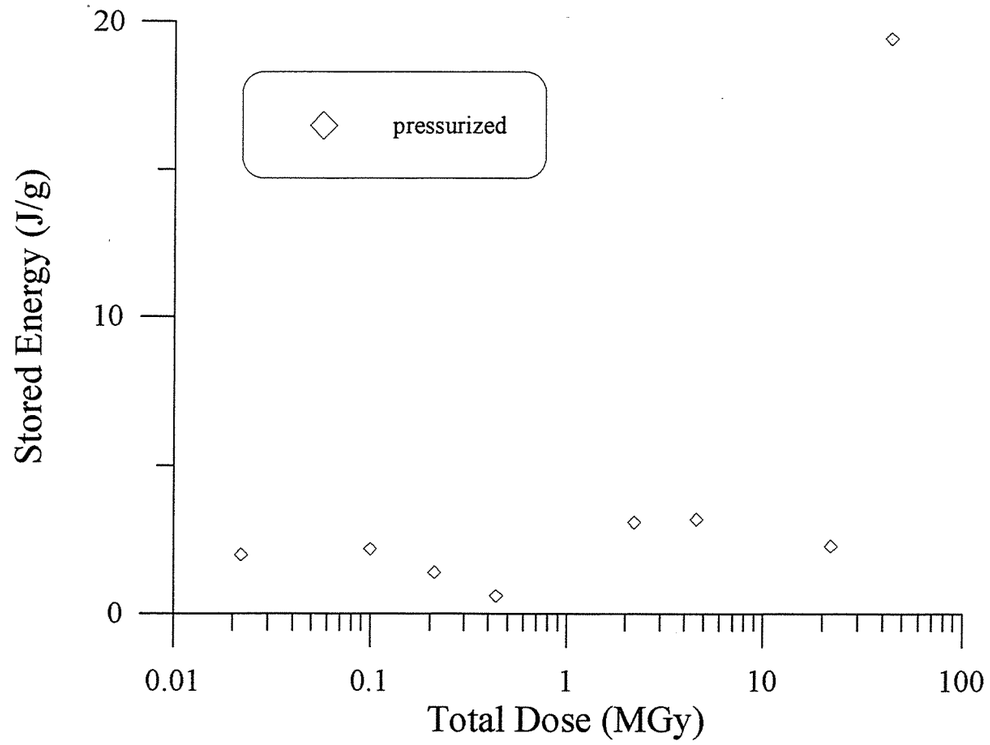


Figure 19: *Stored energy of Dutch Salt samples irradiated in GIF B2 (4 kGy/h, 100 °C)*

### 4. 9. Dutch Salt samples

The measured stored energy values obtained for the Dutch salt samples irradiated in GIF B2 are shown in Fig. 19. The results obtained for these samples are also similar to those of the other samples.

## 5. CONCLUSIONS

For total doses between 0.02 and 44 MGy, a temperature of 100 °C and dose rates of either 4 or 15 kGy/h it can be conluded that in general the stored energy developed in the most damaged parts of salt samples of different composition and microstructure, irradiated under the same conditions, is approximately equal



Hydrostatic pressure of 200 bar or less has no effect on the stored energy developed in pure NaCl single crystals during irradiation.

At a total dose of 44 MGy the stored energy developed in pure NaCl single crystals irradiated at 4 kGy/h is about a factor three higher then that developed at 15 kGy/h.

In most of the irradiated samples recrystallized material has been found. Since for the stored energy measurements presented in this article the most damaged material of the irradiated samples was selected, this means that in general bulk stored energy values will be lower than the values presented in this article.

We strongly suspect, stored energy at crystal boundaries to follow a different behaviour than at the crystal interior.

## ACKNOWLEDGEMENT

We would like to thank Mr. A.C.G. van Genderen and Dr. P.J. van Ekeren of the Thermodynamics Centre Utrecht for performing the DTA measurements and calculating the stored energy values.

## REFERENCES

A. GARCÍA CELMA, 1993: *"Radiation Damage in Natural and Synthetic Halite, Progress report December 1992 – February 1993"*, ECN–C––93–087, Netherlands Energy Research Foundation ECN, Petten, 99 p.

A. GARCÍA CELMA and H. DONKER, 1994a: *"Stored energy in irradiated salt samples"*, Nuclear Science and Technology series, EUR–14845, Commission of the European Communities, Luxembourg, 127 p.

A. GARCÍA CELMA and H. DONKER, 1994b: *"Radiation–Induced Creep of Confined NaCl"*, Rad. Eff. Def. Solids **132**, 223–247.

A. GARCÍA CELMA, H. VAN WEES and L. MIRALLES, 1991: *"Methodological developments and materials in salt–rock preparation for irradiation experiments"*, Nuclear Science and Technology Series, EUR 13266 EN, Commission of the European Communities, Luxembourg, 67 p.

A. GARCÍA CELMA, J.C. MAYOR, C. DE LAS CUEVAS and J.J. PUEYO, 1992: *"Radiation Damage in Salt"*, in: "Pilot Tests on Radioactive Waste Disposal in Underground Facilities", Ed. B. Haijtink, Nuclear Science and Technology Series, EUR 13985 EN, Commission of the European Communities, Luxembourg, p. 75–89.

A. GARCÍA CELMA, H. DONKER, W.J. SOPPE and L. MIRALLES, 1993: *"Development and Anneal of Radiation Damage in Salt: End Report August 1988 – August 1993"*, ECN–C––93–086, Netherlands Energy Research Foundation ECN, Petten, 77 p.

A. GARCÍA CELMA, A.J. NOLTEN, W.A. FELIKS and H. VAN WEES, 1995: *"Methodology of Irradiation Experiments on Non–Ground Salt Performed at the HFR in Petten"*, article 6 of this volume.

M. JIMÉNEZ DE CASTRO and J.L. ÁLVAREZ RIVAS, 1990: *"The Surface Effect on the Stored Energy in Gamma–Irradiated NaCl and LiF"*, J. Phys. Condens. Matter **2**, 1015–1019.

N. JOCKWER, 1981: *" Untersuchungen zur Art und Menge des im Steinsalz des Zechsteins enthaltenen Waser sowie dessen Freisetzung und Migration im Temperaturfeld endlagerter radioaktiver Abfälle"*, Ph.D. Thesis, Technische Universität Clausthal, 135 p.

J.J. PUEYO, C. DE LAS CUEVAS, J. GARCÍA, P. TEIXIDOR and L. MIRALLES, 1992: *"Geochemical Characterization"*, in "Textural and Fluid Phase Analysis of Rock Salt Subjected to the Combined Effects of Pressure, Heat and Gamma Radiation, Part A". Ed. F. Huertas, J.C. Mayor and C. Del Olmo, Nuclear Science and Technology Series, EUR 14169 EN, Commission of the European Communities, Luxembourg, p. 3–64.

T. ROTHFUCHS, K. DUIJVES and R. STIPPLER, 1988: *"Das HAW–projekt. Demonstrationseinlagerung Hochradioaktiver Abfälle im Salzbergwerk Asse"*, Nuclear Science and Technology Series, EUR–11875–DE/EN, Commission of the European Communities, Luxembourg, 227 p.

P. SCHUTJENS, 1991: *"Intergranular Pressure Solution in Halite Aggregates and Quartz Sands: an Experimental Investigation"*, Ph. D. Thesis, Utrecht University, p.123–124.

C.J. SPIERS, J.L. URAI, G.S. LISTER, J.N. BOLAND and H.J. ZWART, 1986: *"The Influence of Fluid–Rock Interaction on the Rheology of Salt Rock"*, Nuclear Science and Technology Series, EUR–10399, Commission of the European Communities, Luxembourg, 131 p.

J.L. URAI, C.J. SPIERS, H.J. ZWART and G.S. LISTER, 1986: *"Weakening of Rock Salt by Water During Long–Term Creep"*, Nature **324**, 554–557.



# ON THE SATURATION OF RADIATION DAMAGE IN IRRADIATED NATURAL ROCK SALT

**H. Donker and A. Garcia Celma**

## ABSTRACT

Natural rock salt samples of the 800 m. level from the Asse mine, Remlingen, Germany were gamma–irradiated at 100 °C with spent fuel elements from the High Flux Reactor at Petten, The Netherlands. Dose rates in the experiments varied between 200 and 20 kGy/h in monthly cycles. After irradiation the radiation induced stored energy was studied as a function of total dose. Total doses of up to 1200 MGy were reached. Initially there is an approximately linear increase of stored energy with increasing total dose, which levels of at higher doses until it reaches a saturation value of about 140 J/g. The results of the stored energy measurements were compared with those obtained by other scientists for irradiated pure and K–doped NaCl single crystals.

## 1. INTRODUCTION

One of the considered options for the disposal of radioactive waste consists of depositing the waste in deep rock salt formations. Rock salt however, is known to be very susceptible to radiation damage when exposed to ionizing radiation. Therefore, much research on radiation damage in rock salt and its safety aspects for repository concepts has been performed during the last decades.

The primary defects formed upon irradiation of alkali halides are F– and H–centres, which result from the radiation–less decay of excitons [Itoh, 1982]. Upon prolonged irradiation, depending on the temperature, the F–centres can aggregate forming colloidal metallic particles [Hughes, 1983; Hughes and Jain, 1979]. Also prismatic dislocation loops have been observed to develop during irradiation of alkali halides. According to Hobbs et al. [1973] these dislocation

A. GARCÍA CELMA, J.C. MAYOR, C. DE LAS CUEVAS and J.J. PUEYO, 1992: *"Radiation Damage in Salt"*, in: "Pilot Tests on Radioactive Waste Disposal in Underground Facilities", Ed. B. Haijtink, Nuclear Science and Technology Series, EUR 13985 EN, Commission of the European Communities, Luxembourg, p. 75–89.

A. GARCÍA CELMA, H. DONKER, W.J. SOPPE and L. MIRALLES, 1993: *"Development and Anneal of Radiation Damage in Salt: End Report August 1988 – August 1993"*, ECN–C––93–086, Netherlands Energy Research Foundation ECN, Petten, 77 p.

A. GARCÍA CELMA, A.J. NOLTEN, W.A. FELIKS and H. VAN WEES, 1995: *"Methodology of Irradiation Experiments on Non–Ground Salt Performed at the HFR in Petten"*, article 6 of this volume.

M. JIMÉNEZ DE CASTRO and J.L. ÁLVAREZ RIVAS, 1990: *"The Surface Effect on the Stored Energy in Gamma–Irradiated NaCl and LiF"*, J. Phys. Condens. Matter **2**, 1015–1019.

N. JOCKWER, 1981: *" Untersuchungen zur Art und Menge des im Steinsalz des Zechsteins enthaltenen Waser sowie dessen Freisetzung und Migration im Temperaturfeld endlagerter radioaktiver Abfälle"*, Ph.D. Thesis, Technische Universität Clausthal, 135 p.

J.J. PUEYO, C. DE LAS CUEVAS, J. GARCÍA, P. TEIXIDOR and L. MIRALLES, 1992: *"Geochemical Characterization"*, in "Textural and Fluid Phase Analysis of Rock Salt Subjected to the Combined Effects of Pressure, Heat and Gamma Radiation, Part A". Ed. F. Huertas, J.C. Mayor and C. Del Olmo, Nuclear Science and Technology Series, EUR 14169 EN, Commission of the European Communities, Luxembourg, p. 3–64.

T. ROTHFUCHS, K. DUIJVES and R. STIPPLER, 1988: *"Das HAW–projekt. Demonstrationseinlagerung Hochradioaktiver Abfälle im Salzbergwerk Asse"*, Nuclear Science and Technology Series, EUR–11875–DE/EN, Commission of the European Communities, Luxembourg, 227 p.

P. SCHUTJENS, 1991: *"Intergranular Pressure Solution in Halite Aggregates and Quartz Sands: an Experimental Investigation"*, Ph. D. Thesis, Utrecht University, p.123–124.

C.J. SPIERS, J.L. URAI, G.S. LISTER, J.N. BOLAND and H.J. ZWART, 1986: *"The Influence of Fluid–Rock Interaction on the Rheology of Salt Rock"*, Nuclear Science and Technology Series, EUR–10399, Commission of the European Communities, Luxembourg, 131 p.

J.L. URAI, C.J. SPIERS, H.J. ZWART and G.S. LISTER, 1986: *"Weakening of Rock Salt by Water During Long–Term Creep"*, Nature **324**, 554–557.



# ON THE SATURATION OF RADIATION DAMAGE IN IRRADIATED NATURAL ROCK SALT

**H. Donker and A. Garcia Celma**

## ABSTRACT

Natural rock salt samples of the 800 m. level from the Asse mine, Remlingen, Germany were gamma–irradiated at 100 °C with spent fuel elements from the High Flux Reactor at Petten, The Netherlands. Dose rates in the experiments varied between 200 and 20 kGy/h in monthly cycles. After irradiation the radiation induced stored energy was studied as a function of total dose. Total doses of up to 1200 MGy were reached. Initially there is an approximately linear increase of stored energy with increasing total dose, which levels of at higher doses until it reaches a saturation value of about 140 J/g. The results of the stored energy measurements were compared with those obtained by other scientists for irradiated pure and K–doped NaCl single crystals.

## 1. INTRODUCTION

One of the considered options for the disposal of radioactive waste consists of depositing the waste in deep rock salt formations. Rock salt however, is known to be very susceptible to radiation damage when exposed to ionizing radiation. Therefore, much research on radiation damage in rock salt and its safety aspects for repository concepts has been performed during the last decades.

The primary defects formed upon irradiation of alkali halides are F– and H–centres, which result from the radiation–less decay of excitons [Itoh, 1982]. Upon prolonged irradiation, depending on the temperature, the F–centres can aggregate forming colloidal metallic particles [Hughes, 1983; Hughes and Jain, 1979]. Also prismatic dislocation loops have been observed to develop during irradiation of alkali halides. According to Hobbs et al. [1973] these dislocation

loops are formed due to the displacement of neighbouring $Na^+$ and $Cl^-$ ions from their normal lattice sites to the extra half–plane of the dislocation loop. The $Na^+$ and $Cl^-$ ion are displaced by two H–centres which on their turn form molecular halide centres which occupy the created divacancies. These molecular halide centres surrounding the dislocation loops can possibly collapse into halide gas bubbles [Hobbs, 1974]. A detailed discussion on the basic principles of the damage formation process in NaCl can be found in [Soppe et al., 1994]

One of the considered risks for a repository is the possibility of a sudden back reaction of the Na colloids and the molecular $Cl_2$ produced under irradiation. Such a back reaction could occur if the concentration of these defects exceeds a certain percolation threshold. It has been reported that such a back reaction might have an explosive character [den Hartog et al., 1993]. Therefore, one of the questions that has to be answered for a repository is whether the created damage will only reach a saturation level well below the percolation threshold or whether this treshold will be reached, making a back reaction possible.

The experimental results obtained for pure single crystals of NaCl by Jenks and Bopp [1974; 1977] and Groote and Weerkamp [1990] show a saturation of damage at a few mol%. These experimental results can be satisfactorily described by the modified Jain–Lidiard model [Jain and Lidiard, 1977; Lidiard, 1979; van Opbroek and den Hartog, 1985]. Calculations with this model simulating repository conditions showed that if a proper disposal strategy is chosen the damage in a repository would also be limited to a few mol% [Bergsma et al, 1985; de Haas and Helmholdt, 1989]. However, results obtained by Den Hartog and coworkers for some doped single crystalline samples showed that for these samples the damage levels were much higher than for pure NaCl, reaching up to 10 mol% damage [den Hartog et al., 1993; Groote and Weerkamp, 1990]. Furthermore Den Hartog claims that natural rock salt samples show a similar behaviour as these doped samples [den Hartog et al., 1993]. The modified Jain–Lidiard model cannot explain the enhancement of damage formation by impurities. Since the natural rock salts in a repository are usually highly impure, the results of Den Hartog et al. put doubts on the predictions obtained with the modified Jain–Lidiard model. The model recently developed by Soppe [1993] however, reasonably reproduces the damage enhancement found for K–doped samples. Simulations of repository conditions with this model showed that also for doped NaCl the damage in a repository would not exceed a few mol% [Soppe and Prij, 1994]. The model of Soppe was shown to be capable of reproducing a broad spectrum of experimental results.



The natural rock salt in a repository is, however, very different from the homogeneous single crystals studied in most experiments. Natural rock salts are polycrystalline and very heterogeneous. Although some irradiation experiments on natural rock salts have been performed [Swyler et al., 1979; 1980; Levy, 1983; Levy et al., 1980; 1983; 1984; Levy and Kierstead, 1982; Loman et al., 1982], very little is known about the effects of polycristallinity and heterogeneity on the formation of radiation damage. It has been known that after irradiation Fluid Assisted Recrystallization occurs in polycrystalline salt samples [Garcia Celma et al., 1988]. Recently, Garcia Celma and Donker [1994a] have shown that in natural samples irradiated at relatively low dose rates various recrystallization and recovery processes occur during irradiation.

In this paper the results of stored energy measurements on natural rock salt samples (Asse speisesalz of the 800 meter level) irradiated at relatively high dose rates (see below) are presented. These irradiation experiments have been performed in order to see whether the damage in these samples would reach a saturation and if so at which level. And also in order to check whether these samples would behave like K–doped single crystals as claimed by den Hartog et al.[1993] or not. The results will therefore, be compared with results obtained by other scientists for pure and doped NaCl.

## 2. EXPERIMENTAL

### 2.1. Samples

For the presently described experiment we have used natural salt samples, i.e. Speisesalz from the 800 meter level of the Asse mine, Remlingen, Germany (Sp–800). These salt samples consist of a relatively high purity ( > 99.0 % ) polycrystalline halite rock, with a grain size of 3 – 10 mm. The main impurity phase in these samples is polyhalite ($K_2MgCa_2(SO_4)_4.2H_2O$ – ~1%), while occasionally anhydrite ($CaSO_4$) is also present. The material has besides the structurally bound water (polyhalite) a water content of about 0.05 wt % which is mainly present in fluid inclusions at grain boundaries. Dislocation densities within individual grains are rather low while slip and kink bands are almost entirely absent [Spiers et al., 1986; Gies, 1995].

Samples in the shape of cylindrical tablets with a diameter of about 24 mm and a height of 10 mm were prepared as described in [Garcia Celma et al., 1991] and placed in golden sample holders. Five of these golden sample holders were placed on top of each other in a stainless steel holder where they were held in position by a spring. Care was taken that the fitting between the samples and the holders and between the golden and steel holders was as tight as possible to ensure a good thermal contact between the samples and the irradiation facility. Eight of the stainless steel holders were placed in one of the Gamma Irradiation Facilities (GIF) in the pool of the reactor at Petten (the Netherlands) so that 40 samples were irradiated at the same time [Garcia Celma et al., 1995].

## 2.2. Irradiation set-up

The Gamma Irradiation Facility (GIF) of the ECN is extensively described in [Garcia Celma and Donker, 1994b]. Essentially each GIF experiment is performed in a long container equipped with heating and cooling devices in which eight sample holders can be placed. The container is placed between the spent fuel elements in the cooling pool of the High Flux Reactor (HFR). The temperature for the experiments was kept at 100°C. For the GIF A experiment, fresh spent fuel elements from the HFR were used in order to obtain a dose rate as high as possible. Each month four of the older spent fuel elements were replaced by fresh elements. As a consequence, the dose rate in our experiment varied between 200 and 20 kGy/h in monthly cycles. Each month one of the samples was retrieved from the facility and replaced by a new one.

Dose rates were measured at regular intervals using red perspex dosimeters. The measurements are performed by temporarily removing the sample container from its position and lowering a measuring tube containing the perspex between the spent fuel elements at the position of the sample container. The measuring tube is designed in such a way that its absorbing power for gamma rays is equal to that of the sample container. To calculate the total dose received by the samples in each cycle the measured dose rates are fitted to the equation:

$$D = A_0 + A_1 e^{(-A_2 t)} + A_3 t \qquad (1)$$



in which D is the dose rate, t is time and $A_0$, $A_1$, $A_2$ and $A_3$ are fitting parameters. This equation is then integrated to calculate the total dose. As an example the measured dose rates and obtained fits for one of the samples are shown in Fig. 1.

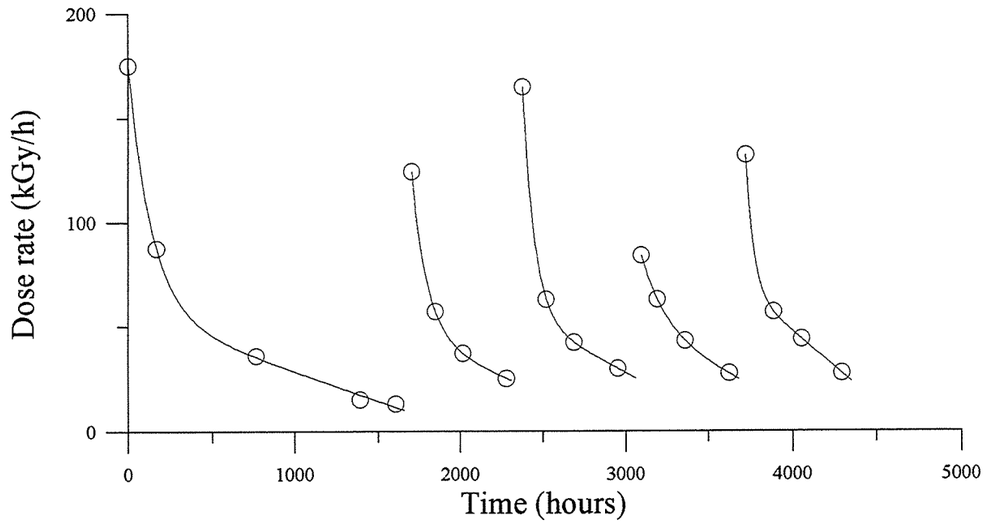


Figure 1: *Dose rate history of one of the irradiated Sp-800 samples.*

## 2.3. Stored energy measurements

The stored energy measurements were carried out by means of differential thermal analysis on a SETARAM DSC-111. Calibrations were performed by melting Indium metal. Anneals take place in "closed" Pt capsules with a small capillary hole to allow gases to escape in order to avoid explosion of the capsule when pressure builds up. The heating rate used for these measurements was, if not indicated otherwise, 10 K/min. In a first run the sample is measured against an empty reference sample holder up to a temperature of 750 K. Then the sample and reference are allowed to cool down and a background signal is measured in a second run. The result of the second run is subtracted from that of the first. The area closed by the resulting curve and the base line is then integrated to obtain the released stored energy.

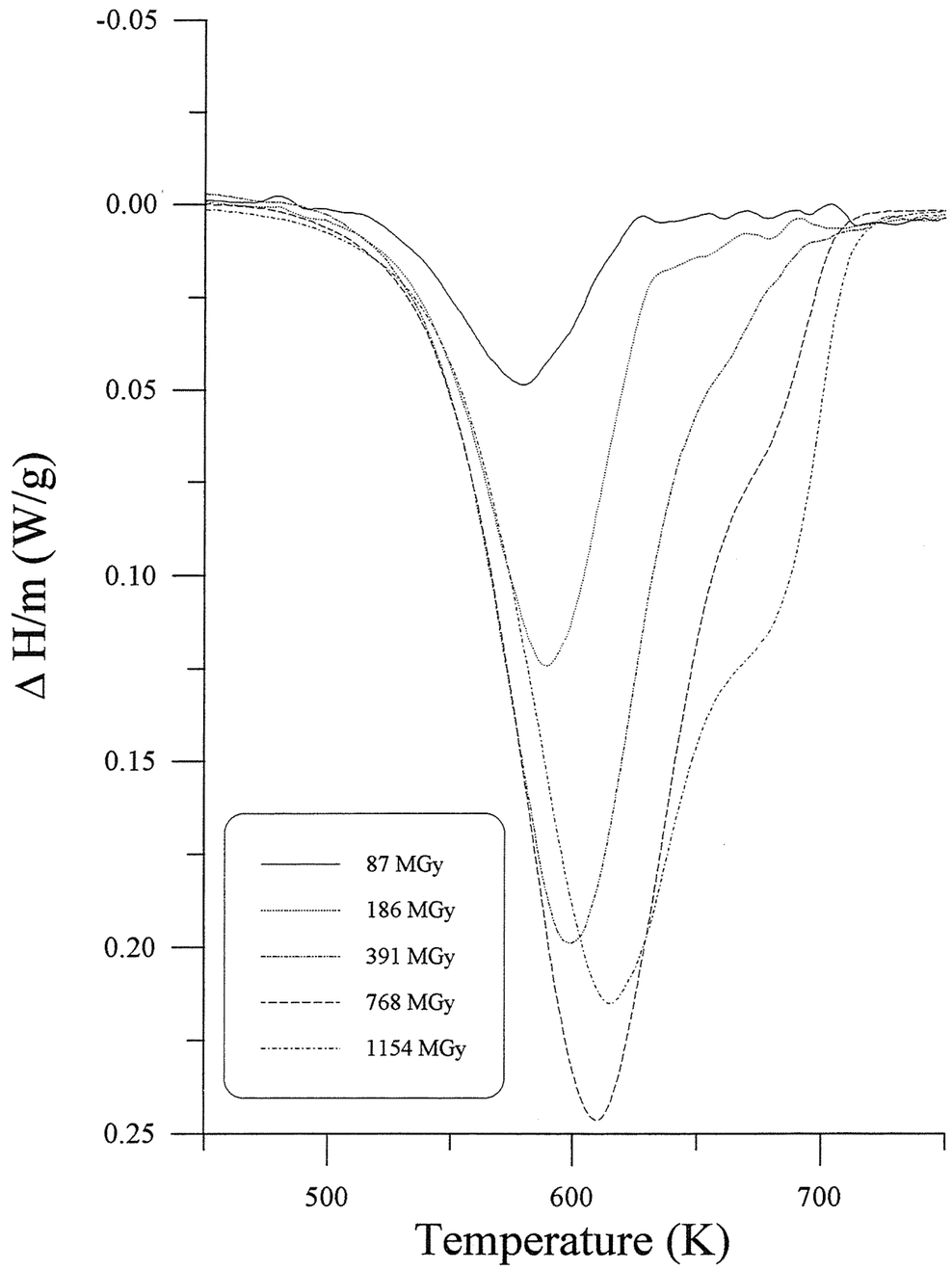


Figure 2: *DTA curves of irradiated Sp–800 samples. Heating rate 10 K/min.*



For the stored energy measurements, parts of the irradiated samples were cut in small pieces. The darkest of those pieces (i.e. free from secondary minerals and recrystallized material) were selected with the naked eye. Small portions of secondary minerals and recrystallized material may however, still have been present in the analyzed material.

According to the measurements of Jockwer [1981], polyhalite loses its crystal water between 235 and 350 °C. Our analysis showed that the dehydration of polyhalite takes place in the same temperature interval as the release of stored energy. This results in the presence of an endothermal peak superposed on the exothermal release of stored energy. When necessary our results have therefore, been corrected for the dehydration of polyhalite.

## 3. RESULTS AND DISCUSSION

A few representative results of the DTA measurements on the irradiated Sp–800 samples are shown in Fig. 2 where the heat flow (Δ H) divided by the sample weigth (m) is plotted versus temperature (T). At low total dose only one single stored energy peak is observed which maximum lies at about 600 K. At higher total doses, however, a shoulder develops on the high temperature side of this peak. The results of the DTA measurements performed on Sp–800 samples irradiated up to high total doses are similar to the results of the DSC measurements on Ba, K or F doped NaCl reported by Grootte and Weerkamp [1990]. We have considered that the shoulder might be caused by a possible endothermal signal from the dehydration of polyhalite. However, we have to reject this possibility for two reasons:

a) In Sp–800 samples in which large amounts of polyhalite are present the temperature of the maximum of the endothermal peak corresponding to the dehydration is situated at 625 K. If the shoulder in the presently described measurements would be due to the dehydration of polyhalite it ought to appear at a lower temperature.

b) The dehydration of polyhalite is normally accompanied by a considerable mass loss due to the evaporation of water. For most of the Sp–800 samples showing the shoulder in their DTA curve, the mass loss during these measurements was negligible.

Therefore, we have to conclude that the DTA curves consist of a double stored energy peak.

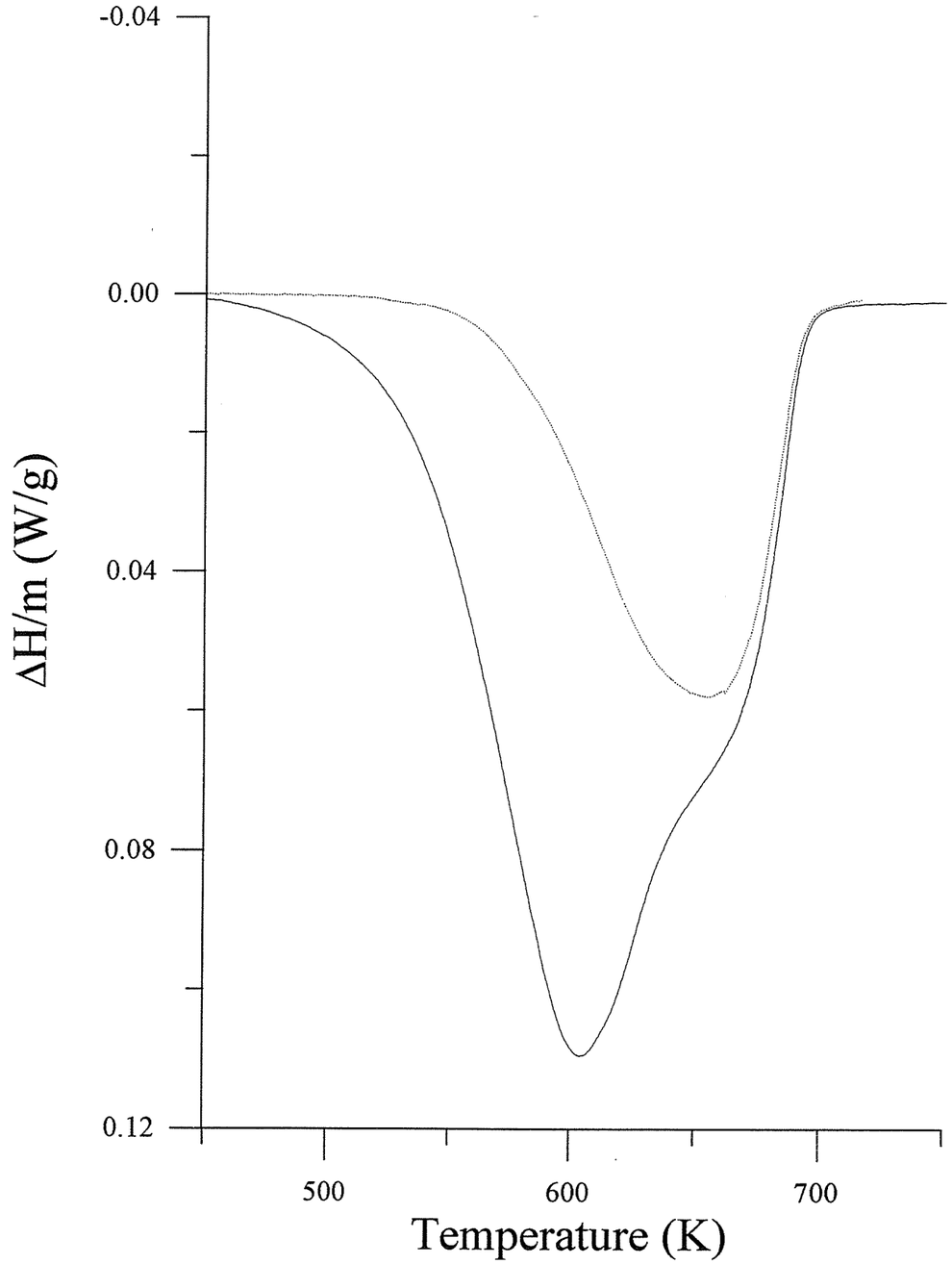


Figure 3: *DTA curves of irradiated Sp–800 sample (Total dose 1223 Mgy). Drawn line: non–annealed sample, dashed line: sample annealed for 30 minutes at 575 K. Heating rate 5 K/min.*



To check this conclusion we annealed one of the irradiated samples showing this double peak during 30 minutes at about 575 K. Then the sample was allowed to cool down to about 400 K. After that we performed a stored energy measurement as usual. The thus obtained DTA curve (Fig. 3) shows a single exothermal peak with a maximum at 655 K. This confirms our conclusion since if the shoulder would have been caused by an endothermal signal we ought to have observed it also after the anneal, what is clearly not the case. The area under the peak observed at 655 K corresponds to a stored energy of 56 J/g. After the anneal at 575 K the sample was still dark blue coloured, almost black. We therefore have to conclude that both stored energy peaks are caused by sodium colloids in the samples and that obviously there are two different kinds of colloids. A closer look at the DTA curves of all samples irradiated above 800 MGy shows that, with increasing total dose, the peak at 655 K seems to grow at the expense of the peak at 600 K, while the total stored energy remains approximately constant (see below). This indicates that one kind of colloid is converted into the other. A possible explanation for this conversion might be a phase transition which occurs when the colloids grow bigger. For very small colloids the sodium atoms are expected to retain the positions of the FCC Na sublattice of NaCl. The crystal structure of bulk sodium however, is BCC. A phase transition from FCC to BCC sodium colloids is therefore expected. Another explanation for the two kinds of colloids might be that certain sizes of colloids are energetically favourable due to the mismatch between the lattice parameters of the Na–lattice and the NaCl–lattice. Further research on this subject is however necessary.

The results of the stored energy measurements on the irradiated Sp–800 samples are shown in Fig. 4 as a function of total dose. The results show that, at low total doses, there is an approximately linear increase of stored energy with increasing total dose. At high doses (> 400 MGy) this increase levels off and the stored energy reaches a saturation value of approximately 140 J/g. In Fig. 4, the results obtained by Jenks and Bopp [1977] for pure NaCl Harshaw crystals, irradiated at 95 °C and a constant dose rate of 100 kGy/h and the results obtained by Den Hartog and coworkers [den Hartog et al., 1993; Groote and Weerkamp, 1990] for pure and 1 mol% K doped NaCl samples irradiated at 100 °C and a constant dose rate of 120 kGy/h are shown for comparison. From Fig. 4 it can be seen that the dependence of the stored energy on total dose observed for the Sp–800 samples is similar to that observed by Jenks and Bopp and Den Hartog and coworkers for pure NaCl single crystals although the results for the Sp–800 samples always are somewhat lower than the results obtained for pure NaCl by the other authors. We estimate the error for our data at about 20 % (both in the measured stored energy as in the calculated total

dose) while probably the same applies for the other experiments. In view of these large errors the correspondence between the experiments is quit good

.

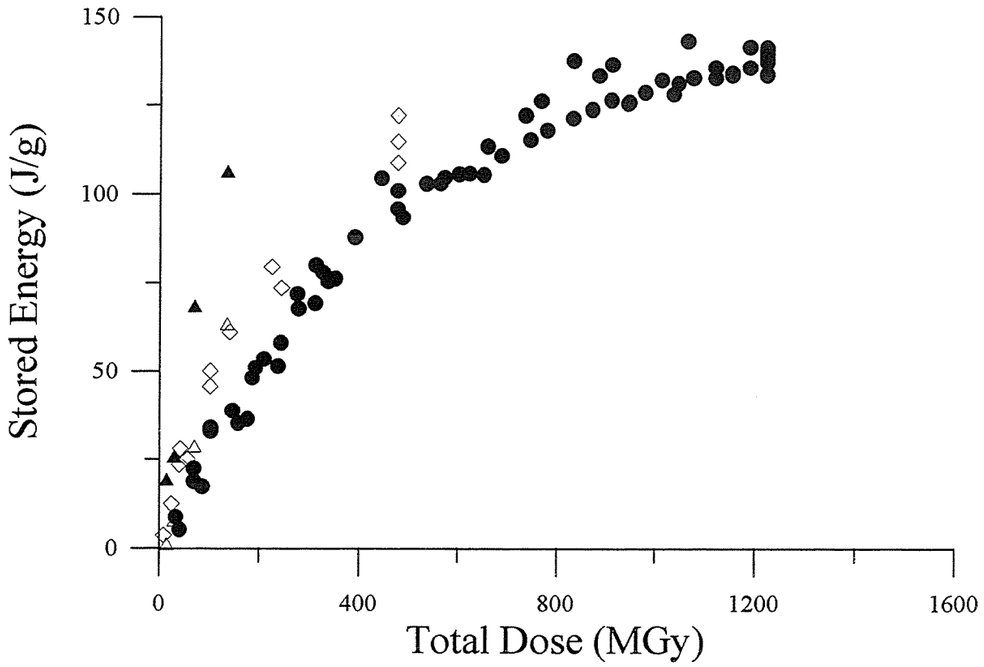


Figure 4: *Stored energy as a function of total dose. Full circles: Sp–800 samples, open squares: pure NaCl irradiated at 95 °C and 100 kGy/h by Jenks and Bopp, open triangles: pure NaCl and closed triangles: K–doped NaCl both irradiated at 100 °C and 120 kGy/h by den Hartog et al.*

The differences with the K–doped samples irradiated by Den Hartog et al. are, however, larger. Together with the Sp–800 samples shown in Fig. 4, we have also irradiated a Harshaw NaCl single crystal. The stored energy in this single crystal is approximately equal to that of the Sp–800 sample with the same irradiation history (total dose 279 MGy, stored energy 63 and 67 J/g respectively). Also from many other experiments in which we have irradiated Harshaw crystals and Sp–800 samples simultaneously we have observed that although their DTA curves are very different, the amount of stored energy developed in these samples is not very different



[Garcia Celma and Donker, 1994b]. We therefore have to conclude that the Sp–800 samples in this aspect do not show a similar behaviour as K–doped samples, contrary to the natural samples studied by Den Hartog et al. Moreover, as can be seen from Fig. 4, we have clearly observed a saturation behaviour for the stored energy developed in our Sp–800 samples. Den Hartog et al have reported that their K–doped samples (although irradiated at a much higher dose rate) do not show a saturation behaviour.

For Sp–800 samples irradiated at low dose rate (15 kGy/h) to relatively low total dose (0.02 to 44.6 MGy) we have shown that various recrystallization and recovery mechanisms are operative, competing with the damage development process [Garcia Celma and Donker, 1994a]. One of these processes, Fluid Assisted Recrystallization (FAR) can take place provided that intergranular brine is present in the salt [Garcia Celma et al., 1988; 1993]. Sp–800 samples on the average contain 0.05 wt% of water, mainly in fluid inclusions at their grain boundaries [Spiers et al., 1986]. It is therefore very unlikely that FAR will not have operated in our samples. However, if colloids are present in the salt the water needed for FAR will be decomposed during its operation. Since we have observed, from the dark blue colour of the samples, that colloids are present in all presently reported samples, FAR can only have played a role in the low dose region of the described experiment. In the high dose region all the water in the sample will have been decomposed and the operation of FAR will have been stopped. To what extent other recrystallization and recovery processes have played a role we do not know since the irradiated samples are so deeply coloured that it was impossible to produce mechanically the thin sections in which the microstructures of the samples could be observed. Recently, we produced the desired thin sections by etching with water, but the thus produced thin sections are of course not too reliable.

## 4. CONCLUSION

Sp–800 samples irradiated in the GIF A facility, to total doses up to 1200 MGy, show a saturation of damage at a level of about 140 J/g stored energy. The amounts of stored energy observed for these samples are not higher than those observed by other scientists for pure NaCl single crystals irradiated under comparable conditions.

## ACKNOWLEDGEMENT

We would like to thank Mr. A.C.G. van Genderen and Dr. P.J. van Ekeren of the Thermodynamics Centre Utrecht for performing the DTA measurements and calculating the stored energy values.

## REFERENCES

J. BERGSMA, R.B. HELMHOLDT and R.J. HEIJBOER, 1985: *"Radiation Dose Deposition and Colloid Formation in a Rocksalt Waste Repository"*, Nuc. Techn. **71,** 597.

J.B.M. DE HAAS and R.B. HELMHOLDT, 1989: *"Stralingsschade rond KSA–Containers in Steenzout"*, ECN–89–23, OPLA Report Nº 23, Ministry of Economic Affairs, The Hague, 45 p.

H.W. DEN HARTOG, J.C. GROOTE, J.R.W. WEERKAMP, J. SEINEN and H. DATEMA, 1993: *"Storage of Nuclear Waste in Salt Mines: Radiation Damage in NaCl"*; in "Defects in Insulating Materials", Ed. O. Kanert and J.M. Spaeth (World Scientific, Singapore) p. 410 – 423.

A. GARCÍA CELMA and H. DONKER, 1994a: *"Stored energy in irradiated salt samples"*, Nuclear Science and Technology series, EUR–14845, Commission of the European Communities, Luxembourg, 127 p.

A. GARCÍA CELMA and H. DONKER, 1994b: *"Radiation–Induced Creep of Confined NaCl"*, Rad. Eff. Def. Solids **132**, 223–247.

A. GARCÍA CELMA, J.L. URAI and C.J. SPIERS, 1988: *"A Laboratory Investigation into the Interaction of Recrystallization and Radiation Damage Effects in Polycrystalline Salt Rocks"*, Nuclear Science and Technology Series, EUR 11849 EN, Commission of the European Communities, Luxembourg, 125 p.

A. GARCÍA CELMA, H. VAN WEES and L. MIRALLES, 1991: *"Methodological developments and materials in salt–rock preparation for irradiation experiments"*, Nuclear Science and Technology Series, EUR 13266 EN, Commission of the European Communities, Luxembourg, 67 p.

A. GARCÍA CELMA, C. DE LAS CUEVAS, P. TEIXIDOR, L. MIRALLES and H. DONKER, 1993: *"On the Possible Continuous Operation of an Intergranular Process of Radiation Damage Anneal in Rock Salt Repositories"*, in: "Geological Disposal of Spent Fuel and High Level and Alpha–Bearing Wastes, Proceedings of a symposium, Antwerp, 19–23 October 1992", International Atomic Energy Agency, Vienna, p. 133–144.

A. GARCIA CELMA, A.J. NOLTEN, W.A. FELIKS and H. VAN WEES, 1995: *"Gamma Irradiation Experiments in Natural and Synthetic Halite"*, article 6 in this volume.



H. GIES, 1995: *" Salt of the Upper Permian (Zechstein–) Salt Diapir of the Asse"*, article 11 in this volume.

J.C. GROOTE and J.R.W. WEERKAMP, 1990: *"Radiation Damage in NaCl; Small Particles"*, Thesis, Groningen University, 270 p.

L.W. HOBBS, 1974: *"Transmission Electron Microscopy of Extended Defects in Alkali Halide Crystals"*, in "Surface and Defect Properties of Solids", Vol. 4, Chap. 6, Ed. M.W. Roberts and J.M. Thomas (The Cemical Society, London), p. 152–250.

L.W. HOBBS, A.E. HUGHES and D. POOLEY, 1973: *"A Study of Interstitial Clusters in Irradiated Alkali Halides using Direct Electron Microscopy"*, Proc. R. Soc. Lond. **A332,** 167–185.

A.E. HUGHES, 1983: *"Colloid Formation in Irradiated Insulators"*, Radiation Effects **74,** 57–76.

A.E. HUGHES and S.C. JAIN, 1977: *"Metal Colloids in Ionic Crystals"*, Adv. Phys. **28,** 717–828.

N. ITOH, 1982: *"Creation of Lattice Defects by Electronic Excitation in Alkali Halides"*, Adv. Phys. **31,** 491–551.

U. JAIN and A.B. LIDIARD, 1977: *"The Growth of Colloidal Centres in Irradiated Alkali Halides"*, Phil. Mag. **35**, 245–259.

G.H. JENKS and C.D. BOPP, 1974: *"Storage and Release of Radiation Energy in Salt in Radioactive–Waste Repositories"*, Oak Ridge Natn. Lab. Rep., ORNL–TM–4449, 77 p.

G.H. JENKS and C.D. BOPP, 1977: *"Storage and Release of Radiation Energy in Salt in Radioactive–Waste Repositories"*, Oak Ridge Natn. Lab. Rep., ORNL–5058, 97 p.

G.H. JENKS, E. SONDER, C.D. BOPP, J.R. WALTON and S. LINDENBAUM, 1975: *"Reaction Products and Stored Energy Released from Irradiated Sodium Chloride by Dissolution and by Heating"*, J. Phys. Chem. **79**, 871–875.

N. JOCKWER, 1981: *"Untersuchungen zur Art und Menge des im Steinsalz des Zechsteins enthaltenen Waser sowie dessen Freisetzung und Migration im Temperaturfeld endlagerter radioaktiver Abfälle"*, Thesis, Technische Universität Clausthal, 135 p.

P.W. LEVY, 1983: *"Radiation Damage Studies on Natural Rock Salt from Various Geological Localities of Interest to the Radioactive Waste Disposal Program"*. Nuc. Techn. **60,** 231–243.

P.W. LEVY and J.A. KIERSTEAD, 1982: *"Very Rough Preliminary Estimate of the Sodium Metal Colloid Induced in Natural Rock Salt by the Radiations from Radioactive Waste Canisters"*, Brookhaven Natn. Lab. Rep., BNL 32004, 76 p.

P.W. LEVY, K.J. SWYLER and R.W. KLAFFKY, 1980: *"Radiation Induced Color Center and Colloid Formation in Synthetic NaCl and Natural Rock Salt"*, J. Physique **41** Colloque C6, 344–347.

P.W. LÈVY, J.M. LOMAN, K.J. SWYLER and R.W. KLAFFKY, 1981: *"Radiation Damage Studies on Synthetic NaCl Crystals and Natural Rock Salt for Radioactive Waste Disposal Applications"*, in "The Technology of High-Level Nuclear Waste Disposal", Vol. 1, (DOE/TIC-4621), ed. P.L. Hoffmann, (Tech. Info. Ctr., U.S. Dept. of Energy, Oak Ridge, TN), p. 136-167.

P.W. LEVY, J.M. LOMAN and J.A. KIERSTEAD, 1984: *"Radiation Induced F-center and Colloid Formation in Synthetic NaCl and Natural Rock Salt: Applications to Radioactive Waste Repositories"*, Nuc. Instr. Meth. Phys. Res. **B1,** 549-556.

A.B. LIDIARD, 1979: *"Energy Stored in Irradiated NaCl"*, Phil. Mag. **A39**, 647-659.

J.M. LOMAN, P.W. LEVY and K.J. SWYLER, 1982: *"Radiation Induced Sodium Metal Colloid Formation in Natural Rock Salt from Different Geological Localities"*, in "Scientific Basis for Nuclear Waste Management", Vol. 6, Ed. S.V. Topp, (Elsevier, New York), p. 433-440.

G. VAN OPBROEK and H.W. DEN HARTOG, 1985: *"Radiation Damage of NaCl: Dose Rate Effects"*, J. Phys. C: Solid State Phys. **18**, 257-268.

W.J. SOPPE, 1993: *"Computer Simulation of Radiation Damage in NaCl by using a Kinetic Rate Reaction Model"*, J. Phys.: Condensed Matter **5,** 3519-3540.

W.J. SOPPE and J. PRIJ, 1994: *"Radiation Damage in a Rock Salt Nuclear Waste Repository"*, Nuc. Techn. **107**, 243-253.

W.J. SOPPE, H. DONKER, A. GARCIA CELMA and J. PRIJ, 1994: *"Radiation Induced Stored Energy in Rock Salt"*, J. Nuc. Mat. **217**, 1-31.

C.J. SPIERS, J.L. URAI, G.S. LISTER, J.N. BOLAND and H.J. ZWART, 1986: *"The Influence of Fluid-Rock Interaction on the Rheology of Salt Rock"*, Nuclear Science and Technology Series, EUR-10399, Commission of the European Communities, Luxembourg, 131 p.

K.J. SWYLER, R.W. KLAFFKY and P.W. LEVY, 1979: *"Radiation Damage Studies on Natural and Synthetic Rock Salt for Waste disposal Applications"*, in "Scientific Basis for Nuclear Waste Management", Vol. 1, Ed. G.J. McCarthy (Plenum, New York), p. 349-354.

K.J. SWYLER, R.W. KLAFFKY and P.W. LEVY, 1980: *"Recent Studies on Radiation Damage Formation in Synthetic NaCl and Natural Rock Salt for Radioactive Waste Disposal Applications"*, in "Scientific Basis for Nuclear Waste Management", Vol. 2, Ed. C.J.M. Northrup Jr.,(Plenum, New York), p. 553-560.



# ON THE RELATIONSHIP BETWEEN STORED ENERGY AND COLLOIDAL SODIUM PRODUCTION IN IRRADIATED ROCK SALT

**H. Donker, W.J. Soppe and A. García Celma**

## ABSTRACT

A few parameters of the theoretical models used to describe the formation of radiation damage in rock salt were critically reviewed. It is discussed that the back reaction used in the models should be described as $\gamma = 10^{16} \exp(-0.4/kT)$ and that for the conversion factor between defect concentrations and stored energy a value of 5 eV/F-H pair should be used. With these modified parameters the models were compared with the experimental results of Jenks and Bopp and the experimental results obtained from the GIF A irradiation experiments.

## 1. INTRODUCTION

The first model describing the formation of radiation damage in alkali halides was developed by Jain and Lidiard [1977]. This model was later modified by Van Opbroek and den Hartog [1985], according to a proposal of Lidiard [1979]. This modification, the inclusion of a back reaction, was introduced in order to be able to explain the experimental results of Jenks and Bopp [1974;1977] and Jenks et al. [1975].

A disadvantage of this model is that it does not describe the nucleation stage of the colloids and dislocation loops. Moreover, the effects of impurities, strain and grain boundaries are not taken into account. Recently two new, slightly different models based on the old Jain-Lidiard model, but with extensions describing the nucleation stage have been developed [Soppe, 1993; Seinen et al.,1992].

In a recent paper [Soppe et al., 1994] the experimental results on radiation damage